On The Nature of Invasive *Salmonella* Typhi and African *Salmonella* Typhimurium

Larissa A. Singletary

A dissertation

submitted in partial fulfillment of the

requirements for the degree of

Doctor of Philosophy

University of Washington

2017

Reading Committee:

Ferric C. Fang, Chair

Brad T. Cookson

Jason G. Smith

Program Authorized to Offer Degree:

Microbiology

University of Washington

Abstract

On The Nature of Invasive Salmonella Typhi and African *Salmonella* Typhimurium

Larissa A. Singletary

Chair of the Supervisory Committee:

Professor Samuel I. Miller

Department of Microbiology

Invasive typhoidal and nontyphoidal Salmonelloses are a significant global burden affecting tens of millions of individuals each year. Typhoid fever and invasive nontyphoidal Salmonellosis (iNTS) are caused by *Salmonella enterica* serovar Typhi (*S*. Typhi) and Typhimurium (*S*. Typhimurium) respectively but share similar disease manifestations in humans like high fever, hepato-splenomegaly and infrequent diarrhea. Despite these clinical similarities each serovar interacts differently with the human immune system. Individuals with congenital or acquired immunodeficiencies resulting in impaired T_h1 immunity, such as HIV/AIDS, are more susceptible to iNTS but not typhoid fever. This suggests nontyphoidal serovars and *S*. Typhi differ in their propensity to initiate a T_h1 immune response in infected hosts. I have found that *S*. Typhi-infected macrophages exhibit reduced innate immune responses to infection including macrophage apoptosis, pyroptosis and M1 activation in comparison to *S*. Typhimurium-infected cells. A hu-SRC-SCID humanized mouse model of infection mirrors these results. Apoptosis, pyroptosis and M1 polarization of human macrophages by *S*. Typhimurium is dependent upon the *Salmonella* pathogenicity island 2 (SPI2) type three secretion system (T3SS). While the

specific effector(s) required for *S*. Typhimurium-induced pyroptosis and M1 activation have not been identified, intramacrophage expression of SPI2 is lower in *S*. Typhi compared to *S*. Typhimurium. Differences in intramacrophage SPI2 expression may account for differences in *S*. Typhi- and *S*. Typhimurium-induced pyroptosis and M1 activation.

While *S*. Typhi dampens intramacrophage SPI2 expression to evade M1/T_h1 responses to infection, iNTS strains exploit the compromised host immune system to cause systemic infection. Non-typhoidal *S.* Typhimurium is a frequent cause of bloodstream infections in children and HIV-infected adults in sub-Saharan Africa. Most isolates from African patients with bacteremia belong to a single sequence type, ST313, which is genetically distinct from gastroenteritis-associated ST19 strains such as 14028s. One important difference between ST19 strains and the sequenced ST313 strain D23580 is an increase in genomic decay in D23580, a hallmark of host-adaptation. ST313 strains were originally hypothesized as becoming more typhoid-like and thereby explaining the increased incidence of associated invasive infections. We have found that, like the enteritis-associated strain 14028s, D23580 is able to elicit an acute inflammatory response and cause enteritis in mice and rhesus macaque monkeys. However, iNTS strains are becoming more typhoid-like in their ability to survive in the environment. We have identified and demonstrated two loss-of-function mutations in D23580, not present in the ST19 strain 14028s, that impair multicellular stress resistance associated with survival outside the host. These mutations result in inactivation of the KatE stationary-phase catalase that protects high-density bacterial communities from oxidative stress and the BcsG cellulose biosynthetic enzyme required for the RDAR (red, dry and rough) colonial phenotype. Collectively, these observations suggest that African *S.* Typhimurium ST313 strain D23580 is becoming adapted to an anthroponotic mode of transmission while retaining the ability to infect and cause enteritis in multiple host species.

We have also identified a novel, 5-gene operon in *S*. Typhi and *S*. Typhimurium that is required for virulence in mice. Previously, humanized mice susceptible to *S*. Typhi infection

were infected with a high-density *S*. Typhi transposon mutant library to identify novel determinants required for invasive *S*. Typhi disease. From the screen, a novel, 5-gene operon was identified as required for virulence. We confirmed this requirement in additional mouse models of invasive *Salmonella* infection. Multiple genes in the operon have homology to carbohydrate metabolism genes. While we were unable to identify a role for these genes during growth on single carbon sources we identified a putative role for this operon in maintaining bacterial membrane stability. We measured the membrane polarization of *Salmonella* 5-gene operon mutant strains and found they were hyperpolarized as compared to wt further confirming a role for these genes in maintaining bacterial membrane stability. While the specific function of these genes is still unknown we continue to investigate how this novel operon promotes membrane stability in *Salmonella*.

TABLE OF CONTENTS

CHAPTER 1: Introduction……11

CHAPTER 2: *Salmonella enterica* serovar Typhi elicits reduced macrophage death and M1/T_h1 polarization in infected human macrophages and humanized mice via reduced intramacrophage SPI2 expression……24

2.1: Introduction

2.2: Results

2.2.1: *S*. Typhi persists in human macrophages by avoiding macrophage death and dampening innate immune responses to infection

Figure 1: *Salmonella* persistence in a human macrophage cell line

Figure 2: Innate immune responses of a human macrophage cell line to *Salmonella*

Table 1: Immune defects causing increased susceptibility to invasive Salmonellosis

Figure 3: Immune responses of primary human macrophages and humanized mice to *Salmonella* infection

2.2.2: Activation of *S*. Typhimurium-induced innate immune responses is dependent upon *Salmonella* Pathogenicity Island 2 and it's regulator PhoP

Figure 4: Innate immune responses of a human macrophage cell line to wild-type and mutant *Salmonella* strains

2.2.3: The ADP-ribosylating toxin SpvB of *S*. Typhimurium, absent from *S*. Typhi, contributes to reduced persistence in human macrophages

Table 2: *Salmonella* Pathogenicity Island-2 (SPI2) effectors

Figure 5: Determinants of wild-type and mutant *Salmonella*-induced cell death or persistence in human macrophages

2.2.4: Differential STAT1 activation cannot be attributed to differences in LPS sensing between serovars

Figure 6: Determinants of innate immune activation in a human macrophage cell line infected with *Salmonella*

Figure 7: Determinants of innate immune activation across time in a human macrophage cell line infected with *Salmonella*

2.2.5: *S*. Typhi has reduced intramacrophage SPI2 expression in human macrophages

Figure 8: Intramacrophage *Salmonella* SPI2 expression

2.3: Discussion

Figure 9: Immune responses of moribund humanized mice to *Salmonella* infection

2.4: Materials and Methods

Table 3: Strains, plasmids, primers

CHAPTER 3: Loss of multicellular behavior in epidemic African non-typhoidal *Salmonella enterica* serovar Typhimurium ST313 strain D23580……67

3.1: Introduction

3.2: Results

3.2.1: D23580 is adhesive, invasive and cytotoxic for mammalian cells

Figure 10: D23580 is more adhesive and invasive for cultured cells than 14028s

Figure 11: D23580 is more invasive and cytotoxic for cultured cells than 14028s

3.2.2: D23580 is highly invasive following oral infection

Figure 12: D23580 efficiently colonizes the murine intestine

3.2.3: D23580 induces inflammation in the intestinal tract

Figure 13: D23580 elicits acute inflammation in the rhesus macaque intestine

3.2.4: D23580 exhibits enhanced susceptibility to oxidative stress due to mutation of the *katE* catalase gene

Figure 14: D23580 exhibits deficient detoxification of hydrogen peroxide despite retaining σ^S-dependent gene expression

Figure 15: D23580 fails to detoxify hydrogen peroxide due to a mutation in the stationary-phase catalase KatE

3.2.5: D23580 is unable to form RDAR (red, dry and rough) colonies due to a mutation of the *bcsG* cellulose biosynthetic gene

Figure 16: D23580 is unable to form RDAR colonies due to a mutation in the cellulose synthetic enzyme BcsG

Figure 17: Survival of D23580 and 14028s in water over 5 days

3.3: Discussion

3.4: Materials and Methods

Table 4: Strains, plasmids, primers

CHAPTER 4: Characterization of a novel operon contributing to *Salmonella enterica* serovar Typhi virulence……..110

4.1: Introduction

4.2: Results

4.2.1: A novel, putative 4-gene operon is important for typhoid virulence in humanized mice

Figure 18: *Salmonella STM14_5332-5335* mutants are less virulent in non-humanized mice

Figure 19: Survival of *Salmonella* in a murine macrophage cell line

4.2.2: The 4-gene operon has no role in carbohydrate metabolism despite *in silico* predictions

Table 5: Protein structure/function prediction analysis reveals a potential role during carbohydrate metabolism

Figure 20: Growth of *Salmonella* on single carbon sources

4.2.3: The 5-gene operon is important to maintaining membrane stability in *Salmonella*

Table 6: Biolog phenotypic microarray results summary

Figure 21: Ty2 *t4474-4478* mutants are hyper-susceptible to EDTA stress

Figure 22: Growth of *Salmonella* in the presence of the toxic, host-metabolite D-serine

Figure 23: *Salmonella* 5-gene operon mutants have hyper-polarized membranes

4.3: Discussion

4.4: Materials and Methods

Table 7: Strains, plasmids, primers

4.5: Appendix

Appendix 4.5.1: The Biolog phenotypic microarray compound list for plates PM1-10

Appendix 4.5.2: The Biolog phenotypic microarray compound list for plates PM11-20

Appendix 4.5.3: Growth analysis for *S*. Typhimurium 14028s wt, Δ*STM14_5331-5335,* and Δ*spvR* on plates PM1-20

CHAPTER 5: Future directions……137

REFERENCES……141

This dissertation is passionately dedicated to my parents.

Thank you for always encouraging the curiosity that has made this research possible.

Chapter 1

Background and significance

Typhoid fever and invasive nontyphoidal Salmonellosis: A growing burden for developing nations

Typhoid fever, caused by the bacterium *Salmonella enterica* serovar Typhi (*S.* Typhi) has plagued man since ancient times (1) but remains a serious public health issue, causing an estimated 21.7 million illnesses and 217,000 deaths each year (2). In developed nations like the United States, typhoid fever is primarily of concern to persons traveling abroad. However, in developing nations where sanitation measures are poor and water sources contaminated, typhoid fever remains a great concern and public health burden (3).

In contrast to invasive salmonellosis in most parts the world, which consists primarily of typhoid or paratyphoid fever, bloodstream *Salmonella* infections in sub-Saharan Africa are primarily caused by non-typhoidal serovars such as *Salmonella* Typhimurium (*S*. Typhimurium), Enteritidis (*S*. Enteritidis) and Dublin (*S*. Dublin) (3–6). The last three decades have witnessed an epidemic of invasive non-typhoidal Salmonellosis (iNTS) in this region. A recent study estimates the global burden of iNTS to be 3.4 million cases per year, with the highest burden in children and young adults (7). Prior to the advent of the HIV pandemic, iNTS in sub-Saharan Africa primarily afflicted young children, often with malaria co-infection, and was rarely seen in adults (4, 8). However, as HIV began to sweep across sub-Saharan Africa in the 1980s, *Salmonella* was increasingly identified as the most common cause of bacterial bloodstream infection in HIV-infected adults (9–11).

Salmonella evolution and host-adaptation

The genus *Salmonella* is comprised of gram negative, rod-shaped, facultative anaerobic bacteria found in the intestines of animals. The pathogen *Salmonella* evolved from the enteric commensal *Escherichia coli* (*E. coli*). The evolution of *Salmonella* can be described as occurring

in three phases with each phase being punctuated by the acquisition of foreign DNA enabling survival in new host niches (12, 13). The acquisition of *Salmonella* pathogenicity island 1 (SPI1) marked the initial divergence of *Salmonella* from *E. coli* (14–16). SPI1 enabled *Salmonella* to invade intestinal epithelial cells and escape the competitive environment in the intestinal lumen (17). The *Salmonella* genus is comprised of only two species: *enterica* and *bongori*. *Salmonella enterica* and *bongori* are distinguished by the presence or absence of *Salmonella* pathogenicity island 2 (SPI2), respectively (18). SPI2 is important for survival and replication in phagocytes and systemic infection (19). SPI2 enabled *Salmonella enterica* to survive gut-associated immune barriers and colonize extra-intestinal sites. While the acquisition of foreign DNA by bacteria can be advantageous it also presents challenges. Unchecked gene expression can be toxic to an organism (20). *Salmonella* minimizes this toxicity by dampening or restricting expression of foreign genes by employing nucleoid-associated, gene-silencing proteins like H-NS (21). H-NS does not recognize specific nucleotide sequences but instead binds foreign DNA based on its reduced GC content (21). H-NS counter-silencers, like PhoP, facilitate integration of foreign DNA expression into existing *Salmonella* regulatory networks (22, 23). *Salmonella enterica* is further divided into the subspecies I, II, IIIa, IIIb, IV and VI (13). *Salmonella enterica* subspecies I (*enterica)* includes 99% of the *Salmonella* that infect warm-blooded animals (13). The remaining subspecies and *bongori* mostly infect cold-blooded animals (13). Within subspecies *enterica*, over 2,500 known serovars exist, a designation that reflects the organism's unique cell-surface antigenic structure, specifically the O and H antigens (24). *S*ubspecies *enterica* serovars are diverse in their host-range including generalists like Typhimurium (*S*. Typhimurium) that can infect multiple animals including mice, cows, chickens and humans. In contrast, serovar Typhi (*S*. Typhi) is host-restricted, only causing disease in humans (25). Despite their differences, serovars Typhimurium and Typhi are closely related, with 89% shared gene content (26). Increased genomic decay is correlated with *Salmonella* host adaptation. The *S*. Typhimurium genome is only 0.6% pseudogenes in contrast to 5% in *S*. Typhi (26).

Human Salmonellosis

In humans, the clinical outcome of *Salmonella* infection depends upon the infecting *Salmonella* strain and the immunological status of the host. Most *Salmonella* infections in humans can be described as one of three syndromes: 1) invasive typhoid fever in immunocompetent hosts 2) nontyphoidal *Salmonella* gastroenteritis in immunocompetent hosts and 3) nontyphoidal *Salmonella* bacteremia in immunocompromised hosts.

The onset of symptoms in *S*. Typhi-infected immunocompetent humans occurs approximately 1-2 weeks following exposure (27). Symptoms of typhoid fever may include high fever (up to 104°F), anorexia, prostration and abdominal tenderness due to hepato-splenomegaly (27). Diarrhea is infrequent. Antibiotic treatment is required for timely resolution of disease and may decrease the rate of carriage (which occurs following ~2-10% of infections) (27, 28). In the absence of antibiotic treatment the fatality rate of *S*. Typhi infection is 10-30%, compared to 1-4% with treatment (2). The high fatality rate in the absence of antibiotic treatment is of great concern given the increase in multiple-drug resistant strains of *S*. Typhi worldwide (29–33). Asymptomatic carriers of *S*. Typhi intermittently shed bacteria in their feces for an indefinite period of time (27). The most famous typhoid carrier, Mary Mallon, also known as Typhoid Mary, shed *S*. Typhi in her stool for her entire life following her initial infection and was responsible for directly infecting at least 122 people (34). Typhoid carriers shed bacteria in the feces that arise in the gallbladder. Asymptomatic carriage has been associated with gallstones, likely due to *S*. Typhi's ability to form robust biofilms on their surfaces (35, 36).

In contrast, the incubation period for nontyphoidal *Salmonella* infections (NTS) in immunocompetent humans is brief: 12-72 hours following exposure. After ingestion, *S*. Typhimurium induces an influx of neutrophils to the site of infection (37–39). The presence of neutrophils in the stool is a hallmark of *S*. Typhimurium-induced diarrhea (40, 41). Symptoms of *S*. Typhimurium infection include gastroenteritis (inflammatory diarrhea), nausea and vomiting

(41, 42). *S*. Typhimurium-induced gastroenteritis is typically self-limiting and rarely requires medical intervention except in complicated cases. Carriage and fecal shedding of *S*. Typhimurium occurs in less than 1% of infected patients (43).

Symptoms of invasive nontyphoidal *Salmonella* infections (iNTS) in immunocompromised hosts are diverse and share features with both typhoid and non-typhoidal infections of immunocompetent humans. While diarrhea is infrequent in typhoid patients and minimal or absent in 20-50% of children and HIV-infected adults with iNTS infections in sub-Saharan Africa it is the most common symptom of nontyphoidal *Salmonella* (NTS) infections in immunocompetent hosts (44, 45). Additionally, as in typhoid fever, high fever and hepato-splenomegaly are common symptoms associated with iNTS infections (45). The fatality rate of iNTS infections in sub-Saharan Africa is high (~20-25%), presumably due to the lack of supportive medical care, the compromised immune status of infected patients, and the prevalence of multi-drug resistant isolates causing infections (6, 45).

Vaccines against invasive Salmonellosis

Two vaccines are currently available to protect against typhoid fever: the Vi antigen polysaccharide and the live attenuated vaccine strain Ty21a (46). The Vi antigen subunit vaccine contains purified *S*. Typhi Vi capsule. Unlike *S*. Typhimurium, *S*. Typhi possesses a polysaccharide capsule that resists phagocytosis and impairs innate immune responses by host cells (47–50). The Ty21a live attenuated vaccine strain contains multiple metabolic mutations and lacks the Vi capsule (46). Both vaccines confer incomplete protection: ~70% protection is elicited by the Vi antigen vaccine with revaccination required every 2-3 years, and 60-70% protection is elicited by the Ty21a vaccine with revaccination required every 5-7 years (51). Both vaccines are unsuitable for widespread distribution in developing countries where they are most needed. Ty21a requires cold-chain storage and a multiple dosing regimen for maximal protection, a requirement that is impractical for rural, impoverished areas where refrigeration

and reliable electricity is scarce. Unlike Ty21a, the Vi antigen vaccine does not require refrigeration and is dispensed as a single dose. However, administration of this vaccine requires trained health professionals. Since the Vi antigen vaccine only recognizes a *S.* Typhi-specific antigen, it is ineffective against *Salmonella enterica* Paratyphi serovars, which have similar clinical manifestations and geographical distribution to typhoid fever (52). In contrast, the Ty21a vaccine protects against paratyphoid fever but is not suitable for immunocompromised individuals due to the live nature of the vaccine (53). Therefore improved typhoid vaccines with improved efficacy and ease of storage and administration are needed. Large-scale immunization campaigns have shown to be effective and feasible (54). Currently, no vaccines against invasive or diarrheal NTS are available, although several conjugate and attenuated live oral vaccines are currently in development (51).

Salmonella interactions with the small intestine

Much of what we know regarding *Salmonella* pathogenesis in humans has been gleaned from the study of nontyphoidal *Salmonella* infection of mice. *S*. Typhi is a host-specific human pathogen that fails to replicate and cause disease in mice. However, susceptible mice infected with *S*. Typhimurium succumb to a somewhat typhoid-like illness. Animal models of infection have been further developed to examine both the acute gastroenteritis and chronic phases of *Salmonella* infection (55).

Salmonella infection of animals begins when bacteria are orally ingested through consumption of fecally-contaminated water or food. Over 99% of ingested *Salmonellae* are killed in the stomach or pass through the intestine without consequence (56). Remaining bacteria invade the intestinal epithelium, primarily Microfold (M) cells, using the *Salmonella* pathogenicity island 1 (SPI1)-encoded type III secretion system (T3SS) (57–59). The SPI1 T3SS translocates effectors from the bacterium into the host cell cytosol to facilitate internalization of *Salmonella* by host cells (60). Invasion of M cells allows direct access to the

underlying lymphoid tissue known as Peyer's patches (61). Once within the Peyer's patches, *Salmonella* preferentially infects phagocytic cells, specifically macrophages and dendritic cells, that traffic to the mesenteric lymph nodes and beyond (spleen, liver) (62). *Salmonella* can also gain access to systemic sites in a SPI1-independent manner via $CD18^{+}$ dendritic cells that directly sample the intestinal lumen (63). The ability of *Salmonella* to survive and proliferate within mononuclear phagocytes is integral to *Salmonella*'s ability to cause systemic infection (64). The small intestine mounts an immune response against *Salmonella* that is dependent on the infecting serovar. This response and its determinants will be covered in greater depth later in this chapter.

Survival of *Salmonella* within macrophages

In 1986, Fields *et al.* performed a large-scale screen for *S*. Typhimurium transposon mutants that were unable to survive in cultured murine macrophages (64). These investigators demonstrated that *S*. Typhimurium mutants unable to proliferate within macrophages failed to cause systemic infection in mice. This highlights the importance of intramacrophage survival for the establishment of invasive Salmonellosis. No comparable study has been performed for *S*. Typhi in human macrophages.

Once inside macrophages, *Salmonella* utilizes a second T3SS, encoded on *Salmonella* pathogenicity island 2 (SPI2), to translocate effectors across the phagosomal membrane into the host cell cytoplasm (65). *S*. Typhimurium SPI2 mutants are defective for survival and proliferation in murine macrophages as well as in their ability to cause systemic disease (66). There are over 30 known SPI2 effectors with roles ranging from manipulation of the host cell's actin cytoskeleton, vesicular trafficking and signal transduction pathways (65). Interestingly, Forest *et al.* reported that SPI2 is not required for the survival of *S*. Typhi in either primary or immortalized human macrophages (67), although the same group reported in a 2001 study that *S*. Typhi up-regulates SPI2 expression inside human macrophages (68). Although the prevailing

paradigm has held that SPI2 is required for *Salmonella* survival inside host macrophages, SPI2 may serve an alternative role in *S*. Typhi interactions with the host immune system. This possibility will be discussed further in Chapter 2.

Intracellular defenses against *Salmonella*

Despite *Salmonella*'s ability to manipulate the host and shape its replicative niche, host mechanisms exist to prevent the replication of intracellular *Salmonella*. Macrophages have an extensive repertoire of anti-bacterial defense mechanisms. Upon phagocytosis of bacteria, vacuolar pH decreases to ~5.0-5.5, thereby activating phagosomal enzymes with potent anti-microbial activity (69–71). Bactericidal reactive oxygen species (ROS) are produced rapidly upon bacterial internalization via the NADPH phagocyte oxidase (Nox2), and production of reactive nitrogen species (RNS) by inducible nitric oxide synthase (iNOS) occurs subsequently (72–75). The generation of ROS in response to bacterial internalization is also observed in neutrophils (73, 76). The phagosomal compartment deprives microbes of essential nutrients such as metals like iron, which are withheld from the phagosome by metal pumps like the natural resistance associated membrane protein 1 (Nramp1, also known as Slc11a1). The importance of Nramp1 during *Salmonella* infection is demonstrated by the severe susceptibility of Nramp1-/- mice to *Salmonella* infection (77). Programmed host cell death is another mechanism by which *Salmonella* infection can be controlled. The most well studied form of *Salmonella*-induced cell death, pyroptosis, is described in more detail below.

***Salmonella*-induced macrophage death**

Salmonella-induced host cell death occurs at multiple sites in the body and in multiple cell types including macrophages and epithelial cells (78). For the purposes of this discussion, only *Salmonella*-induced macrophage death will be considered. The best-characterized mechanism of *Salmonella*-induced macrophage death is pyroptosis. *Salmonella*-induced

macrophage pyroptosis was initially regarded as apoptotic in nature, however it was later designated as a distinctive form of macrophage death that is more inflammatory than apoptosis (79, 80).

Pyroptosis is an inflammatory form of cell death that releases intracellular bacteria into the extracellular milieu where they are ingested and killed by neutrophils (81). Additionally, pyroptosis stimulates systemic innate immune responses through the production and secretion of the inflammatory cytokines IL-1β and IL-18 (82–85). Pyroptosis is characterized as either rapid or delayed in onset. Rapid pyroptosis is dependent upon the *Salmonella* SPI1 T3SS (86, 87). During invasion of host cells, *Salmonella* employs the SPI1 T3SS to translocate effector proteins into the host cell cytosol and facilitate invasion (17). Simultaneously, flagellin and SPI1 T3SS structural components may be translocated through the secretion apparatus into the host cytosol. Host cells have exploited these events to detect and respond to invading intracellular bacteria. Host cytosolic pattern-recognition receptors called NAIPs (NLR family apoptosis inhibitor proteins) directly bind *Salmonella* flagellin or the SPI1 T3SS rod protein PrgJ (88–90). The NAIP-bound protein then associates with the NOD-like receptor (NLR) NLRC4 (88–90). Mice encode seven different NAIPs, with NAIPs 5 and 6 specifically recognizing flagellin and NAIP2 specifically recognizing PrgJ (88). Interestingly, humans only encode a single NAIP that does not recognize flagellin or PrgJ but instead recognizes the T3SS needle protein PrgI (91). The NAIP/NLRC4 oligomer then associates with the inflammasome adapter protein ASC to form an active inflammasome complex (86, 90). Pro-caspase-1 is recruited to the inflammasome and cleaved into its active form (78, 83, 84). Consequently, the inflammatory cytokines IL-1β and IL-18 are processed and activated by caspase-1 and released from infected cells (82). Membrane pores are formed in the infected host cell in a caspase-1-dependent manner, eventually resulting in host cell swelling and osmotic lysis that culminates in the release of intracellular bacteria (85). Cell lysis is not required for the release of IL-1β and IL-18, which recruit additional immune cells including neutrophils to the site of infection to aid in killing of *Salmonella* (78).

NLRC4 and a second inflammasome-associated NLR protein, NLRP3, are thought to represent different pathways of inflammasome activation, with NLRP3 recognizing distinctive stimuli from those recognized by NLRC4, although a recent publication has demonstrated recruitment of NLRP3 by NLRC4 during *Salmonella* infection of macrophages (92).

In contrast to rapid pyroptosis, delayed *Salmonella*-induced macrophage death does not require the SPI1 T3SS but rather requires the SPI2 T3SS (93, 94). While caspase-1 is known to be involved in delayed *Salmonella*-induced macrophage death, the precise inflammasome components involved in this process have not been characterized (78, 94). The rod protein of the SPI2 T3SS, SsaI, has been ruled out as an activator of delayed macrophage pyroptosis (95). However to our knowledge, no reports have yet confirmed or excluded the involvement of flagellin in delayed macrophage cytotoxicity (addressed further in Chapter 2). In fact it is unlikely that flagellin is involved, as flagellin is downregulated following macrophage uptake of *Salmonella* (96). In addition, no studies have directly demonstrated the ability of SPI2 to translocate flagellin under natural conditions (97, 98), although SPI2-dependent detection of heterologously-expressed flagellin in macrophages by NLRC4 has been demonstrated (81). The pro-inflammatory cytokine IL-1β is expressed in delayed as in rapid pyroptosis (94). SpvB, an ADP-ribosylating toxin encoded on the *Salmonella* virulence plasmid pSLT (which is absent in *S*. Typhi) and translocated by the SPI2 T3SS, also triggers delayed macrophage death in infected cells (99–101). However, the mechanism by which SpvB induces macrophage cell death may be distinct from *Salmonella*-induced delayed pyroptosis, which will be discussed in further detail in Chapter 2.

Since pyroptosis has primarily been studied in the context of *S*. Typhimurium-infected murine macrophages and mice, the importance of pyroptosis in *S*. Typhi-human macrophage interactions is less clear. Nevertheless, several studies have addressed the ability of *S*. Typhi to cause cell death in human macrophages. *S*. Typhi induces both rapid and delayed cytotoxicity in cultured human macrophages (79, 80, 93). *S*. Typhi and *S*. Typhimurium induce similar

amounts of rapid SPI1-dependent macrophage cytotoxicity in human macrophages (94), but *S*. Typhi induces less delayed macrophage death than *S*. Typhimurium (102). The ability of *S*. Typhi to persist within human macrophages and disseminate to systemic sites might be related to its ability to modulate macrophage death in a manner distinct from non-typhoidal serovars such as *S*. Typhimurium. However the mechanism by which *S*. Typhi avoids the induction of delayed human macrophage cell death is incompletely understood.

The immune response to *Salmonella* infection

The immune response to *Salmonella* infection begins in the small intestine. Intestinal epithelial cells rapidly respond to *Salmonella* infection by secreting inflammatory cytokines, such as IL-8 and hepoxilin A_3, that recruit neutrophils to the site of infection (50, 103). Neutrophil-rich diarrhea is a hallmark of *Salmonella*-induced gastroenteritis, whereas diarrhea is infrequent in patients with typhoid fever (37–39). This is likely due to the differential interactions of *S*. Typhi and *S*. Typhimurium with the intestinal epithelium. Epithelial cells secrete IL-8 in response to *Salmonella* infection by detecting *Salmonella* flagellin through the pattern-recognition receptor (PRR) TLR5 (50). In contrast, less IL-8 is secreted from the intestinal epithelium and macrophages during infection with *S*. Typhi (50). *S*. Typhi expresses the polysaccharide capsule Vi that prevents TLR recognition of pathogen-associated molecular patterns (PAMPs) like flagellin and LPS. A Vi^- mutant of *S*. Typhi was shown to induce secretion of higher levels of IL-8 from both epithelial cells and macrophages upon infection (50).

In addition to efficiently killing *Salmonella*, neutrophils are also an important early source of interferon-γ (IFN-γ), a potent antimicrobial cytokine that activates resident phagocytes (104). The importance of neutrophils in fighting *Salmonella* infection is highlighted by a study from Cheminay, *et al.*, in which antibody-mediated neutrophil depletion rendered mice more susceptible to oral *Salmonella* infection and resulted in higher organism burdens in Peyer's Patches and spleens compared to wild-type mice (105).

Additional cell types including macrophages and NK cells are also recruited to the site of intestinal infection (104, 106, 107). Resident dendritic cells (DCs) are activated by *Salmonella* PAMPs and migrate to the Peyer's Patches to activate naïve T-cells (108–110). A 2001 study by Sierro, *et al.* demonstrated that recognition of *Salmonella* LPS and flagellin by resident dendritic cells results in maturation and translocation of dendritic cells to the T-cell-enriched area of intestinal lymphoid tissue to initiate an adaptive immune response (108). While T-cells in the Peyer's patches and mesenteric lymph nodes are activated within hours of oral *Salmonella* infection, clonal expansion of *Salmonella*-specific T-cells can take weeks (109, 110).

In addition to a robust cell-mediated immune response, *Salmonella* also induces a strong antibody response (111). Secretory IgA (sIgA) is released from the intestine and is an important local anti-*Salmonella* defense (112). Interestingly, a sIgA response is only initiated when *Salmonella* actively invades via M cells (113). *Salmonella* that bypass M cells to penetrate the intestinal barrier fail to provoke a sIgA response in mice (113), although IgG responses are initiated from both primary and secondary sites of infection (mesenteric lymph nodes and spleen) (113). B cells are not only important during *Salmonella* infection because of their ability to secrete anti-*Salmonella* antibodies, but also serve as antigen-presenting cells (114).

While a variety of host immune responses are generated in response to *Salmonella* infection, we can learn much about which immune responses are integral to restricting *Salmonella* to the intestine by examining immunodeficiencies that predispose individuals to invasive nontyphoidal *Salmonella* infections (iNTS). Three immunodeficiencies are known to predispose individuals to iNTS but not typhoid fever. First, the phagocytes of individuals with chronic granulomatous disease (CGD) are unable to mount a potent enough respiratory burst to kill intracellular bacteria, including nontyphoidal *Salmonella* (115). Second, individuals with defects in their ability produce IL-12/23 in response to infection are more susceptible to iNTS (116). Third, individuals with reduced levels of $CD4^+$ T-cells, such as those infected with HIV^+, are more susceptible to iNTS infections but not typhoid fever (9–11). Immunodeficiencies that

predispose individuals to invasive Salmonellosis primarily appear to involve an inability to initiate or sustain a T_h1 immune response. Additional observations underscore the importance of a robust T_h1 response in controlling iNTS infection, which will be discussed in further detail in Chapter 2 (114, 117). While the host immunodeficiencies that predispose individuals to iNTS inform us of the host defenses important to resisting nontyphoidal *Salmonella* infection, the infections these individuals are not more susceptible to, like typhoid fever, can be just as informative about the pathogenesis of an organism. We know that a robust gut T_h1 immune response is important to preventing iNTS, and that when these defenses are compromised *Salmonella* that normally induce enteritis are able to infect the peripheral organs. However, whether an individual has these same gut immune responses is of little consequence to *S*. Typhi. While *S*. Typhimurium relies upon the absence of these defenses to cause systemic infection, *S*. Typhi does not; suggesting *S*. Typhi possesses mechanisms to neutralize detection by and/or activation of these responses.

Objectives of this thesis

Currently available typhoid vaccines are sub-optimal, and vaccines for invasive nontyphoidal Salmonellosis (iNTS) do not yet exist. However, vaccination against these infections are likely to be an important component of efforts to prevent invasive Salmonellosis until comprehensive infrastructural remedies to ensure universal access to clean water and adequate sewage disposal are instituted. The need for better vaccines is hastened by the rising prevalence of multi-drug resistant strains of both *S*. Typhi and *S*. Typhimurium (118, 119). An improved understanding of immune responses to typhoidal and nontyphoidal *Salmonella* will enhance vaccine development efforts. Human Salmonellosis is most often studied in a murine *S.* Typhimurium model system that recapitulates selected aspects of human typhoid fever. While these studies are essential and useful to understanding the molecular basis of *Salmonella* pathogenesis, unique pathogenic mechanisms employed by *S*. Typhi to subvert human immune

responses cannot be studied in this model. This thesis seeks to understand the novel pathogenic relationship between *S*. Typhi and human macrophages. The specific objectives are three-fold: 1) to understand the molecular basis of *S*. Typhi persistence in human macrophages and avoidance of macrophage cell death; 2) to understand the ability of *S*. Typhi to evade immune detection in human macrophages and humanized mice; and 3) to characterize novel determinants of *S*. Typhi virulence during infection of humanized mice.

Chapter 2

Salmonella enterica serovar Typhi persists in human macrophages by avoiding the elicitation of protective immune responses

LAS contribution: Conceived and designed study with F.C.F. and wrote manuscript. L.A.S. performed all experiments, with assistance from Taylor Stepien on screening of SPI-2 effector mutants for STAT1 phosphorylation and from Stephen J. Libby on humanized mouse infection experiments.

Abstract

The human pathogen *Salmonella enterica* serovar Typhi (*S*. Typhi) causes more than 20 million infections and 200,000 deaths each year. Typhoid fever is characterized by a prolonged incubation period, invasive disease and a high rate of asymptomatic carriage following disease resolution. Survival within macrophages is an essential feature of *Salmonella* pathogenesis. Accordingly, a T_h1 helper T cell response and M1 macrophage activation in response to T_h1 cytokines are important for host resistance to intracellular pathogens such as *Salmonella*. Individuals with congenital or acquired immunodeficiencies resulting in impaired T_h1 immunity, such as HIV/AIDS, are more susceptible to invasive nontyphoidal salmonellosis but not typhoid fever, suggesting that nontyphoidal serovars and *S*. Typhi may differ in their propensity to promote a T_h1 immune response in infected hosts. We have found that *S*. Typhi persists within cultured human THP-1 macrophages, in contrast to the nontyphoidal serovar *S*. Typhimurium, by avoiding *Salmonella*-induced macrophage cell death, an important innate immune defense against intracellular infection. *S*. Typhimurium induces macrophage death via caspase-3 activation as well as by caspase-1/4/5-dependent mechanisms, in a process dependent upon the *Salmonella* pathogenicity island 2 (SPI2) type III secretion system (T3SS) and the ADP-ribosylating toxin SpvB encoded on the *Salmonella* pSLT virulence plasmid. Furthermore, *S*.

Typhi-infected macrophages exhibit reduced activation of the M1 transcription factor STAT1 and secretion of the T_h1 cytokine IL-12 in comparison to *S*. Typhimurium-infected macrophages. A hu-SRC-SCID humanized mouse model mirrors these results, with *S*. Typhi-infected mice displaying significantly lower levels of serum IL-12 and IFN-γ in comparison to *S*. Typhimurium-infected mice. The M1 polarization of human macrophages by *S*. Typhimurium is also SPI2-dependent. However, in contrast to macrophage death, M1 polarization is not dependent on SpvB. Although the specific effector(s) responsible for the observed differences in STAT1 activation have not been identified, intramacrophage *S*. Typhi expresses SPI2 at lower levels relative to *S*. Typhimurium, which may account for the different macrophage responses to these *Salmonella* serovars. Collectively these observations suggest that *S*. Typhi is able to cause persistent infection by avoiding host cell death and the elicitation of M1/T_h1 immune responses related to intramacrophage SPI2 expression.

Introduction

Typhoid fever afflicts more than 20 million people each year resulting in over 200,000 deaths (2). Typhoid fever is a disease characterized by bacterial persistence. Following ingestion of *Salmonella enterica* serovar Typhi (*S*. Typhi), the causative agent of typhoid fever, a prolonged incubation period occurs with symptoms, including high fever, appearing 1-2 weeks after exposure (27). Invasive disease, primarily involving the reticuloendothelial system (27), is a hallmark of typhoid fever. This is in contrast to infection with genetically similar but clinically distinct nontyphoidal serovars such as *Salmonella enterica* serovar Typhimurium (*S*. Typhimurium). Following ingestion of *S.* Typhimurium, infected individuals develop a self-limiting gastroenteritis within 1-2 days. While chronic carriage of *S*. Typhimurium bacteria is rare, approximately 2-10% of typhoid fever patients suffer long-term persistence and fecal shedding of *S*. Typhi from the gallbladder (27, 28, 43).

As *S*. Typhi is an obligate human pathogen, what is known about typhoid fever pathogenesis in humans is largely gleaned from studies of *S*. Typhimurium infection of mice. In immunocompetent humans, *S*. Typhimurium infections cause gastroenteritis, while in mice a typhoid-like, invasive infection occurs (55). However, it is evident from their clinical presentations in humans that *S*. Typhi and *S*. Typhimurium interact differently with the human immune system. Individuals with congenital or acquired immunodeficiencies resulting in impaired T_h1 immunity, such as mutations in the IL-12/23 signaling axis or HIV/AIDS, are more susceptible to invasive nontyphoidal Salmonellosis (iNTS) but not typhoid fever, suggesting that nontyphoidal serovars, like *S*. Typhimurium, and *S*. Typhi may differ in their propensity to initiate a T_h1 immune response in infected hosts (9–11, 116). In addition, *S*. Typhimurium infection of mice cannot recapitulate all aspects of *S*. Typhi infection in humans, as *S*. Typhi possesses unique virulence traits that are absent in *S*. Typhimurium, and vice versa. For example, *S*. Typhi expresses a polysaccharide capsule called Vi, which is absent from *S*. Typhimurium and which masks lipopolysaccharide (LPS) recognition by TLRs to blunt downstream inflammatory cytokine expression (48–50). Conversely, *S*. Typhimurium possesses an ADP-ribosylating toxin called SpvB, which is encoded on the virulence plasmid pSLT and absent from *S*. Typhi, that is important for intracellular *Salmonella* survival and systemic infection of mice (120, 121).

I hypothesize that *S*. Typhi and *S*. Typhimurium interact with and elicit differential immune responses in human macrophages, and that *S*. Typhi avoids and/or dampens immune responses to infection such as M1 macrophage polarization, T_h1 immune responses and macrophage death. Through direct comparison of human macrophage responses to infection with either serovar, we have found that *S*. Typhi is better able to persist in human macrophages compared to *S*. Typhimurium, which may contribute to the ability of *S*. Typhi to cause persistent infection. Persistence in human macrophages correlates with the ability of each serovar to induce macrophage death, with *S*. Typhi inducing less macrophage death than *S*. Typhimurium. Similarly, *S*. Typhi-infected macrophages are less M1-polarized than *S*. Typhimurium-infected

cells, a trend that is mirrored in humanized mice. In addition, the macrophage responses to infection with *S.* Typhi and *S.* Typhimurium correlate with differential intramacrophage expression of virulence genes encoded by SPI2 (*Salmonella* Pathogenicity Island-2) and in the case of *S*. Typhimurium are dependent upon the SPI2 T3SS (Type III Secretion System). These observations suggest *S*. Typhi may have evolved to avoid immune detection during infection, in contrast to *S*. Typhimurium, and that *S*. Typhi may dampen anti-bacterial responses through downregulation of intramacrophage SPI2 expression.

Results

S. Typhi persistence in human macrophages

Typhoid fever is a disease characterized by the sustained survival of *Salmonella* Typhi within host macrophages, an essential aspect of *Salmonella* pathogenesis (64). I therefore compared the ability of *S*. Typhi and *S*. Typhimurium to persist within human macrophages *in vitro*. Phorbol 12-myristate 13-acetate (PMA)-differentiated THP-1 human macrophage-like cells were infected with the human-serum opsonized, stationary-phase *S*. Typhi strain Ty2 or *S*. Typhimurium strain 14028s at a multiplicity of infection (MOI) of ~15. Bacteria were centrifuged onto macrophage monolayers to synchronize infection and internalized for 1 hr. Macrophage monolayers were then washed with medium containing the membrane-impermeant antibiotic gentamicin. Gentamicin was maintained in the medium for the duration of the experiment. At specific timepoints, macrophages were lysed and intracellular colony-forming units (cfu) enumerated. Survival was expressed as the percent intracellular *Salmonella* surviving as compared to 1 hr post-infection (hpi). Both Ty2 and 14028s initially replicated inside human macrophages, but by 48h and 72h, the survival of Ty2 was significantly greater than that of 14028s (Fig. 1). By light microscopy, 14028s-infected macrophages appeared to lose integrity in comparison to Ty2-infected cells, thus I investigated whether differences in macrophage viability

might account for differences in the persistence of *S.* Typhi and *S.* Typhimurium in human macrophages.

Reduced cell death in *S.* Typhi-infected macrophages.

Multiple mechanisms of *Salmonella*-induced macrophage death have been described, including pyroptosis and apoptosis (78, 100). One feature of pyroptotic cell death is the loss of \ membrane integrity followed by leakage of intracellular contents into the supernatant, including the cytoplasmic protein lactate dehydrogenase (LDH) (85). Cleavage of the caspase-3 protease was monitored as a specific indicator of apoptotic cell death (122). Human THP-1 macrophage-like cells were infected as above with *S*. Typhi strain Ty2 or *S*. Typhimurium strain 14028s. At 24 hpi, supernatants from *Salmonella*-infected macrophages were collected and the concentration of LDH quantified (Promega CytoTox96 Cytotoxicity Kit). Macrophage monolayers were then lysed and total protein collected for Western blot analysis of activated caspase-3 levels. The concentration of LDH in the supernatant of 14028s-infected macrophages was higher than from supernatants of Ty2-infected cells (Fig. 2A). LDH release also occurs during necrotic cell death and sometimes during late-stage apoptosis and is not as specific for macrophage pyroptosis as the activation of caspase-1 (78). We therefore employed the caspase-1 inhibitor Z-YVAD-FMK to determine whether *Salmonella*-induced macrophage LDH release is caspase-1 dependent. Human THP-1 macrophage-like cells were pre-treated with 50 μm of the inhibitor for 2 hrs prior to infection, and the inhibitor was maintained throughout infection. At 24 hpi, supernatants from *Salmonella*-infected macrophages were collected, and LDH was quantified. While LDH release from Ty2-infected cells was unchanged in the presence of the caspase-1 inhibitor Z-YVAD-FMK, LDH release from 14028s-infected macrophages was reduced by almost 40%, to levels similar to Ty2-infected cells (Fig. 2A). Similarly, more activated caspase-3 was present in 14028s-infected macrophages than in Ty2-infected cells (Fig. 2B). Taken together, these results indicate that Ty2 is less cytotoxic for human

macrophages than 14028s and that Ty2 elicits less macrophage death than 14028s, including both pyroptosis and apoptosis.

Reduced M1 Polarization in *S.* Typhi-infected Human Macrophages.

Macrophage death is an innate immune response to *Salmonella* infection that releases bacteria from their intracellular niche for killing by neutrophils (81). We hypothesized that *S*. Typhi avoidance of cell death might represent one facet of a coordinated evasion of anti-bacterial host defenses. This is consistent with clinical observations indicating that susceptibility to *S*. Typhi infection does not correlate with impaired M1/T_h1 responses, in contrast to non-typhoidal *Salmonella* infections (Table 1). I hypothesized that *S*. Typhi may inhibit or fail to initiate an M1/T_h1 response in infected hosts, whereas a robust M1/T_h1 response is required for resistance to non-typhoidal Salmonellosis (Table 1). I therefore investigated whether *S*. Typhi-infected human macrophages are less M1-polarized than *S*. Typhimurium-infected cells. Human THP-1 macrophage-like cells were infected as above with *S*. Typhi strain Ty2 or *S*. Typhimurium strain 14028s. At 24 hpi, supernatants from *Salmonella*-infected macrophages were collected and the concentration of the M1 cytokine IL-12 quantified by ELISA. Macrophage monolayers were then lysed and total protein collected for Western blot analysis of phosphorylated (activated) STAT1 (phospho-STAT1), an M1 transcription factor (123). *S*. Typhi Ty2-infected human macrophages were found to contain reduced levels of phospho-STAT1 in comparison to 14028s-infected cells (Fig. 2C). As predicted by differences in STAT1 activation, Ty2-infected human macrophages also secreted less IL-12 than 14028s-infected cells (Fig. 2D), and the quantity of IL-12 secreted by Ty2-infected macrophages was not significantly different from the very low levels of IL-12 produced by uninfected macrophages (Fig. 2D).

I next investigated whether the observations in THP-1 cells were also seen in primary human macrophages. Peripheral mononuclear blood cells (PBMCs) isolated from leukocyte reduction filters were differentiated into macrophages in the presence of 10 ng ml^{-1} human

granulocyte-macrophage colony stimulating factor (hGM-CSF) for 6 d and infected with *S.* Typhi or *S.* Typhimurium under the same experiment conditions used for the THP-1 cells . At 24 hpi, supernatants were collected and the concentration of LDH and IL-12 quantified as previously. Macrophage monolayers were lysed and total protein collected for Western blot analysis of activated caspase-3 and phospho-STAT1 levels. In agreement with the THP-1 infections, Ty2-infected primary human macrophages released less LDH into the supernatant and had reduced activated caspase-3, phospho-STAT1, and IL-12 secretion as compared to 14028s-infected primary human macrophages (Fig. 3A-D), although the difference in LDH release between Ty2- and 14028s-infected cells did not reach statistical significance, possibly as a consequence of variability between cells derived from different human donors.

Reduced T_H1 Polarization in *S.* Typhi-infected Humanized Mice.

I next examined the relevance of these observations in human macrophages to infection in an animal model. This was a challenging proposition, as *S*. Typhi is a human-restricted pathogen that fails to cause disease in normal mice. However, in collaboration with researchers at the University of Massachusetts and Jackson Laboratories, our lab has developed a humanized mouse model of systemic *S*. Typhi infection (124). To create this model, newborn or 21 day-old nonobese diabetic-scid *IL2rγ*^{null} (NOD-*scid IL2rγ*^{null}) mice are irradiated then engrafted with T cell-depleted, CD34$^+$ human umbilical cord hematopoietic stem cells (124–126). Engraftment levels must be confirmed by flow cytometry of peripheral blood to identify human CD45$^+$ (leukocytes), CD3$^+$ (T cells) and CD20$^+$ (B cells) cell subsets. These mice will heretofore be referred to as humanized mice. Humanized mice were infected intraperitoneally (i.p.) with ~6x10^4 cfu of *S*. Typhi Ty2 or ~1x10^3 cfu *S*. Typhimurium 14028s. Uninfected mice received an equal volume of sterile PBS. Inoculua were based on pilot experiments to optimize the infection rate for each group. However since each mouse varies in engraftment level and donor blood cell origin, disease severity and time to death is variable. Infected humanized mice

were sacrificed after becoming moribund or at 7 d post-infection. At the time of sacrifice, peripheral blood, livers and spleens were aseptically harvested. Peripheral blood was immediately frozen and stored at -80°C until assayed for cytokine concentration using an assay that differentiated between human and mouse cytokines. Liver and spleens were homogenized and cfu enumerated. Mice with organ burdens below the limit of detection were excluded from cytokine analysis. *S*. Typhi Ty2-infected humanized mice had nearly 100-fold less circulating human IL-12 than *S*. Typhimurium 14028s-infected humanized mice (Fig. 3E). We also measured the T_h1 cytokine human interferon-γ (IFN-γ). IFN-γ is secreted by T cells that have undergone differentiation to T_h1 cells in response to IL-12 (127). Although the difference in circulating human IFN-γ between Ty2- and 14028s-infected humanized mice did not reach statistical significance, Ty2-infected humanized mice strongly trended towards less circulating human IFN-γ than 14028s-infected humanized mice (Fig. 3E). We also determined the bacterial burden (cfu) of infected mice at the time of sacrifice (Fig. 3F). Taken together these results confirm that *S*. Typhi Ty2 elicits lower levels of pyroptosis, apoptosis and M1 macrophage polarization in THP-1 human macrophage-like cells and primary human macrophages, as well as lower levels of T_h1 cytokine production in humanized mice, consistent with evasion or suppression of host anti-bacterial immune responses.

Genetic Determinants of *Salmonella*-induced Cell Death.

Multiple bacterial and host determinants of *Salmonella*-induced macrophage pyroptosis and apoptosis are known (78). *Salmonella*-induced macrophage pyroptosis is categorized as either rapid (~4 hpi) or delayed (~18-24 hpi) in onset (78). In vitro, rapid onset pyroptosis can be induced by infecting macrophages with bacteria grown to late-logarithmic phase and is dependent upon flagellin and *Salmonella* Pathogenicity Island 1 (SPI1), with the type 3 secretion system (T3SS) proteins PrgJ and PrgI specifically impliclated in inflammasome activation (88, 89, 91). In contrast, delayed onset macrophage pyroptosis is induced when

infecting bacteria are grown to stationary phase and is dependent on *Salmonella* Pathogenicity Island 2 (SPI2) rather than SPI1 (93, 94). I tested the involvement of these determinants in my experimental system. THP-1 human macrophage-like cells were infected as in previous experiments with stationary-phase *S*. Typhi strain Ty2 or *S*. Typhimurium strain 14028s. At 24 hpi macrophage supernatants were collected and LDH release quantified as a measure of macrophage death. Macrophages infected with *S*. Typhimurium 14028s strains lacking the SPI1 T3SS subunit InvA or the flagellar subunits FliC and FljAB exhibited LDH release similar to that of macrophages infected with wild-type *S.* Typhimurium, confirming that SPI1 and flagellin are not required for late 14028s-induced macrophage LDH release (Fig. 4A). In contrast, the loss of SsrB or PhoP, regulators of SPI2 expression, resulted in a significant decrease in LDH release from infected macrophages, demonstrating that 14028s-induced human macrophage cell death is SPI2-dependent (Fig. 4A). *S*. Typhi expresses a polysaccharide capsule called Vi on its surface, which has anti-phagocytic, anti-complement and anti-inflammatory properties (47–50). As Vi is an important typhoid virulence determinant, we investigated whether Vi had an influence on the release of LDH from Ty2-infected human macrophages. However infection of macrophages with a *vexA* mutant of Ty2 (Vi^- phenotype) did not significantly increase levels of macrophage LDH release (Fig. 4A).

Genetic determinants of *Salmonella*-induced macrophage apoptosis are less well characterized than for *Salmonella*-induced pyroptosis. As for delayed *Salmonella*-induced macrophage pyroptosis, SPI2 and its regulators PhoP and OmpR, are required for *Salmonella*-induced macrophage apoptosis (93, 94, 128, 129). To further investigate this question, human THP-1 macrophage-like cells were infected as before with *S*. Typhi Ty2 or *S*. Typhimurium 14028s. At 24 hpi, macrophage monolayers were lysed and total protein collected for Western blot analysis of activated caspase-3 and phospho-STAT1 levels. Macrophages infected with either 14028s *ssrB* or *phoP* mutants had reduced caspase-3 activation and phospho-STAT1 levels as compared to 14028s wt-infected macrophages (Fig. 4B,C). We also tested whether

secretion of T_h1 cytokines in infected humanized mice was dependent upon 14028s SPI2. Humanized mice were infected as before with ~$6x10^4$ cfu of *S*. Typhi Ty2, ~$1x10^3$ cfu *S*. Typhimurium 14028s or ~$1x10^3$ cfu of *S*. Typhimurium 14028s Δ*ssrB*. Uninfected mice received an equal volume of sterile PBS. Serum levels of the human IL-12 in 14028s Δ*ssrB*-infected humanized mice were significantly lower than in 14028s wt-infected humanized mice, similar to *S*. Typhi Ty2-infected humanized mice (Fig. 4D). Although the difference in circulating human IFN-γ between 14028s Δ*ssrB*- and 14028s wt-infected humanized mice did not reach statistical significance, 14028s Δ*ssrB*-infected humanized mice strongly trended towards less circulating human IFN-γ than 14028s wt-infected humanized mice (Fig. 4D). Taken together, these results demonstrate that SPI2, and its regulator PhoP, are required for 14028s-induced pyroptosis, apoptosis, and M1 polarization of human macrophages, as well as for T_h1 cytokine secretion in humanized mice.

We have demonstrated that multiple pathways of *S*. Typhimurium-induced macrophage death as well as M1 macrophage polarization are dependent upon SPI2 (Fig. 4). LDH release, caspase-3 activation and phospho-STAT1 levels in human macrophages infected with 14028s *ssrB* mutants are similar to those observed in *S*. Typhi Ty2-infected cells. This suggested that the differences in macrophage responses to infection with *S*. Typhi or *S*. Typhimurium might relate to serovar-specific variation in SPI2. Extensive genome degradation is a hallmark of host-adapted pathogens such as *S*. Typhi, and *S*. Typhi SPI2 contains a number of pseudogenes in comparison to *S*. Typhimurium (Table 2). I hypothesized that the absence of specific SPI2 effectors in *S*. Typhi might explain serovar-specific differences in intramacrophage persistence, macrophage death and macrophage polarization (Figs. 1, 2). The pSLT virulence plasmid of *S*. Typhimurium, absent in *S*. Typhi, has previously been shown to induce apoptosis in *Salmonella*-infected macrophages (99–101). The ADP-ribosylating toxin and SPI2-translocated effector SpvB is encoded on this plasmid (130). PMA-differentiated THP-1 human macrophage-like cells were infected as before with *S*. Typhi Ty2, *S*. Typhimurium 14028s, or *S.* Typhimurium 14028s

carrying an *spvB* mutation. At 24 hpi macrophage supernatants were collected and LDH release quantified as a measure of macrophage death. Human macrophages infected with 14028s lacking SpvB had no significant change in macrophage LDH release levels as compared to those infected with wt 14028s (Fig. 5A). However, when macrophages were lysed and total protein collected for Western blot analysis of activated caspase-3 and phospho-STAT1 levels, a 14028s *spvB* mutant was found to induce less caspase-3 activation during infection than 14028s wt (Fig. 5B). This result was not entirely surprising given a previous report that apoptosis ofm*S*. Typhimurium-infected primary human macrophages is dependent upon the *spv* regulator SpvR (100). We next investigated the effect of an *spvB* mutation on *S*. Typhimurium intramacrophage persistence. At the timepoints listed in Fig. 5C, macrophages were lysed and intracellular cfu enumerated. Survival is expressed as the percent survival of intracellular *Salmonella* as compared to one hpi. While a, *spvB S.* Typhimurium mutant did not have significantly greater intramacrophage survival at day three as compared to wt 14028s, it did trend towards greater survival (Fig. 5C). A 14028s *ssrB* mutant, lacking SPI2 expression, had greatly increased intramacrophage persistence compared to either the wt or the Δ*spvB* mutant strains of 14028s, indicating that the absence of SpvB does not fully restore 14028s intramacrophage persistence and that additional SPI2-related mechanisms of cell death remain to be characterized (Fig. 5C).

Genetic Determinants of *Salmonella*-induced M1 Polarization of Macrophages.

Finally, the activation of STAT1 was examined in human macrophages infected with a 14028s *spvB* mutant. Human macrophages infected with a 14028s *spvB* mutant had similar levels of phospho-STAT1 as those infected with wild-type *S.* Typhimurium 14028s (Fig. 5D). Collectively these results confirm that *Salmonella*-induced macrophage death influences the persistence of intramacrophage *Salmonella*. We have identified one pro-macrophage death SPI2 effector, SpvB, which both induces apoptosis and impairs *S*. Typhimurium 14028s

intramacrophage persistence (Fig. 5B,C). However, SpvB does not account for the SPI2-dependent differences in LDH release and STAT1 activation observed during human macrophage infection with *S.* Typhi and *S.* Typhimurium (Fig. 5A,D).

Differential STAT1 activation is not attributable to differences in LPS sensing between serovars

Although the *S.* Typhimurium ADP-ribosylating toxin SpvB can account for the different abilities of these *Salmonella* serovars to induce macrophage cell death, it does not explain the differences in STAT1 activation (Fig. 5D). STAT1 is activated in response to IFN-γ or -β stimulation (131). IFN-γ is secreted by differentiated T and NK cells (132), whereas IFN-β is secreted by macrophages in response to TLR4 stimulation by bacterial lipopolysaccharide (LPS) an mediates autocrine STAT1 activation (133, 134). To further investigate the mechanism of STAT1 activation, I first measured the secretion of IFN-β by *S*. Typhi and *S*. Typhimurium-infected human macrophages. PMA-differentiated THP-1 human macrophage-like cells were infected as before with *S*. Typhi Ty2 or *S*. Typhimurium 14028s. At indicated timepoints, macrophage supernatants were collected and IFN-β quantified by ELISA. IFN-β secretion in response to *Salmonella* infection was rapid and robust, but no significant differences at any timepoint were observed between Ty2- and 14028s-infected macrophages (Fig. 6A). This suggested that macrophage TLR4-sensing of *S.* Typhimurium and *S.* Typhi LPS is similar. This conclusion was further supported by infecting THP-1 macrophages with a Vi capsular mutant of Ty2 (Δ*vexA*). Vi is reported to shield *S*. Typhi LPS from TLR4 recognition to reduce inflammatory cytokine stimulation (50, 135). However an *S.* Typhi *vexA* mutation did not restore phospho-STAT1 levels to those of macrophages infected with wt *S.* Typhimurium (Fig. 6B). This indicates that reduced STAT1 activation in *S.* Typhi-infected macrophages is not caused by inhibitory actions of the Vi capsule.

I further determined whether differences in STAT1 phosphorylation were a consequence of pyroptosis. Pyroptotic cell death culminates in the lysis of infected cells and the release of bacteria into the extracellular milieu. Consequently, extracellular bacteria might stimulate TLR4-dependent STAT1 activation in adjacent macrophages. To test this possibility, THP-1 macrophages were pretreated with the pan-caspase inhibitor Z-VAD-FMK, including caspases 1 and 3, for two hours, then infected as above, with Z-VAD-FMK maintained throughout the infection. At 24 hpi macrophage supernatants were collected and LDH release quantified as a measure of macrophage cell death. Addition of the pan-caspase inhibitor Z-VAD-FMK to 14028s-infected macrophages reduced LDH release from cells to a level similar to that measured in Ty2-infected macrophages (Fig. 6C). This effect was specific to caspase inhibition, as the negative control molecule Z-FA-FMK, an inhibitor of non-caspase cysteine proteases, had no effect on LDH release from 14028s-infected macrophages (Fig. 6C). Pan-caspase inhibition of 14028s-infected human macrophages did not significantly change intramacrophage phospho-STAT1 (Fig. 6D). A decrease in phospho-STAT1 levels was observed in infected human macrophages containing the negative control molecule Z-FA-FMK, likely due to a non-specific consequence of cysteine protease inhibition. I conclude that differences in LPS recognition or the amount of macrophage death does not account differential STAT1 activation in human macrophages infected *S.* Typhi and *S.* Typhimurium.

I next investigated whether differences in STAT1 phosphorylation at 24 hpi resulted from the failure of *S*. Typhi-infected macrophages to activate STAT1, or the dephosphorylation of phospho-STAT1. Human THP-1 macrophage-like cells were infected as above with *S*. Typhi Ty2 or *S*. Typhimurium 14028s. At the indicated times macrophage monolayers were lysed and total protein collected for Western blot analysis of phospho-STAT1. At 1 and 6 hpi, phospho-STAT1 levels were similar in Ty2- and 14028s-infected macrophages. However, at later timepoints, differences in phospho-STAT1 levels were evident (Fig. 7A). The activation and deactivation of STAT1 in Ty2-infected macrophages correlated with human IFN-β secretion (Fig.

6A). Having shown that Ty2-infected human macrophages were capable of activating STAT1 to levels similar to that of 14028s-infected cells at initial time points, I tested the ability of Ty2-infected human macrophages to respond to exogenous human IFN-β. In the event that Ty2 infection prevents activation of STAT1, the response of Ty2-infected cells to exogenous IFN-β would be expected to be attenuated. Human THP-1 macrophage-like cells were infected as above but at 18 hpi, exogenous human IFN-β was added and maintained throughout infection. At 24 hpi macrophage monolayers were lysed and total protein collected for Western blot analysis of phospho-STAT1 levels. Ty2-infected human macrophages treated with exogenous IFN-β exhibited reduced phospho-STAT1 levels in comparison to 14028s-infected human macrophages, consistent with the hypothesis that *S.* Typhi blunts the responsiveness of macrophage JAK-STAT signaling pathways (Fig. 7B). Taken together, the observations show that differences in STAT1 activation between Ty2- and 14028s-infected human macrophages cannot be attributed to differential LPS sensing, Vi capsular polysaccharide or pyroptosis (Figs. 6B,D). Rather, *S.* Typhi appears to inhibit JAK-STAT signaling in response to IFN-β, the mechanism of which is an object of ongoing investigation in the lab.

_S_. Typhi Virulence Gene Expression in Human Macrophages.

As my initial studies found that *S.* Typhimurium-induced macrophage pyroptosis, apoptosis, STAT1 activation and T_h1 cytokine secretion are all dependent upon the virulence locus SPI2 (*Salmonella* Pathogenicity Island 2) (Fig. 4), I investigated whether differences in SPI2 between *S.* Typhi and *S.* Typhimurium might be responsible. A preliminary screen (performed with the assistance of Taylor Stepien) in human macrophages infected with *S.* Typhimurium mutants lacking individual SPI2 effectors failed to identify an individual effect required for STAT1 activation. I next measured intramacrophage SPI2 gene expression using a SPI2 expression reporter plasmid from *Ibarra et al.* (136). In this system, the promoter of the SPI2 structural gene *ssaG* drives GFP expression (136). Human THP-1 macrophage-like cells

were infected as above with *S*. Typhi Ty2 or *S*. Typhimurium 14028s carrying the SPI2 reporter plasmid. At 24 hpi, macrophage monolayers were lysed and bacteria separated from macrophage debris by gentle centrifugation. Bacteria were then harvested, fixed and subjected to flow cytometric analysis for GFP expression on a BD FACSCanto II flow cytometer. A pronounced difference in intramacrophage SPI2 expression between *S*. Typhi Ty2 and *S*. Typhimurium 14028s was observed (Fig. 8). Although most intracellular *S.* Typhimurium exhibited high levels of GFP expression, lower levels and a broader distribution of GFP expression was observed in intracellular *S.* Typhi (Fig. 8). In additionally, a larger number of GFP-negative *S.* Typhi-infected macrophages were detected (Fig. 8). These data suggest that differences in intramacrophage SPI2 expression between the *S.* Typhi and *S.* Typhimurium may play an important role in the different host immune responses to these *Salmonella* serovars (Figs. 4,8). Studies in progress to enhance SPI2 expression in *S*. Typhi Ty2 will determine whether macrophage pyroptosis and STAT1 activation are increased as a result.

Discussion

Clinical and epidemiological observations suggest that *S.* Typhi and *S.* Typhimurium have fundamentally different interactions with the human immune system. This study examined the immune response during *S*. Typhi and *S*. Typhimurium infection of human macrophages and humanized mice to test the hypothesis that *S*. Typhi causes persistent infection by evading critical components of the immune response. I found that *S*. Typhi is better able than *S.* Typhimurium to cause persistent infection of human macrophages by avoiding the induction of pyroptosis and apoptosis. Moreover, reduced M1/T_h1 polarization and initiation of T_h1 immune responses were observed in *S*. Typhi-infected human macrophages and humanized mice.

Salmonella gastroenteritis caused by non-typhoidal serovars is an acute self-limited illness, whereas typhoid fever is characterized by bacterial persistence. This is further evidenced by *S*. Typhi's longer incubation period and higher rate of carriage (27, 28). My

research has shown that the same is true for *S*. Typhi and *S.* Typhimurium infection of human macrophage-like cells (Fig. 1). I found that both *S*. Typhi Ty2 and *S*. Typhimurium 14028s are initially able to replicate in THP-1 human macrophage-like cells, but by 48 and 72 hpi, the intramacrophage viability of *S.* Typhi was higher than that of *S.* Typhimurium (Fig. 1). Enhanced persistence of *S*. Typhi in human macrophages may underlie clinical phenomena such as typhoid fever's prolonged incubation period, sustained infection in the host, relapse in convalescent patients and chronic carriage (27). Typhoid fever relapse occurs in ~5-20% of recovering patients and can occur within weeks or months of recovery (137). Few determinants of relapsing typhoid fever are known, although relapse has been demonstrated in a mouse model of persistent infection that *Salmonella* can persist in a mesenteric lymph node reservoir (138). *Salmonella* has also been reported to persist within non-activated monocytes at low levels (138). I have not determined whether the persistent *S*. Typhi that I have observed in cultured human macrophages are metabolically active and replicating.

One mechanism of *S*. Typhi persistence in human macrophages is the avoidance of *Salmonella*-induced macrophage death. *S.* Typhi infection of THP-1 human macrophage-like cells and primary human macrophages elicits less pyroptosis and apoptosis than *S.* Typhimurium (Figs. 2A,B & 3A,B). *S.* Typhimurium-induced pyroptosis and apoptosis is dependent upon the SPI2 T3SS (Fig. 4A,B). The ADP-ribosylating toxin SpvB which is translocated by the SPI2 T3SS (130), has been implicated in *Salmonella*-induced apoptosis. I constructed an isogenic mutation of *spvB* of *S*. Typhimurium 14028s and confirmed that SpvB is required for caspase-3 activation by *S.* Typhimurium in infected human macrophages (Fig. 5B). Importantly, the absence of SpvB allowed *S.* Typhimurium 14028s to persist within human macrophages to an extent similar to *S.* Typhi (Fig. 5C). Interestingly, SpvB is commonly found in gastroenteritis-causing *Salmonella* serovars such as *S.* Typhimurium and *S.* Enteritidis, which rarely cause systemic disease in immunocompetent humans (139), whereas the enteric fever

serovars *S.* Typhi, *S.* Paratyphi A and *S.* Paratyphi B all lack SpvB in their genome, consistent with the idea that the avoidance of apoptosis is required for persistent infection (139).

Although the absence of SpvB in *S.* Typhimurium abrogated caspase-3 activation during infection of human macrophages, it did not influence *Salmonella*-induced pyroptosis or STAT1 activation (Fig 5A,D). The possibility that differential STAT1 activation might result from differences in LPS activation was assessed. Macrophages secrete IFN-β in response to TLR4 activation by bacterial LPS (131, 133, 134). Autocrine responses to IFN-β result in STAT1 activation by the JAK1 kinase (131). I hypothesized that *S.* Typhi might exhibit reduced TLR4 activation due to inhibitory actions of the Vi polysaccharide capsule (12). However, no differences in IFN-β secretion by *S.* Typhi- or *S.* Typhimurium-infected human macrophages were observed (Fig. 6A). Furthermore, , a Vi^- mutation in *S.* Typhi failed to restore phospho-STAT1 activation at 24 hpi (Fig. 6B). Inhibition of cell death with a pan-caspase inhibitor failed to inhibit STAT1 activation by *S.* Typhimurium at 24 hpi, indicating that increased extracellular LPS release from dying macrophages did not account for sustained STAT1 activation in *S.* Typhimurium-infected human macrophages (Fig. 6C,D). Knowing that *Salmonella*-induced cell death, STAT1 activation and the downstream activation of T_h1 immune responses are all dependent on the SPI2 virulence genes, I next investigated whether differences in SPI2 effectors or expression could account for the observed differences in the macrophage immune response to *S.* Typhi and *S.* Typhimurium.

After performing a preliminary screen in human macrophages infected with *S.* Typhimurium mutants lacking individual SPI2 effector proteins and failing to identify a specific effector that was responsible for differences in STAT1 activation, I determined that intramacrophage expression of the SPI2 structural gene *ssaG* was significantly lower in *S.* Typhi than *S.* Typhimurium (Fig. 8). The acquisition of SPI2 was a critical evolutionary event for the ability of *Salmonella* to survive intracellularly and cause invasive infections (Hensel, 2000). Early studies of the systemic virulence of *S*. Typhimurium in mice identified SPI2 as essential for

macrophage and systemic replication (66). However, SPI2 is not required for the persistence of *S*. Typhi or *S*. Typhimurium in human macrophages (Fig. 5C) (67). In fact, SPI2 mutants are better able than wild-type *S.* Typhimurium to survive in human macrophages when assayed at late timepoints (Fig. 5C). The importance of SPI2 for *Salmonella* intracellular and systemic replication appears to depend on the host cell type and time interval. Levels of SPI2 expression are also important, as SPI2 dysregulation can impair *S.* Typhimurium replication and virulence even in murine cells (140). A nucleoid-associated protein called YdgT has been identified as a negative regulator of SPI2 that is thought to optimize expression levels (140). I hypothesize that *S*. Typhi has evolved mechanisms to reduce SPI2 expression levels in order to minimize the stimulation of host immune responses, whereas *S*. Typhimurium expresses SPI2 at higher levels and exploits host inflammation (Geddes, 2010; Rivera-Chavez, 2015).

It must be acknowledged that a role for differences in the complement of SPI2 effectors of *S.* Typhi and *S.* Typhimurium has not been excluded. A number of *S.* Typhimurium SPI2 effectors are absent or present only as pseudogenes in *S.* Typhi (Table 2), and it is also possible that differences in the expression or activity of other factors is contributory. For example, SseL is a SPI2-translocated effector, present in both *S*. Typhi and *S*. Typhimurium, that has been suggested to promote macrophage death and inflammation in mice (141, 142), and PhoP, a regulator of SPI2 expression, can directly activate *sseL* (143). In fact our laboratory has preliminary evidence indicating that PhoP-dependent gene expression is reduced in *S*. Typhi relative to *S*. Typhimurium under *in vitro* conditions (S. Libby, unpublished data). Additional SPI2 effector candidates include PipB, a proinflammatory SPI2 effector (144) and SptP, a SPI2 effector with homology to the *Yersinia* cytotoxin YopE (145). Both PipB and SptB are present in *S*. Typhi and *S*. Typhimurium.

This study is novel in its use of humanized mice to examine *S*. Typhi avoidance of T_h1 immune responses to infection. I have demonstrated that humanized mice infected with *S*. Typhi have significantly lower serum levels of human IL-12 than humanized mice infected with *S*.

Typhimurium 14028s (Fig. 3E). Of note, *S*. Typhimurium-elicited T_h1 cytokine responses in this model are dependent upon SPI2 (Fig. 4D). A caveat with regard to these data is that organ burdens (cfu) between different infection groups were different and might influence serum cytokine levels. At later time points, organ burdens were more similar (Fig. 9B), with IL-12 levels trending higher ($p = 0.11$) in the *S.* Typhimurium 14028s-infected mice than *S*. Typhi Ty2-infected mice (Fig. 9A).

This work has important implications for understanding the pathogenesis of typhoid fever and developing new strategies for the prevention and treatment of *Salmonella* infections. The observations underscore the importance of studying pathogens in their native hosts and host cells whenever possible. While mouse models have proven to be an invaluable resource for understanding *Salmonella* pathogenesis, ordinary laboratory mice cannot recapitulate the aspects of *S*. Typhi infection that are unique to humans. Infection studies in human cells and humanized systems will continue to complement murine Salmonellosis models in the future. The evasion of T_h1 immune responses by *S.* Typhi explain the longstanding observation that only non-typhoidal *Salmonella* serovars cause opportunistic infections in patients with HIV infection and suggest that *S*. Typhi vaccines may require specific strategies to augment cellular immune responses. The importance of STAT1 for MHC class I expression (Zhou, 2009) suggests that antigen presentation may also be inhibited by *S.* Typhi, as has been demonstrated during *S*. Typhimurium infection of murine dendritic cells (146). Like *S.* Typhi itself, further elucidation of the mechanisms of evasion of host immunity during typhoid fever will require both persistence and ingenuity.

Materials and Methods

Bacterial genetic manipulations, growth conditions and chemicals

Unless otherwise stated, chemicals were purchased from Sigma-Aldrich (St. Louis, MO) or Fisher Scientific (Waltham, MA). The λ-red recombinase system was used to construct

Salmonella mutants (147). PCR was performed with primers containing ~40 bp of homology to the 5' or 3' end of the gene of interest and ~20 bp of homology to the kanamycin-resistance gene of pKD4 or pKD13. Mutant construction was confirmed by PCR. Strains were cultured in Luria-Bertani (LB) media for 18 hrs with shaking at 250 rpm at 37°C. Kanamycin and carbenicillin were supplemented in the appropriate cultures at 50 μg ml^{-1}.

Animals

All animal experiments were approved by the University of Washington Institutional Animal Care and Use Committee in accordance with guidelines regarding animal welfare.

***Salmonella* intramacrophage survival assay**

Prior to infection, human THP-1 monocytes were differentiated into macrophage-like cells with 100 nm of phorbol 12-myristate 13-acetate (PMA) for 48 hrs. PMA-free medium was added to macrophages 24 hrs prior to infection. Human peripheral blood mononuclear cells (PBMCs) were harvested from leukocyte reduction filters (Bloodworks Northwest) and differentiated in 10 ng ml^{-1} human granulocyte-macrophage colony stimulating factor (GM-CSF) for 6 d. GM-CSF-free media was added to macrophages 24 hrs prior to infection. *Salmonella* strains were grown in LB broth (Fisher Scientific) for 18 hrs with shaking at 37°C. *Salmonella* cultures were adjusted to OD_{600} 1.0 and washed twice with sterile PBS (Cellgro). Equal parts *Salmonella* and 100% AB human serum (Cellgro) were mixed and incubated at 37°C in 5% CO_2 for 20 min to opsonize bacteria. Opsonized bacteria were then used to infect $3x10^5$ THP-1 human macrophage-like cells/well or human peripheral blood mononuclear cells/well (24-well plate) at a MOI of ~15. Infected monolayers were centrifuged for 5 min at 1000 rpm to synchronize infection then incubated at 37°C for 1 hr to promote internalization. Following internalization, monolayers were washed with RPMI supplemented with 20 μg ml^{-1} gentamicin to

kill extracellular bacteria. At the times listed, medium was removed from wells and macrophages lysed with 1% Triton X-100 to enumerate intramacrophage bacteria.

***Salmonella*-induced human macrophage cytotoxicity assay**

The concentration of lactate dehydrogenase in the supernatant of infected human macrophages was assayed using the CytoTox96 Cytotoxicity Kit per the manufacturer's protocol (Promega). Percent cytotoxicity was calculated as follows: ((Experimental release-Spontaneous release)/(Maximum release-Spontaneous release)) x 100. For caspase inhibitor assays, the inhibitors Z-YVAD-FMK (R&D Systems) and Z-VAD-FMK (BD Biosciences) were added to medium 2 hrs prior to infection at 50 and 20 μm, respectively, and maintained throughout the infection. The negative control molecule Z-FA-FMK (BD Biosciences) was used at the same concentration used for its respective caspase inhibitor.

Humanized mouse infections

Humanized mice susceptible to *S*. Typhi infection were constructed as previously described (124). Briefly, NOD-SCID IL2rγ null mice engrafted with human umbilical cord stem cells were infected with ~$6x10^4$ cfu of *S*. Typhi Ty2 Nal^R, ~$1x10^3$ cfu *S*. Typhimurium 14028s wt or ~$1x10^3$ cfu of *S*. Typhimurium 14028s Δ*ssrB*. Infection inoculua were chosen to obtain similar duration of infection in humanized mice. Humanized mice were sacrificed upon becoming moribund or at 7 d post-infection, whichever occurred first. Upon sacrifice, intracardiac blood was harvested then centrifuged in BD Microtainer tubes with serum separator additive for 5 min at 15000 rpm. Serum was removed, transferred to a new tube, then stored at -80°C until analysis. Serum cytokines were measured with a cytokine bead array (Becton Dickinson) followed by analysis on a LSRII flow cytometer (Becton Dickinson) or on a multiplex microbead cytokine array with analysis on a Luminex 200 (Luminex). Mice with no detectable organ burden were excluded from cytokine analysis. The spleen and liver from each mouse were aseptically

removed, weighed, then homogenized in 1 ml sterile PBS using a Power Gen 125 tissue homogenizer (Fisher Scientific). Homogenates were serially diluted in sterile PBS, plated on LB agar plates and incubated overnight at 37°C. Cfu/gram tissue were enumerated.

Cell culture

Human THP-1 monocytes were obtained from the American Type Culture Collection (ATCC). THP-1 cells were cultured in RPMI 1640 1X (Mediatech, Manassas, VA) supplemented with 10% heat-inactivated fetal bovine serum (Cellgro). THP-1 cells were propagated according to ATCC recommendations at 37°C in 5% CO_2.

Human peripheral blood mononuclear cell harvest

One-day-old leukocyte reduction filters (LRFs) were purchased from Bloodworks Northwest (Seattle, WA). Each LRF was backflushed with 100 ml sterile PBS (Cellgro). Eluate was overlaid on Ficoll-Paque PLUS (GE Healthcare) and centrifuged at room temp for 35 min at 2000 rpm (brake off). Following gradient separation, the monocyte-containing layer was removed and washed twice in sterile PBS. Cells were suspended in a solution of RPMI 1640 1X containing human granulocyte macrophage colony stimulating factor (GMCSF, Peprotech) at a concentration of 10 ng ml^{-1} and filtered using a 70 μm nylon mesh sterile cell strainer (Fisherbrand) to remove coagulated material. Cells were incubated in untreated tissue culture flasks for 48 hrs. Adherent cells were scraped and seeded into tissue culture wells where they were allowed to adhere for 5 more d. GMCSF-free media was added to cells 24 hrs prior to infection.

Immunoblotting

Infected human macrophages were lysed in 1X RIPA buffer (Cell Signaling Technology) with added 1X phosphatase and protease inhibitors (Cell Signaling Technology). Total protein

lysates were frozen at -20°C until assayed. Total protein was quantified using the BCA protein assay kit (Pierce). Fifty µg total protein was combined with SDS loading dye and incubated for 5 min at ~95°C. Denatured total protein was loaded into a 4-15% SDS polyacrylamide gel (Bio-rad) and electrophoresed with 150 volts for 45 min. Proteins were wet-transferred onto a Immobilon-P Polyvinylidene fluoride (PVDF) membrane (Millipore) with 120 milliamps for 42 min. Protein-containing membranes were blocked in 5% bovine serum albumin (RPI Corp.) for 30 min. Membranes were then incubated with rabbit anti-human caspase-3 or rabbit anti-human phospho-STAT1 (Tyr701) antibodies (Cell Signaling Technology) at a 1:500 or 1:1000 dilution, respectively, overnight at 4°C with gentle rocking. Membranes were washed three times for 5 min each in 1X Tris-buffered saline with 0.05% Tween (TBST). Membranes were then incubated in goat, anti-rabbit IgG HRP-linked secondary antibody (Cell Signaling Technology) at a 1:1000 or 1:2000 dilution for caspase-3 and phospho-STAT1, respectively, for 30 min at 25°C with rocking. Membranes were washed three times for 5 min each in 1X TBST. Chemiluminescent substrate (ECL western blotting substrate, Thermo Scientific) was applied to the membrane and immediately exposed to CL-X Posure film (Thermo Scientific). Film was developed using an AFP Imageworks MM90. Membranes were subsequently stripped and reprobed with rabbit anti-human β-actin antibody (Cell Signaling Technology) at a 1:1000 dilution to confirm equal loading. All washes, secondary antibody incubations and developing were as above.

Measurement of secreted cytokines from macrophages

Supernatants were collected from infected human macrophages and stored at -20°C until assayed for human interferon-β or IL-12p70. Human IL-12p40 was assayed on fresh material. Human interferon-β (PBL Assay Science Verikine ELISA), IL-12p70 and IL-12p40 (R&D systems Quantikine ELISA) were assayed by ELISA per the manufacturer's protocol.

Interferon-β macrophage stimulation assay

Exogenous human interferon-β (Peprotech) was added to infected human THP-1 macrophage-like cells at a final concentration of 10 ng ml^{-1} at 18 hrs post-infection. Exogenous human interferon-β remained in the medium until the end of infection.

Intramacrophage bacterial SPI2 expression assay

Bacterial cultures were grown with carbenicillin overnight and used to infect human macrophages as described previously. Infected macrophages were lysed in 1% Triton. Lysates were gently centrifuged at 2500 rcf for 5 min. The supernatants were removed and bacteria pelleted by centrifugation at 15000 rpm for 5 min. Bacterial pellets were resuspended in freshly-made 2.5% paraformaldehyde and fixed for 10 min at 37°C. Fixed bacteria were washed once in PBS then analyzed for GFP expression using a BD FACSCanto II flow cytometer.

Acknowledgments

We thank Michael Brehm and Dale Greiner (University of Massachusetts) and Leonard Schultz (Jackson Laboratories) for providing us with humanized mice. We thank Olivia Steele-Mortimer (NIH Rocky Mountain Laboratories) for providing us with the pMPMA3 ΔP_{lac} P_{ssaG} GFP and pMPMA3 ΔP_{lac} null GFP expression plasmids.

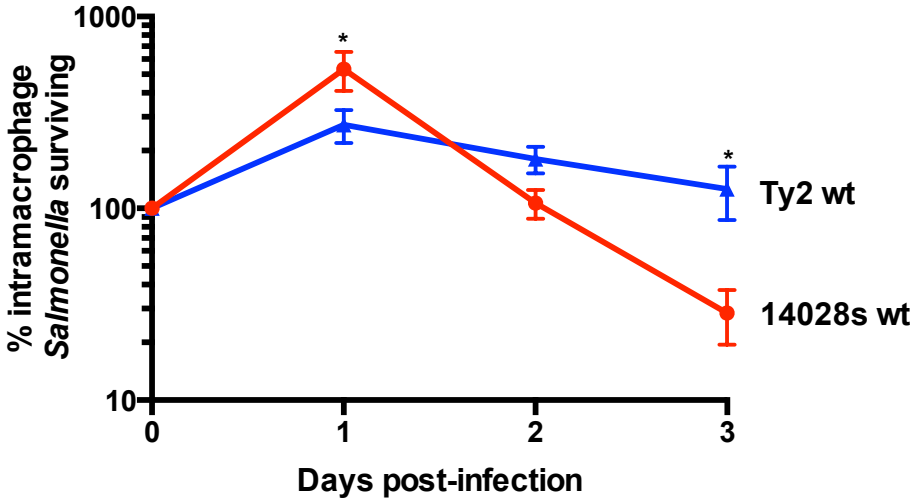

Figure 1. *Salmonella* persistence in a human macrophage cell line. Differentiated human THP-1 macrophage-like cells were infected with opsonized stationary-phase *S*. Typhi Ty2 or *S*. Typhimurium 14028 at an MOI of ~15. At designated timepoints, macrophages were lysed and intracellular bacteria enumerated. *Salmonella* survival is expressed as the proportion of internalized bacteria at 1 h post-infection. Statistical significance was determined using a RM one-way ANOVA and is indicated as * $P < 0.05$.

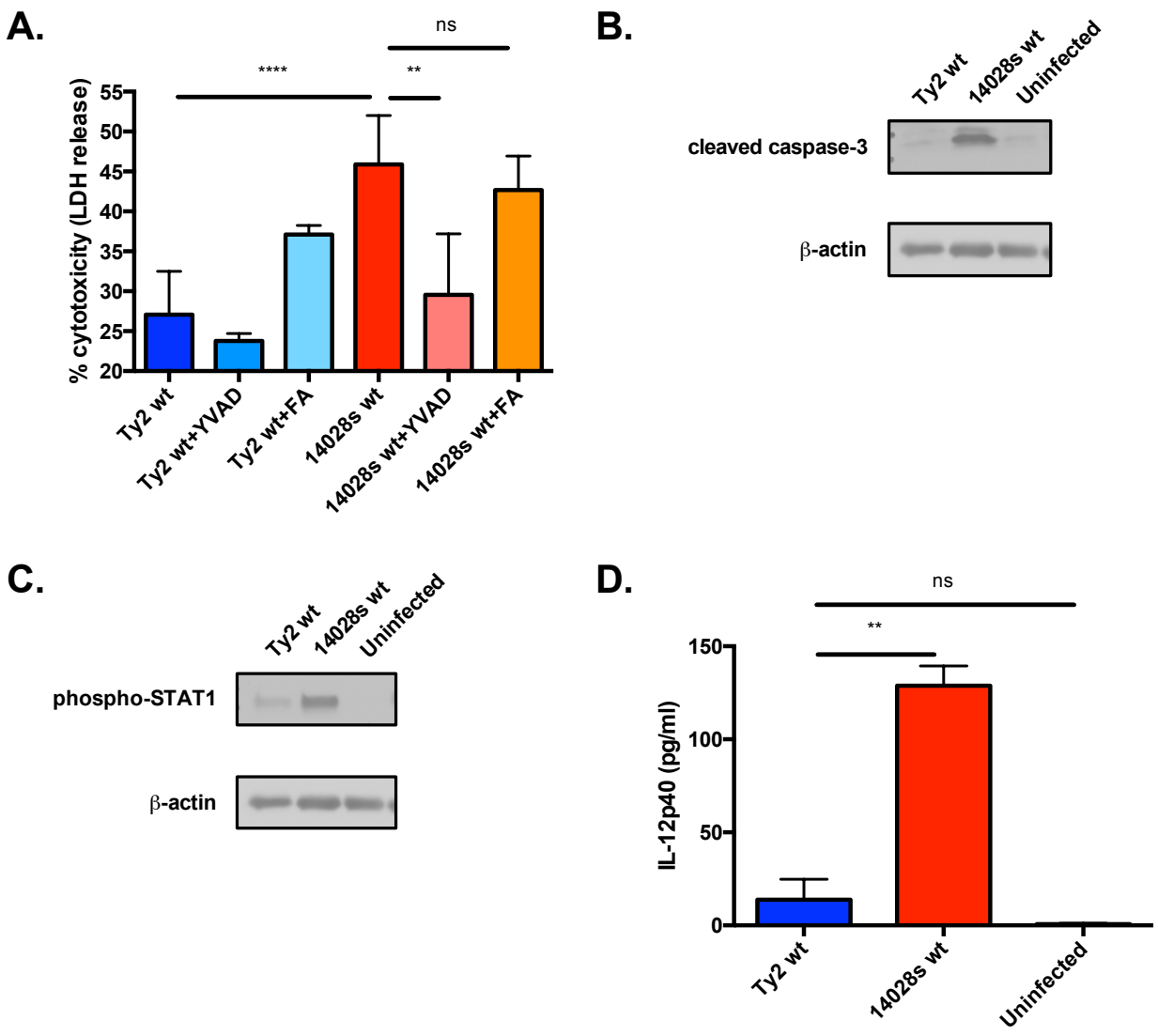

Figure 2. Innate immune responses of a human macrophage cell line to *Salmonella*. Differentiated human THP-1 macrophage-like cells were infected with opsonized stationary-phase *S*. Typhi Ty2 or *S*. Typhimurium 14028 at an MOI of ~15. (A) Fifty μM of the caspase-1, 4, and 5 inhibitor Z-YVAD-FMK or the non-specific control molecule Z-FA-FMK were administered to differentiated THP-1 cells beginning 2h prior to infection. Supernatants were collected 24h post-infection and LDH quantified as a measure of macrophage cell death. (B) Fifty μg of total protein from macrophages 24h post-infection were subjected to Western blot analysis for activated Caspase-3, an executioner caspase of apoptosis. β-actin was included as

a loading control. (C) Fifty μg of total protein from macrophages 24h post-infection were subjected to Western analysis for phosphorylated STAT1, an M1 transcription factor. β-actin was included as a loading control. D) Supernatants from macrophages 24h post-infection were assayed for human IL-12p40, a T_h1 cytokine. Statistical significance was determined using a Ordinary one-way ANOVA and is indicated as ** $P < 0.01$; **** $P < 0.0001$

	Increased susceptibility to	
Congenital/Acquired Immune Defect	**Invasive non-typhoidal Salmonellosis (iNTS)?**	**Typhoid fever?**
NADPH phagocyte oxidase/respiratory burst (e.g. chronic granulomatous disease)	yes	no
IL-12 and IFN-γ signaling	yes	no
$CD4^+$ T-cells (e.g. HIV/AIDS)	yes	no

Table 1. Immune defects causing increased susceptibility to invasive Salmonellosis. Multiple congenital or acquired immune defects predispose individuals to invasive nontyphoidal Salmonellosis but not typhoid fever.

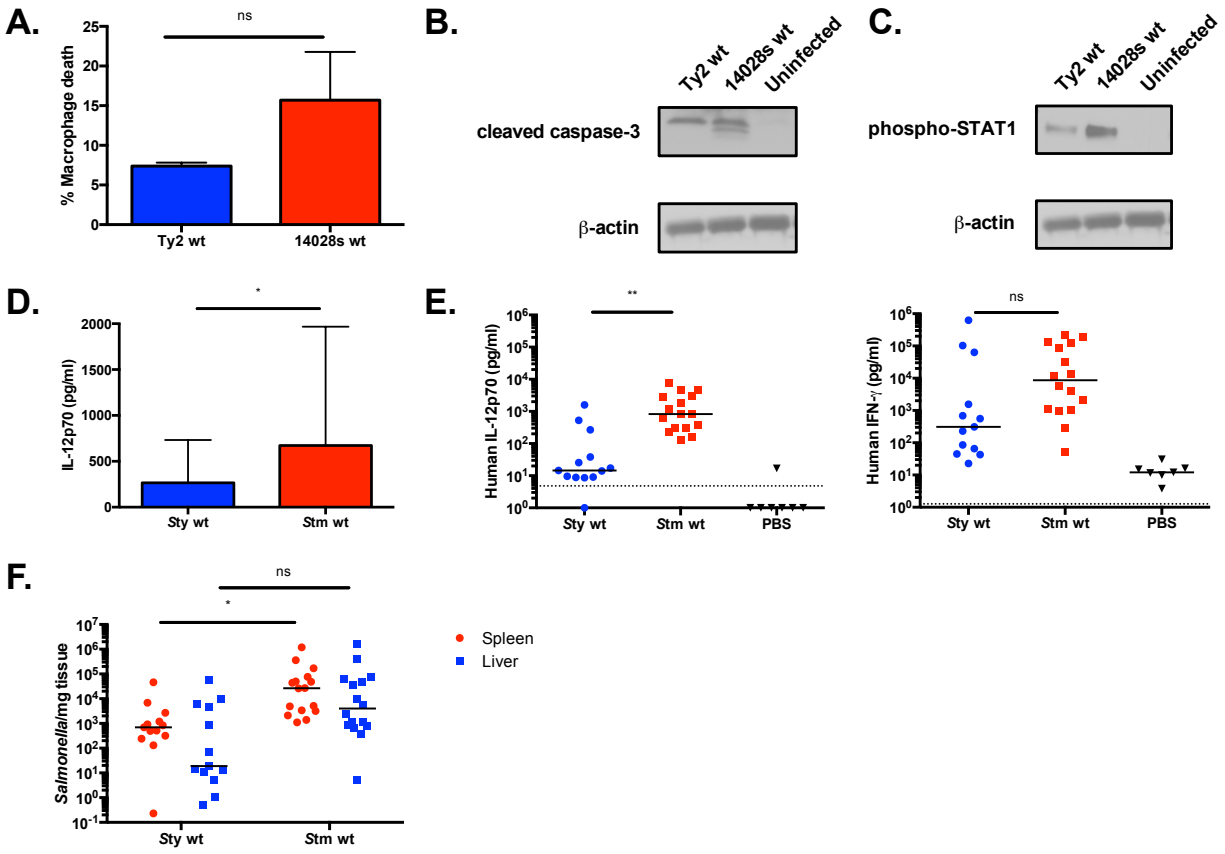

Figure 3: **Immune responses of primary human macrophages and humanized mice to *Salmonella* infection.** (A-D) Whole-blood was recovered from leukocyte reduction filters ~24h post-collection from human volunteers. Peripheral blood mononuclear cells (PBMCs) were isolated from PBS-diluted whole blood following Ficoll gradient separation. After washing, PBMCs were incubated in the presence of human GM-CSF for 7d prior to *Salmonella* infection. Infection of PBMCs was identical to that of THP-1 human macrophage-like cells in Figure 2. (A) Supernatants were collected 24h post-infection and LDH quantified as a measure of macrophage cell death. (B) Fifty µg of total protein from PBMCs 24h post-infection were subjected to Western analysis for the presence of activated caspase-3. (C) Fifty µg of total protein from PBMCs 24h post-infection were subjected to Western analysis for the presence of phosphorylated STAT1. (D) 24h post-infection, culture supernatants were assayed for the presence of IL-12p70 by ELISA. (E,F) Humanized NOD-SCID IL2rγ null mice engrafted with

human umbilical cord stem cells were infected with ~$6x10^4$ cfu wild-type *S*. Typhi or ~$1x10^3$ cfu wild-type *S*. Typhimurium. Humanized mice were sacrificed when moribund or 7d post-infection, whichever came first. (E) Serum human IL-12p70 and IFN-γ were measured by cytokine bead array (Becton Dickinson) or multiplex microbead cytokine array (Luminex). Dotted line indicates assay limit of detection. (F) Spleens and livers were aseptically harvested from infected humanized mice and homogenized for enumeration of cfu. Mice without detectable organ burdens were excluded from analysis. Each symbol represents one mouse with the horizontal lines representing the median. Statistical significance for PBMC LDH release data was determined using a ordinary one-way ANOVA. Statistical significance for PBMC IL-12p70 data was determined using a ratio paired t-test. Statistical significance for humanized mouse data was determined using a Kruskal-Wallis test. Statistical significance is indicated as * $P < 0.05$; ** $P < 0.01$.

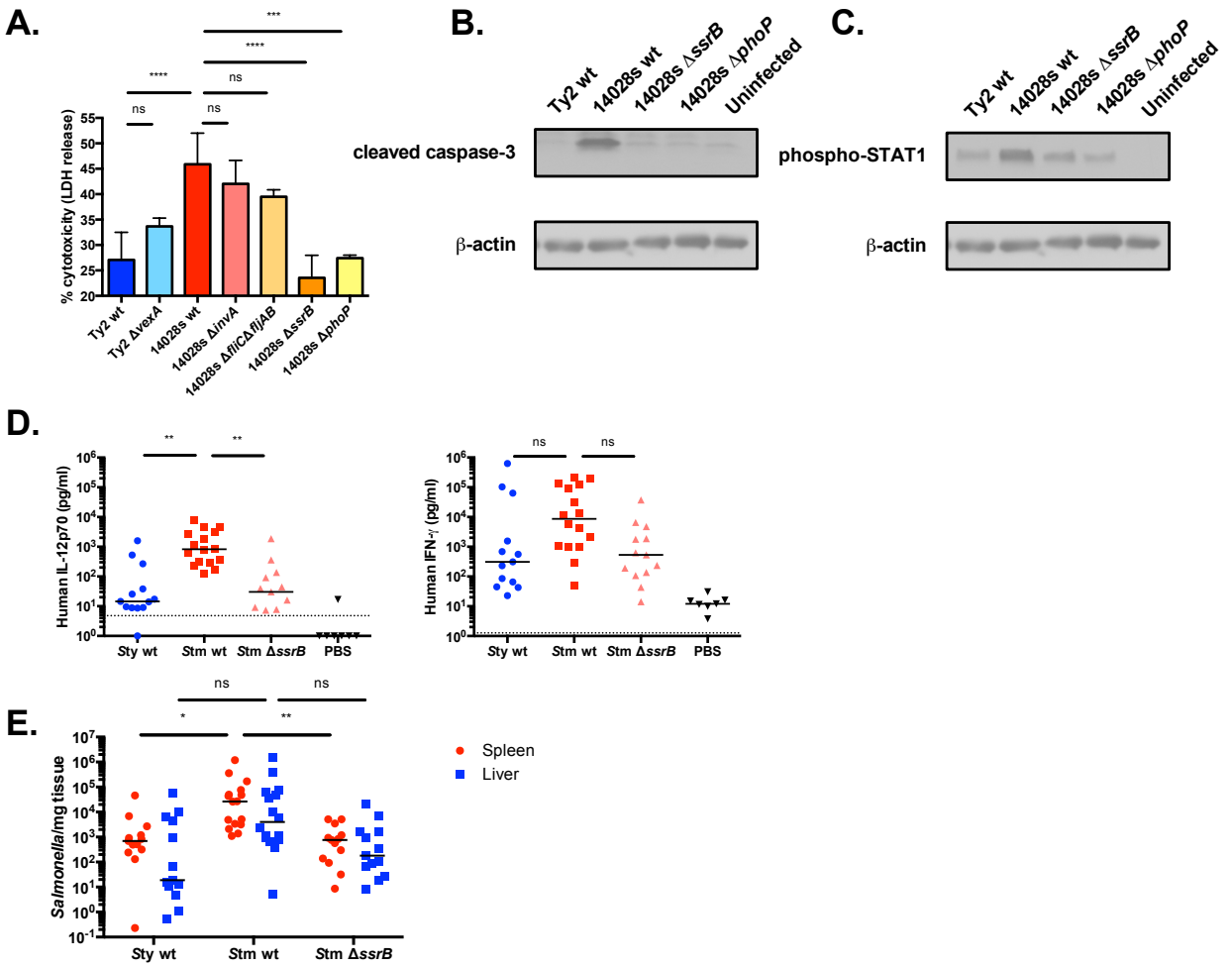

Figure 4: **Innate immune responses of a human macrophage cell line to wild-type and mutant *Salmonella* strains.** (A-C) Differentiated human THP-1 macrophage-like cells were infected with opsonized stationary-phase *Salmonella* at an MOI of ~15. Mutant bacterial strains included *S*. Typhi *vexA* lacking the Vi polysaccharide capsule, *S*. Typhimurium *invA* lacking a functional SPI1 T3SS (type III secretion system), *S*. Typhimurium *fliC fljAB* lacking flagellin, *S*. Typhimurium *ssrB* lacking the SPI2 T3SS regulator SsrB, and *S*. Typhimurium *phoP* lacking the transcriptional regulator PhoP. (A) Lactate dehydrogenase (LDH) was quantified in supernatants 24h post-infection as a measure of macrophage cell death. (B) Fifty µg of total protein from macrophages 24h post-infection were subjected to Western blot analysis of activated Caspase-3. β-actin was included as a loading control. (C) Fifty µg of total protein from

macrophages 24h post-infection were subjected to Western blot analysis of phosphorylated STAT1. β-actin was included as a loading control. *S.* Typhimurium-induced caspase-3 activation, THP-1 cell death and STAT1 activation are dependent on SPI2 and PhoP. (D,E) Humanized NOD-SCID IL2rγ null mice engrafted with human cord blood hematopoietic stem cells were infected with ~$6x10^4$ cfu wild-type *S*. Typhi, ~$1x10^3$ cfu wild-type *S*. Typhimurium or ~$1x10^3$ cfu of *S*. Typhimurium 14028s Δ*ssrB*. Humanized mice were sacrificed when moribund or 7d post-infection, whichever came first. (D) Serum human IL-12p70 and IFN-γ were measured by cytokine bead array (Becton Dickinson) or multiplex microbead cytokine array (Luminex). Dotted line indicates assay limit of detection. (E) Spleens and livers were aseptically harvested from infected humanized mice and homogenized for enumeration of cfu. Mice without detectable organ burdens were excluded from analysis. Each symbol represents one mouse with horizontal lines representing the median *Salmonella* organ burden for each group. Statistical significance for THP-1 data was determined using ordinary one-way ANOVA. Statistical significance for humanized mouse data was determined using a Kruskal-Wallis test. Statistical significance is indicated as * $P < 0.05$; ** $P < 0.01$; ***<0.001; **** $P < 0.0001$.

SPI-2 effector	+/- in *S.* Typhi
gogB	-
cigR	pseudogene
gtgA	-
pipB	+
pipB2	+
sifA	+
sifB	+
sopD2	pseudogene
spiC/ssaB	+
spvB	-
spvC	-
spvD	-
srfJ	-
sseF	+
sseG	+
sseI/srfH	-
sseJ	pseudogene
sseK1	-
sseK2	-
sseK3	-
sseL	+
sspH2	+
steC	+
steD	+
steE	-
gtgE	-
avrA	-
slrP	pseudogene
sptP	+
sspH1	-
steA	+
steB	-

Table 2. *Salmonella* Pathogenicity Island-2 (SPI2) effectors. Multiple *S.* Typhimurium SPI2 effectors are absent or present only as pseudogenes in *S.* Typhi. Each effector listed has a Ty2 gene number designation and a published demonstration of translocation by the SPI2 T3SS.

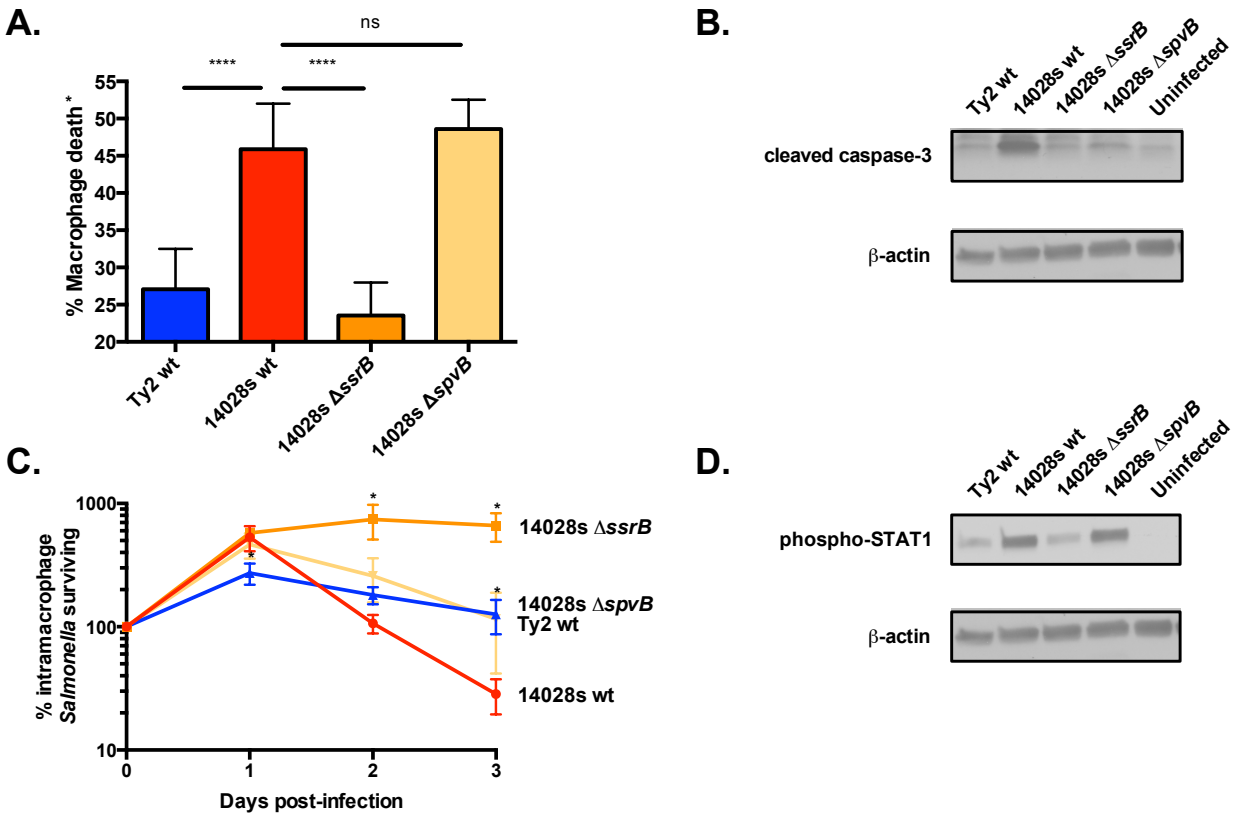

Figure 5. **Determinants of wild-type and mutant *Salmonella*-induced cell death or persistence in human macrophages.** Differentiated human THP-1 macrophage-like cells were infected with opsonized stationary-phase *Salmonella* at an MOI of ~15. Mutant bacterial strains included *S*. Typhimurium *spvB* lacking the SPI2-translocated ADP-ribosylating toxin SpvB and *S*. Typhimurium *ssrB* mutant lacking the SsrB regulator of the SPI2 T3SS. (A) Lactate dehydrogenase (LDH) was quantified in supernatants 24h post-infection as a measure of macrophage cell death. (B) Fifty µg of total protein from macrophages 24h post-infection were subjected to Western blot analysis of activated Caspase-3. β-actin was included as a loading control. (C) At designated timepoints, macrophages were lysed and intracellular bacteria enumerated. *Salmonella* survival is expressed as the proportion of internalized bacteria at 1h post-infection. (D) Fifty µg of total protein from macrophages 24h post-infection were subjected to Western blot analysis of phosphorylated STAT1. β-actin was included as a loading control. *S.* Typhimurium-induced cell death under these conditions is dependent on SPI2 but not SpvB.

Caspase-3 activation correlates with the failure of *S.* Typhimurium to persist in THP-1 cells and is dependent on SPI2 and partially dependent on SpvB. *S.* Typhimurium-induced STAT1 activation is not dependent on SpvB. Statistical significance was determined using a ordinary one-way ANOVA (A) and RM one-way ANOVA (C) and is indicated as * $P < 0.05$; ** $P < 0.01$; *** $P < 0.001$; **** $P < 0.0001$.

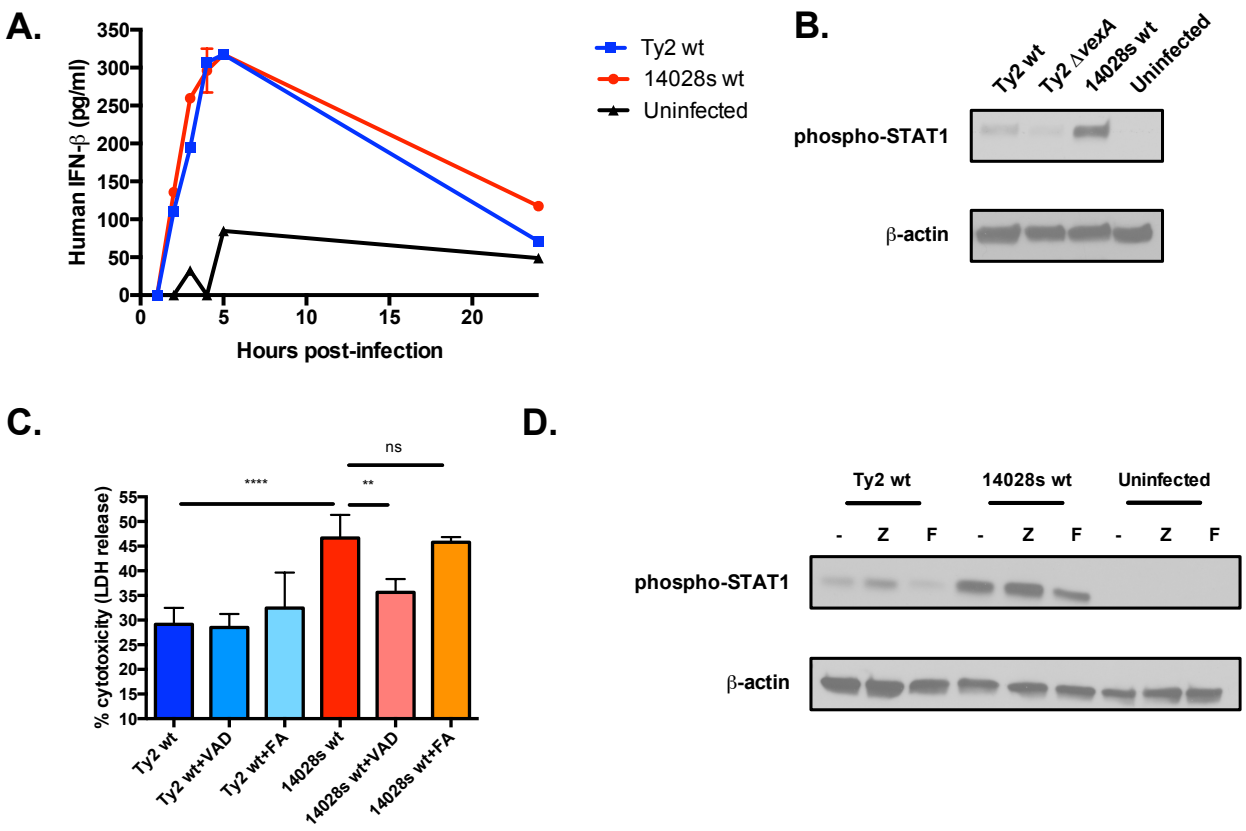

Figure 6. Determinants of innate immune activation in a human macrophage cell line infected with *Salmonella.* Differentiated human THP-1 macrophage-like cells were infected with opsonized stationary-phase *Salmonella* at an MOI of ~15. (A) At designated timepoints, culture supernatants were assayed for the presence of human interferon-β by ELISA. (B) Fifty µg of total protein from macrophages 24h post-infection were subjected to Western blot analysis of phosphorylated STAT1. β-actin was included as a loading control. *S.* Typhi *vexA* mutant lacks the Vi polysaccharide capsule. (C-D) THP-1 cells were treated with 20 µm of the pan-caspase inhibitor Z-VAD-FMK or the non-specific control molecule Z-FA-FMK beginning 2h prior to infection. (C) Lactate dehydrogenase (LDH) was quantified in supernatants 24h post-infection as a measure of macrophage cell death. (D) Fifty µg of total protein from macrophages 24h post-infection were subjected to Western blot analysis of phosphorylated STAT1. β-actin was

included as a loading control. Statistical significance was determined using a ordinary one-way ANOVA and is indicated as ** $P < 0.01$; **** $P < 0.0001$.

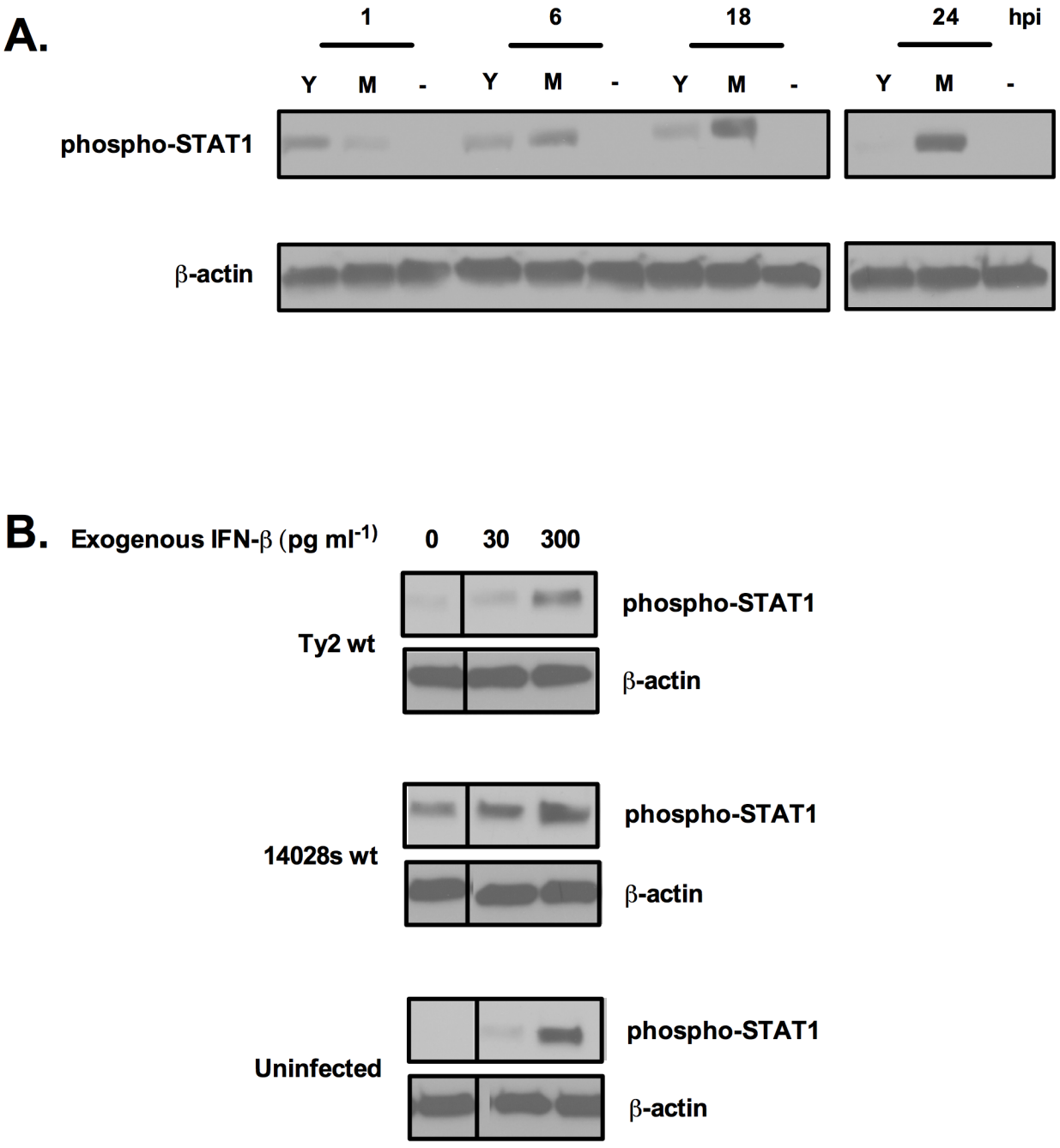

Figure 7. STAT1 activation over time in a human macrophage cell line infected with *Salmonella.* (A) Differentiated human THP-1 macrophage-like cells were infected with opsonized stationary-phase *Salmonella* at an MOI of ~15. Fifty µg of total protein from macrophages at designated time intervals were subjected to Western analysis for phosphorylated STAT1. Y = *S*. Typhi Ty2, M = *S*. Typhimurium 14028s, - = Uninfected. β-actin

was included as a loading control. (B) Thirty-to-three hundred pg ml^{-1} of human interferon-β were administered to differentiated THP-1 cells 18h post-infection to stimulate STAT1 phosphorylation. Fifty μg of total protein from macrophages at 48h post-infection were subjected to Western analysis for phosphorylated STAT1. β-actin was included as a loading control.

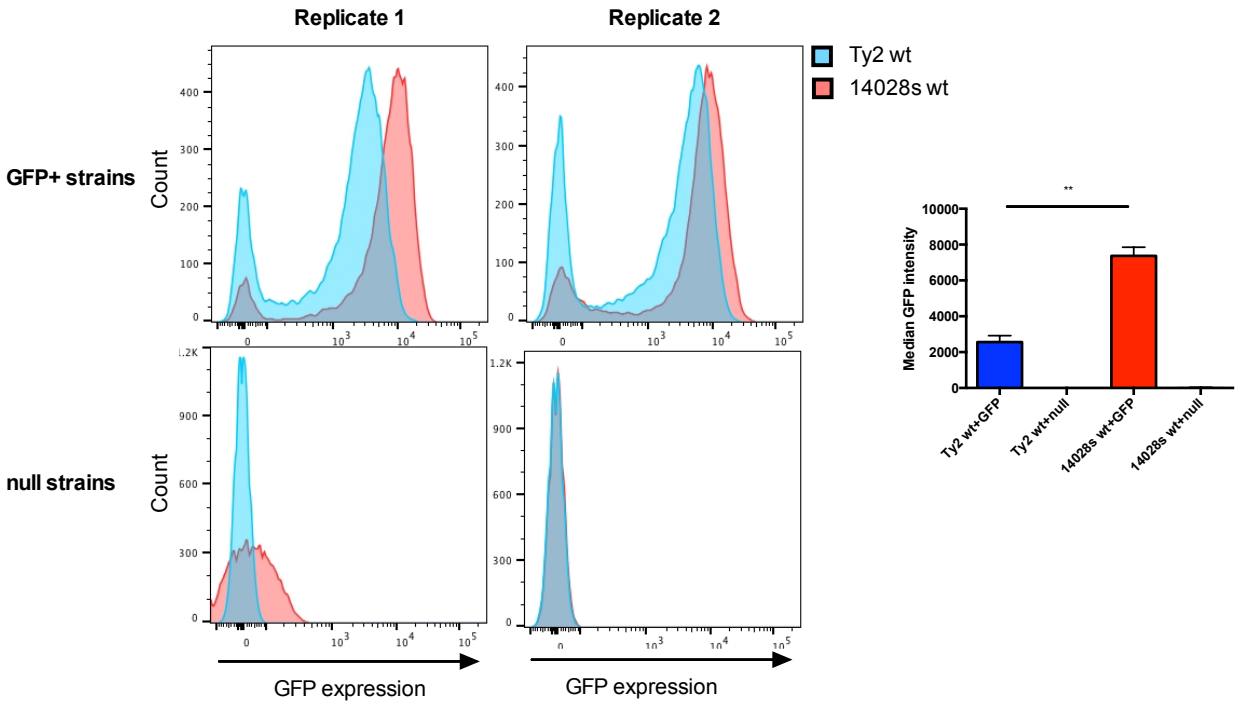

Figure 8. Intramacrophage *Salmonella* SPI2 expression. Differentiated human THP-1 macrophage-like cells were infected with opsonized, stationary-phase *Salmonella* carrying *ssaG::gfp* reporter plasmids at an MOI of ~15. Macrophages were lysed 24h post-infection and bacteria separated by gentle centrifugation. Isolated bacteria were fixed and then assayed for GFP expression as a measure of SPI2 *ssaG* expression. Histograms depicting individual biological replicates demonstrate a leftward shift in GFP intensity in intracellular *S*. Typhi in comparison to *S*. Typhimurium. The median GFP intensity of bacteria is also plotted. Intramacrophage *S*. Typhi exhibit reduced expression of SPI2 *ssaG* in comparison to *S*. Typhimurium. Statistical significance was determined using a ordinary one-way ANOVA and is indicated as ** $P < 0.01$.

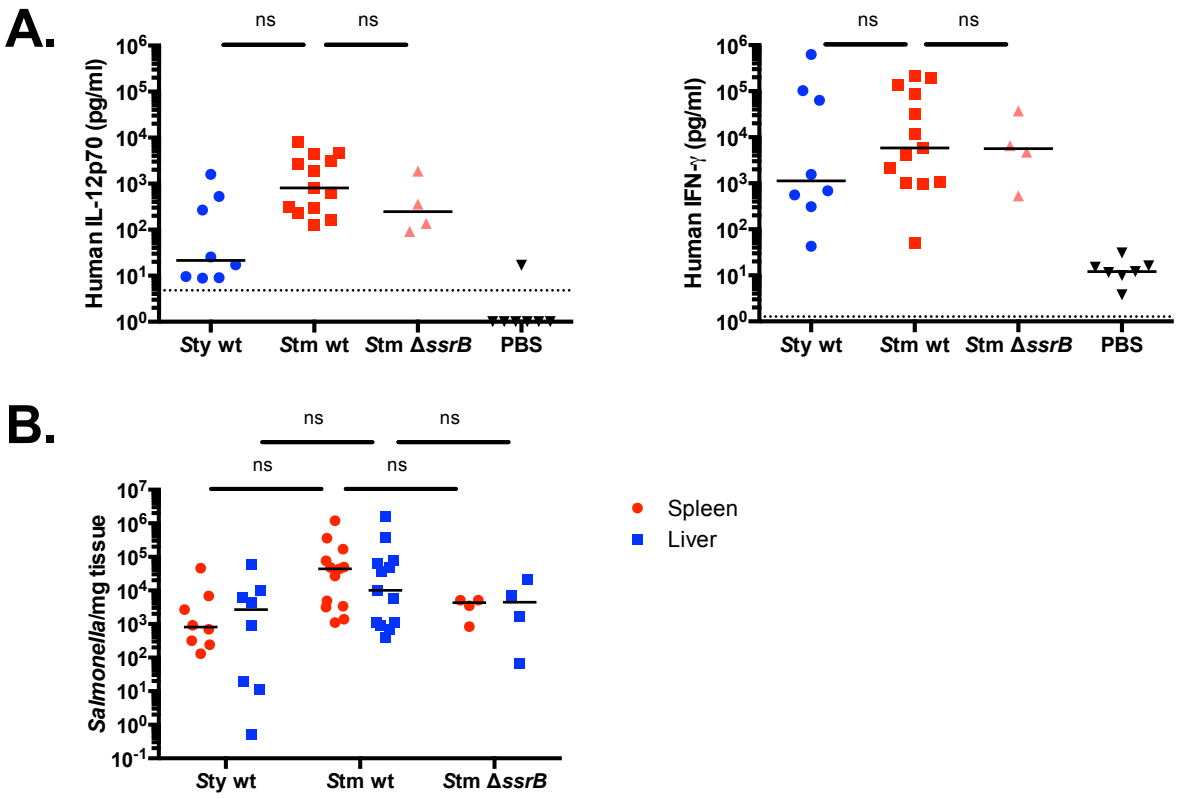

Figure 9. Immune responses of humanized mice to *Salmonella* infection. Humanized NOD-SCID IL2rγ null mice engrafted with human umbilical cord stem cells were infected with ~6x10^4 cfu wild-type *S*. Typhi, ~1x10^3 cfu wild-type *S*. Typhimurium or ~1x10^3 cfu of *S*. Typhimurium 14028s Δ*ssrB* cfu. Mice were sacrificed when moribund. (A) Serum human IL-12p70 and IFN-γ was measured by cytokine bead array (Becton Dickinson) or multiplex microbead cytokine array (Luminex). Dotted line indicates assay limit of detection. (B) Spleens and livers were aseptically harvested from infected humanized mice and homogenized for enumeration of cfu. Mice without detectable organ burdens were excluded from analysis. Each symbol represents one mouse with horizontal lines representing the median *Salmonella* organ burden for each group. Statistical significance was determined using a Kruskal-Wallis test.

Table 3. Strains, plasmids, primers.

Strain, plasmid or primer	Genotype, relevant characteristics, or sequence[a]	Source or reference
JK377	*Salmonella* Typhimurium 14028s *fliC::tetRA fljAB*::FRT-*kan*	This study (constructed by J. Karlinsey)
JK1217	*Salmonella* Typhimurium 14028s *invA*::FRT-*kan*	(148)
LAS5	*Salmonella* Typhimurium wild-type strain 14028s	ATCC
LAS18	*Salmonella* Typhimurium 14028s *ssrB*::FRT-*kan*	This study
LAS85	*Salmonella* Typhimurium 14028s *spvB*::FRT-*kan*	This study (constructed by S. Libby)
LAS269	*Salmonella* Typhimurium 14028s pMPMA3 ΔP_{lac} P_{ssaG} GFP	This study; (136)
LAS270	*Salmonella* Typhimurium 14028s pMPMA3 ΔP_{lac} null GFP	This study; (136)
LAS273	*Salmonella* Typhi Ty2 pMPMA3 ΔP_{lac} P_{ssaG} GFP	This study; (136)
LAS274	*Salmonella Typhi Ty2* pMPMA3 ΔP_{lac} null GFP	This study; (136)

SL4330	*Salmonella* Typhimurium 14028s *phoP*::FRT-*kan*	This study (constructed by S. Libby)
TY3	*Salmonella* Typhi wild-type strain Ty2	JSG624 from J. Gunn
TY76	*Salmonella* Typhi Ty2 *vexA*::FRT-*kan*	This study (constructed by J. Karlinsey)
TY196	*Salmonella* Typhi Ty2 Nal^R (mouse infections)	This study (constructed by J. Karlinsey)

Chapter 3

Loss of multicellular behavior in epidemic African non-typhoidal *Salmonella enterica* serovar Typhimurium ST313 strain D23580

Published as: Singletary LA, Karlinsey JE, Libby SJ, Mooney JP, Lokken KL, Tsolis RM, Byndloss MX, Hirao LA, Gaulke CA, Crawford RW, Dandekar S, Kingsley RA, Msefula CL, Heyderman RS, Fang FC. (2016) Loss of Multicellular Behavior in Epidemic African Nontyphoidal *Salmonella enterica* Serovar Typhimurium ST313 Strain D23580. MBio. Mar 1;7(2). pii: e02265-15. doi: 10.1128/mBio.02265-15.

LAS contribution: Working with F.C.F., wrote manuscript. For Fang lab data, L.A.S., J.E.K. and F.C.F. conceived of studies. The experiments in Figures 1, 2 (except 2B), 3C, 5A, 6, 7, and 8 were performed by L.A.S. The experiments in Figures 2B and 5B,C were performed by J.E.K of the Fang laboratory. The experiments in Figures 3A,B were performed by J.P.M. and K.L.L. of the Tsolis laboratory. The experiments in Figure 4 were performed by L.A.H. of the Dandekar laboratory.

Abstract

Non-typhoidal *Salmonella* enterica serovar Typhimurium (*S.* Typhimurium) is a frequent cause of bloodstream infections in children and HIV-infected adults in sub-Saharan Africa. Most isolates from African patients with bacteremia belong to a single sequence type, ST313, which is genetically distinct from gastroenteritis-associated ST19 strains such as 14028s and SL1344. Some studies suggest that the rapid spread of ST313 across the African subcontinent has been facilitated by anthroponotic (person-to-person) transmission, eliminating the need for *Salmonella* survival outside the host. While these studies have not ruled out zoonotic or other means of transmission, the anthroponotic hypothesis is supported by evidence of extensive genomic

decay, a hallmark of host-adaptation, in the sequenced ST313 strain D23580. We have identified and demonstrated two loss-of-function mutations in D23580, not present in the ST19 strain 14028s, that impair multicellular stress resistance associated with survival outside the host. These mutations result in inactivation of the KatE stationary-phase catalase that protects high-density bacterial communities from oxidative stress and the BcsG cellulose biosynthetic enzyme required for the RDAR (red, dry and rough) colonial phenotype. However, we have found that like 14028s, D23580 is able to elicit an acute inflammatory response and cause enteritis in mice and rhesus macaque monkeys. Collectively, these observations suggest that African *S.* Typhimurium ST313 strain D23580 is becoming adapted to an anthroponotic mode of transmission while retaining the ability to infect and cause enteritis in multiple host species.

Introduction

Prior to the advent of the HIV pandemic, invasive *Salmonella* infections in sub-Saharan Africa primarily afflicted young children, often with malaria co-infection, and were rarely seen in adults (4, 8). However, as HIV began to sweep across sub-Saharan Africa in the 1980s, *Salmonella* was increasingly identified as the most common cause of bacterial bloodstream infections in HIV-infected adults (9–11). In contrast to invasive salmonellosis elsewhere in the world, which consists primarily of typhoid or paratyphoid fever, bloodstream *Salmonella* infections in sub-Saharan Africa are non-typhoidal and most often caused by the *Salmonella enterica* serovars Typhimurium (*S*. Typhimurium), Enteritidis (*S*. Enteritidis) and Dublin (*S.* Dublin) (3–6). Of note, while inflammatory enteritis is the most common clinical manifestation of *S.* Typhimurium and *S.* Enteritidis infections among immunocompetent hosts in the developed world, diarrhea may be minimal or absent in as many as 20-50% of children and HIV-infected adults with invasive *Salmonella* infections in Africa (44, 45).

Initial reports emphasized the genetic diversity of non-typhoidal *Salmonella* (NTS) causing bloodstream infections in Africa and their similarity to strains responsible for

uncomplicated gastroenteritis (149). However, multi-locus sequence typing of more than 50 *Salmonella* isolates isolated from blood or cerebrospinal fluid specimens of patients in Malawi and Kenya found that many belong to a dominant sequence type, ST313 (150). Subsequent analysis has shown that the majority of invasive *S.* Typhimurium strains from sub-Saharan Africa fall within two closely related ST313 lineages that emerged during the HIV pandemic (151). These isolates are genetically distinct from well-characterized gastroenteritis-inducing ST19 strains such as 14028s and SL1344. Sequencing of a representative ST313 isolate, D23580, revealed a large number of pseudogenes and deletions (150). As genomic degradation is a hallmark of host-adapted or -restricted *Salmonella* serovars like *Salmonella enterica* serovar Typhi (*S*. Typhi), in contrast to most strains of generalist serovars like *S*. Typhimurium (25, 26), *S*. Typhimurium ST313 is thought to be evolving to become more host-adapted to humans (150). This suggestion is consistent with earlier reports that failed to detect *Salmonella* strains resembling invasive human isolates in the food and household animals of index patients with NTS infections (152) and suggests that *S.* Typhimurium in sub-Saharan Africa might be transmitted from person-to-person rather than from common-source vehicles (153). The latter investigation analyzed fecal samples from relatives, animals and the home environments of Kenyan index patients with NTS bloodstream infections (153). A majority of isolates from human fecal samples, but not from animals or the environment, matched the index patient isolates.

Since those initial studies, it has been demonstrated that *S.* Typhimurium ST313 strains are not host-restricted, as they have retained the ability to infect a variety of hosts including chickens and mice (154–156). The absence of diarrhea in some patients with invasive *S.* Typhimurium ST313 infections has been attributed to a reduced propensity of these strains to elicit host inflammatory responses and suggested to result from the absence of *pipD* and *ratB* in the D23580 genome, genes associated with diarrhea and colonization of the mammalian intestine by *S*. Typhimurium ST19 strains (144, 150, 157–160). However, we show in the

present study that *S.* Typhimurium ST313 strain D23580 is comparable to the conventional *S.* Typhimurium ST19 strain 14028s in its ability to cause invasive disease and inflammation in murine and primate models of intestinal and systemic infection. However, *S.* Typhimurium D23580 is distinctive in its loss of oxidative stress resistance and the ability to form RDAR (red, dry and rough) colonies that are required for multicellular development (161–164). These phenotypes result from point mutations in the *katE* and *bcsG* genes, encoding stationary-phase catalase and a cellulose biosynthetic protein, respectively. These observations suggest that although, in contrast to S. Typhimurium ST19 strain 14028s, *S.* Typhimurium D23580 appears to have adapted to an anthroponotic mode of transmission by losing traits associated with environmental persistence, it remains typical of other *S.* Typhimurium strains in its virulence characteristics and ability to cause enteritis in multiple host species.

Results

D23580 is adhesive, invasive and cytotoxic for mammalian cells

Clinical descriptions of *S.* Typhimurium ST313 and ST19 human infections have suggested that these NTS strains differ in their interactions with the intestinal tract. *S.* Typhimurium ST313 infections appear to be less frequently associated with diarrheal symptoms than ST19 infections (44). We compared the interaction of *S.* Typhimurium ST313 strain D23580 and ST19 strain 14028s with cultured human epithelial cells. Confluent layers of HeLa human cervical epithelial cells were infected with stationary phase *Salmonella*. Bacteria were centrifuged onto HeLa monolayers to synchronize infection, and bacteria were allowed to adhere to the cells for 15 minutes at 37°C. Infected monolayers were then washed four times with sterile PBS to remove transiently associated bacteria before lysing of the cells and enumeration of adherent bacterial colony-forming units (cfu). Bacterial adherence is expressed as the percent of the bacterial inoculum that adhered to HeLa cells normalized to total 14028s adherence. D23580 was over three times more adherent to HeLa cells than 14028s (Fig. 10A).

We next assayed the invasiveness of D23580 for HeLa cells. Confluent layers of HeLa cells were infected with late-logarithmic phase bacteria at a multiplicity of infection (MOI) of ~100. Ten minutes post-invasion, cell monolayers were washed and then lysed to enumerate intracellular bacteria. D23580 was approximately three times as invasive for HeLa cells in comparison to 14028s (Fig. 10B). Strains lacking the *Salmonella* pathogenicity island 1 (SPI1) type 3 secretion system (T3SS) subunit InvA were completely non-invasive, confirming that invasion by either strain is dependent upon the SPI1 T3SS.

We next compared the ability of D23580 and 14028s to induce early macrophage pyroptosis (pro-inflammatory cell death), another SPI1-dependent phenotype. Early *Salmonella*-induced pyroptosis occurs when flagellin is translocated through the SPI1 T3SS into the host cell cytoplasm (78). One hallmark of pyroptotic cell death is the loss of membrane integrity and subsequent leakage of intracellular contents into the extracellular milieu, including the host cell protein lactate dehydrogenase (LDH). RAW264.7 murine macrophage-like cells were infected with late-logarithmic phase bacteria at an MOI of ~10. Following infection, macrophages were washed to remove extracellular bacteria and incubated at 37°C for 4 hrs. Supernatant samples were then assayed for the release of LDH. In agreement with the epithelial cell invasion experiments, D23580 was more than three times as cytotoxic for macrophages as 14028s (Fig. 11A). Uptake of D23580 by macrophages was three times more efficient than uptake of 14028s, which may account for the enhanced cytotoxicity. This phenotype was dependent upon the SPI1-encoded T3SS, as isogenic *invA* mutants of each strain failed to induce a significant degree of macrophage pyroptosis (Fig. 11A). Despite the differences in early pyroptosis, both D23580 and 14028s exhibited similar levels of long-term survival within murine macrophages (Fig. 11B). The transcription factor PhoP, of the two-component PhoPQ regulatory system, was required for intramacrophage survival of both 14028s and D23580, as isogenic *phoP* mutants of either strain failed to replicate or survive inside murine macrophages (Fig. 11B). We also assayed the ability of D23580 to induce

macrophage death and survive in human THP-1 macrophage-like cells. Phorbol 12-myristate 13-acetate (PMA)-differentiated THP-1 human macrophage-like cells were infected with late-logarithmic phase bacteria at an MOI of ~10. Following infection, macrophages were washed to remove extracellular bacteria and incubated at 37°C for 4 hrs. Supernatant samples were then assayed for LDH release. In contrast to the observations in murine macrophages, D23580 and 14028s were similarly cytotoxic for THP-1 human macrophages (Fig. 11C). This phenotype was partially dependent upon the SPI1-encoded T3SS, as isogenic *invA* mutants of each strain induced less macrophage pyroptosis (Fig. 11C). A second type of *Salmonella*-induced macrophage death known as delayed pyroptosis was assayed in infected THP-1 human macrophages. PMA-differentiated THP-1 cells were infected with human-serum opsonized, stationary-phase bacteria at an MOI of ~15. Bacteria were centrifuged onto macrophage monolayers to synchronize infection and internalized for one hr. Macrophage monolayers were then washed with medium containing the membrane-impermeant antibiotic gentamicin. Twenty-four hpi supernatants were assayed for LDH release. *S.* Typhimurium D23580 and 14028s induced similar amounts of delayed pyroptosis in THP-1 cells (Fig. 11D). This phenotype was dependent upon the SPI2-encoded T3SS, as isogenic *ssrB* mutants of each strain failed to induce as much delayed macrophage pyroptosis as wt strains (Fig. 11D). D23580 and 14028s exhibited similar levels of survival within human THP-1 macrophages (Fig. 11E). Collectively these results demonstrate that D23580 is adherent, invasive and cytotoxic for mammalian cells, and these phenotypes are dependent on the SPI1 and SPI2 T3SS, as observed in other *Salmonella* strains.

D23580 is highly invasive following oral infection

To better understand how *S.* Typhimurium ST313 interacts with the mammalian intestine, D23580 and IR715 (a spontaneous nalidixic-acid resistant mutant of ST19 strain 14028s) were orally administered to mice and monitored in the feces, mesenteric lymph nodes

and Peyer's patches. D23580 has previously been shown to cause systemic disease in mice following intragastric (i.g.) or intraperitoneal (i.p.) inoculation (155, 156, 165). However, early interactions between D23580 and the mammalian gut and the subsequent course of infection have been less well studied. CBA/J mice were administered streptomycin i.g. prior to *Salmonella* infection to disrupt the gut microbiota and allow *Salmonella* to establish colonization of the intestinal tract. Following streptomycin treatment, 10^8 cfu of a ~1:1 mixture of D23580 and IR715 were administered i.g. At the indicated time points, mice were sacrificed and their organs homogenized prior to plating on selective medium to enumerate cfu of each strain. Values greater than 1 indicate a competitive advantage of D23580 over IR715. Similar to the observations in cultured human epithelial cells, D23580 was able to invade the murine intestinal tract to a greater degree than IR715 on the first day post-infection (Fig. 12A). In the small intestine, *Salmonella* gains access to lymphoid immune follicles known as Peyer's patches via specialized epithelial cells called M cells or can be taken up by dendritic cells in the lamina propria (63). The former pathway is SPI1-dependent, whereas the latter is SPI1-independent (63, 166). Following translocation across the intestinal epithelium by either route, the bacteria are able to reach the mesenteric lymph nodes. On day 1 post-infection, D23580 was found in 10-fold greater abundance than IR715 in the mesenteric lymph nodes and nearly 100-fold greater abundance in the colonic contents (Fig. 12A). In parallel, D23580 was shed at 10- to 100-fold higher levels in fecal pellets (Fig. 12B). However, by day 4 post-infection, levels of D23580 in the Peyer's patches, mesenteric lymph nodes, colon and fecal pellets were comparable to those of IR715, or even somewhat reduced in certain sites (Figs. 3A, B). Despite rapid transit from the small intestinal lumen to deeper lymphoid tissues, D23580 was not found in higher abundance in the spleen and liver on day 1 and was only found in moderately higher abundance on day 4 post-infection (Fig. 12A). We also examined long-term fecal shedding of *Salmonella* in 129/Sv mice. These mice were orally infected with approximately $4x10^8$ cfu of a ~1:1 mixture of *S.* Typhimurium D23580 and 14028s. At the timepoints indicated, fresh fecal

pellets were harvested from individual mice, homogenized in sterile PBS, and cfu were enumerated. The quantity of D23580 in each sample was determined by patching 100 colonies onto selective medium. In contrast to short-term fecal shedding, there was no significant difference in the quantity of D23580 and 14028s shed in the feces of infected mice (Fig. 12C).

D23580 induces inflammation in the intestinal tract

Having determined that *S.* Typhimurium D23580 is able to colonize and disseminate from the murine intestinal tract, we next sought to determine whether D23580 differs from the ST19 strain IR715 (a spontaneous nalidixic-acid resistant mutant of 14028s) in its ability to elicit mucosal inflammation. As mentioned previously, the absence of significant diarrhea in some patients with invasive ST313 infections and the reduced inflammatory responses observed in tissue culture (157, 158) have suggested that D23580 might elicit less inflammation than IR715. Previous studies in mice and cattle have also suggested that D23580 elicits less inflammation than ST19 strains in the intestine (157, 159), although the strain of *S.* Typhimurium ST19 used in those studies (SL1344) is recognized to be particularly pro-inflammatory (167). In contrast to these findings, Parsons et al. reported that D23580 elicits more inflammation in the chicken intestine early in infection (154). In an attempt to clarify these disparate findings, we performed histopathological examination of infected cecal tissue from streptomycin pre-treated mice inoculated i.g. with *S.* Typhimurium. The results of these experiments revealed no significant difference in intestinal pathology, with both D23580- and IR715-infected samples exhibiting moderate to severe levels of inflammation (Fig. 12D). Further, similar degrees of cecal exudate, epithelial damage, submucosal edema and infiltration of the lamina propria by mononuclear and polymorphonuclear cells were noted (Fig. 12D).

To determine whether D23580 and IR715 differ in their early interaction with the intestinal mucosa, we compared inflammatory responses in a rhesus macaque ligated ileal loop assay after intraluminal inoculation with *S.* Typhimurium. Comparable quantities of fluid

accumulation, a correlate of intestinal inflammation, were measured following inoculation of D23580 or IR715 (Fig. 13A). Similarly, no significant differences in the expression of inflammatory cytokine genes *Lcn2* (lipocalin-2), *Mip3α* (macrophage inflammatory protein-3α), *Ifnγ* (interferon-γ), *Il17* (interleukin-17) and *Il22* (interleukin-22) were measured following inoculation of D23580 or IR715 into ligated ileal loops (Fig. 13B). The numbers of tissue-associated IR715 and D23580 bacteria in infected ileal loops were also similar (Fig. 13C). In summary, *S.* Typhimurium ST313 strain D23580 is capable of eliciting an inflammatory response in the mammalian intestine and does not appear to differ in this regard from the well-characterized ST19 strain IR715.

D23580 exhibits enhanced susceptibility to oxidative stress due to mutation of the *katE* catalase gene

Following investigation of host-related phenotypes, we evaluated D23580 for traits associated with environmental stress resistance, which may be lost during host-adaptation of pathogens. First we evaluated the enzyme catalase, which converts hydrogen peroxide (H_2O_2) to oxygen and water. H_2O_2 detoxification by catalase is dispensable for *Salmonella* survival in phagocytes or during infection but required during high density or multicellular colonial growth (161, 168). Catalase activity can be detected by adding H_2O_2 to cultured bacteria and monitoring the elaboration of oxygen bubbles over time. *S.* Typhimurium ST313 strain D23580 was found to exhibit decreased catalase activity by this assay when compared to the ST19 strains 14028s and SL1344, a phenotype that has also been recently reported by others (156) (Fig. 14A, left panel). The ST19 strains LT2, 14028s *rpoS** and 14082s Δ*rpoS* carry mutations in *rpoS,* rendering them extremely sensitive to H_2O_2. 14028s *rpoS** has an *rpoS* mutation resulting in reduced expression of the σ^S (RpoS) regulon and enhanced sensitivity to H_2O_2. These strains were included as known catalase-deficient controls (169) (Fig. 14A, left panel). Often, laboratory-passaged bacteria may appear catalase-negative due to the loss of a fully-

functional RpoS, prompting us to determine whether this was a universal characteristic of ST313 strains. Nine additional ST313 isolates were tested and all were found to be catalase-deficient, in contrast to the ST19 strains 14028s and SL1344 (Fig. 14A, right panel).

The reduced catalase expression of *S.* Typhimurium ST313 strain D23580 correlated with enhanced susceptibility to H_2O_2 (Fig. 14B). The lag phase of D23580 cultured in the presence of H_2O_2 was prolonged in comparison to 14028s (Fig. 14B). Growth of D23580 in the presence of H_2O_2 was similar to that of *rpoS* mutant strain 14028s *rpoS** (Fig. 14B). As *rpoS* mutations are common among archival *Salmonella* isolates (170) and result in reduced catalase expression, the possibility of an *rpoS* mutation in D23580 was investigated. However, sequencing of the D23580 *rpoS* promoter and coding region yielded no mutations when compared to 14028s. Moreover, expression of the σ^S-dependent *spvB* (encoding an ADP-ribosylating toxin), *otsA* (trehalose biosynthesis) and *katE* (catalase) genes was found to be comparable in *S.* Typhimurium D23580 and 14028s (Fig. 14C). In contrast, the *rpoS** 14028s derivative showed 5-to-10-fold lower expression of *spvB, otsA* and *katE* in comparison to wild-type 14028s (Fig. 14C). Thus the reduced catalase activity of D23580 could not be attributed to a defect in σ^S regulation.

We next examined the sequence of *katE*, encoding the stationary-phase catalase, in D23580 and 14028s. A single amino acid change distinguishing KatE in the 2 sequence types was identified at position 117, with glutamic acid in 14028s corresponding to glycine in D23580. We also examined the KatE sequence of 8 additional ST313 isolates for which sequence was available and found the E117G mutation present in all strains analyzed. The 14028s allele of *katE*, including its promoter, was cloned onto a plasmid and transformed into D23580, thereby restoring catalase activity (Fig. 15). In contrast, replacement of the 14028s *katE* allele with the D23580 *katE* allele abolished catalase activity (Fig. 15). As a control to exclude involvement of the heat-labile *Salmonella* catalase KatG, samples were heat-treated for 15 min and catalase activity measured. No difference in catalase activity before and after heat treatment was

observed (Fig. 15). We conclude that D23580 has lost catalase activity as the result of an E117G KatE mutation.

D23580 is unable to form RDAR (red, dry and rough) colonies due to a mutation of the *bcsG* cellulose biosynthetic gene

At room temperature, many strains of *Salmonella* are able to form RDAR (red, dry and rough) colonies resulting from the formation of thin aggregative fimbriae (curli) and the production of cellulose and other polysaccharides (162, 171, 172). RDAR colonies represent a form of multicellular behavior that enhances *Salmonella* stress resistance in the environment and allows biofilm formation (173). To observe RDAR colony formation, *Salmonella* strains were grown on no-salt, Congo Red-containing medium at room temperature (~25°C) for 7 days (162). D23580 is unable to form RDAR colonies in contrast to the ST19 strain 14028s, which exhibits the typical RDAR colonial phenotype (Fig. 16, top panel). RDAR colony formation was not observed at 37°C in 14028s or D23580 because RDAR gene expression is repressed at this temperature (Fig. 16, bottom panel). Three genes implicated in RDAR colony formation were found to differ between D23580 and 14028s: *csgE*, required for the production of curli fimbriae, and 2 genes required for cellulose biosynthesis, *bcsC* and *bcsG* (174). CsgE in D23580 contains the amino acid mutation Q36H, whereas the only difference in *bcsC* between the two sequence types is a synonomous single nucleotide change from T to G at position 1461. The most impactful sequence change between 14028s and D23580 occurs in BcsG, with the introduction of a premature stop codon approximately halfway through the protein at position 247 (W→STOP). The 14028s *bcsG* allele, with promoter, was cloned into a plasmid and transformed into D23580. Transformants were plated onto nutrient-rich, no-salt Congo Red medium and incubated for 7 days at 25° or 37°C. The 14028s *bcsG* gene rescued the RDAR-deficient colonial phenotype of D23580 (Fig. 16), confirming that D23580 has lost the ability to form RDAR colonies and biofilms as the result of a *bcsG* nonsense mutation. The difference in

appearance of the *bcsG*-complemented colony from 14028s is likely due to enhanced expression of *bcsG* from a multi-copy plasmid (175). Overexpression of cellulose-synthetic genes has previously been shown to enhance the RDAR phenotype (176). Eight additional ST313 isolates were tested for the RDAR morphology. Five isolates, all of lineage II, were negative for the RDAR morphology and harbored the mutant *bcsG* allele identical to lineage II isolate D23580 (unpublished data). The remaining three isolates, of lineage I, had weak or intermediate RDAR morphologies and contained the wild-type *bcsG* allele. The basis of the defective RDAR morphology of lineage I isolates is not known. The incidence of invasive nontyphoidal Salmonellosis increases during the rainy season (177). We therefore hypothesized that the RDAR status of D23580 could influence its survival in water. *Salmonellae* were inoculated into sterile water and incubated at room temperature without shaking. At the timepoints listed, cfu were enumerated. Despite differences in the RDAR phenotype of each strain, no difference in the survival of D23580 and 14028s in water were evident (Fig. 17).

Discussion

This study examines *S.* Typhimurium ST313, an NTS (non-typhoidal *Salmonella*) lineage responsible for invasive infections in young children and HIV-infected adults throughout sub-Saharan Africa, to test the hypothesis that *S.* Typhimurium ST313 represents an evolutionary transition to a more typhoid-like pathogen that is host-adapted to humans and preferentially causes systemic infection rather than inflammatory enteritis (150). We did not find that *S.* Typhimurium ST313 strain D23580 has become host-restricted for humans, in contrast to S. Typhi, nor impaired in its ability to cause inflammatory enteritis in multiple infection models, including rhesus macaques. However, we found that D23580 has lost its ability to exhibit multicellular behaviors associated with environmental persistence, which is consistent with epidemiological evidence of person-to-person transmission (152, 153).

Clinical reports have suggested that *S.* Typhimurium ST313 has a reduced propensity to cause diarrhea in comparison to conventional *S.* Typhimurium strains (44, 45). However, we found that D23580 has retained the capacity to elicit inflammatory responses in the mammalian intestine. Inflammation-associated pathology and levels of inflammatory cytokines elicited by *S.* Typhimurium D23580 or the ST19 strain IR715, a spontaneous nalidixic acid-resistant mutant of 14028s, were similar in a murine and primate colitis model (Fig. 12D, 4B). These findings, the latter of which represents the first report of ST313 virulence in non-human primates, is consistent with recent reports that D23580 is able to cause enteritis and invasive infections in chickens (154). However, our observations contrast with *in vitro* studies suggesting that D23580 elicits reduced inflammatory responses relative to *S.* Typhimurium ST19 strain SL1344 when infecting cultured cells (157, 158) or murine and bovine models of intestinal infection (159). We suggest that this may in part relate to heterogeneity among ST19 strains with regard to *Salmonella* Pathogenicity Island 1 (SPI1) expression and related proinflammatory sequelae (167). ST19 *S.* Typhimurium strain SL1344 exhibits particularly high levels of SPI1 expression, and this was one of the comparator strains used in previously published *in vitro* and *in vivo* studies. It is also important to point out differences in the genetic backgrounds of the mice used in each study, C57/BL6 (*Salmonella*-susceptible, Nramp1^{-}) versus CBA/J and 129P2/olaHsd (*Salmonella*-resistant, Nramp1^{+}) mice, which may account for some of the differences observed. Regardless of the ST19 comparator strain examined, our observations suggest that D23580 has not in fact lost the ability to induce inflammation in the mammalian intestine and cause enteritis, in contrast to the host-restricted serovar *S.* Typhi (49, 50, 178). The systemic virulence of D23580 also appears comparable to that of IR715 (Fig. 12A). It is therefore likely that the reduced incidence of diarrhea and the high frequency of invasive disease associated with *S.* Typhimurium ST313 in Africa are attributable to differences in host innate immune responses rather than solely to intrinsic properties of ST313. This is supported by recent studies in which experimental malarial co-infection with increased expression of IL-10 was associated with

enhanced susceptibility to invasive NTS infection and blunted intestinal inflammation (165), as well as epidemiological data showing increased incidence of NTS bacteremia in HIV-positive adults, children with malaria, and children less than one year of age (165, 179, 180).

The enhanced adherence and invasiveness of *S*. Typhimurium D23580 in cultured epithelial cells (Fig. 10A, B) correlated with increased cfu in the mesenteric lymph nodes of infected mice (Fig. 12A) and with enhanced fecal shedding at early time points following infection (Fig. 12B). Both epithelial cell invasion and fecal shedding of *Salmonella* are influenced by the SPI1 type III secretion system (181). Previous studies have reported differential expression of the SPI1 effector *sopE2* between ST19 and ST313 strains (157). These observations described here further support that SPI1 genes may be differentially expressed in the ST313 strain D23580 and the ST19 strain 14028s, which might be investigated in future studies.

In corroboration of findings in a recent publication (156), we found that multiple *S.* Typhimurium ST313 strains express reduced catalase activity. Although reduced catalase activity is typically a result of reduced activity of the alternative sigma factor σ^S (RpoS) (182–184), we found that activation of the σ^S regulon is intact in ST313 strain D23580 (Fig. 14C). Instead, an E117G mutation in the stationary phase catalase KatE was found to be responsible for the reduced catalase activity of D23580 (Fig. 15) and other ST313 strains. Other investigators previously reported D23580 to be “weakly positive” for catalase activity (156), while our data indicate that D23580 lacks catalase activity (Fig. 15, lighter bars). This is most likely because we assayed catalase during stationary phase, in which catalase activity is KatE-dependent, whereas the earlier study assayed catalase from growing colonies in which both KatE and KatG catalases are expressed. Catalase is not required for *Salmonella* virulence (168) but is required for oxidative stress resistance during multicellular colonial growth (161). This suggests that *S.* Typhimurium D23580 has lost a functional *katE* gene by mutation because it no longer requires multicellular behavior for transmission and/or survival in the

environment. It is interesting to note that the human-adapted *Salmonella* serovar *S.* Typhi also exhibits reduced catalase activity. However, in the case of *S.* Typhi, the reduced catalase activity is more often a consequence of reduced σ^S activity (184). This difference may reflect the requirement of NTS serovars to retain σ^S in order to preserve expression of *spv* virulence genes carried by the plasmid pSLT (182), whereas the negative regulatory influence of σ^S on Vi polysaccharide expression (185) may favor the accumulation of *rpoS* mutations in *S.* Typhi.

We also found that D23580 no longer exhibits a RDAR (rough, dry and red) colonial phenotype, a correlate of biofilm formation (Fig. 16). RDAR colonies are resistant to a variety of environmental stresses including desiccation and nutrient deprivation (162, 163, 172, 186). The failure of D23580 to form RDAR colonies results from a nonsense mutation in the cyclic-di-GMP-sensitive cellulose biosynthetic gene *bcsG* (171, 174). As with catalase, the RDAR phenotype is not required for *Salmonella* virulence but is required for environmental stress resistance during multicellular growth (187). The RDAR colonial phenotype is seen in a majority of generalist *S.* Typhimurium isolates but is variable in chicken-adapted *S.* Gallinarum and absent in human-adapted *S.* Typhi or swine-adapted *S.* Choleraesuis (188). In addition, the loss of RDAR in *S*. Typhimurium ST313 strain D23580 contrasts with other *S.* Typhimurium isolates associated with endemic infection in Africa (189), which may still require the ability to survive outside the host for effective transmission to susceptible hosts. Alternatively, the loss of RDAR colony formation has also been reported to increase the fitness of *Salmonella* in plants (190), and the involvement of an as-yet unidentified food vector cannot be excluded. Interestingly, the premature stop codon in *bcsG* is only found in ST313 lineage II but not in lineage I isolates. In contrast, the KatE E117G mutation is present in all ST313 isolates tested. This suggests the KatE mutation was acquired prior to lineage divergence, while the *bcsG* mutation was subsequently acquired by lineage II isolates only.

In conclusion, the studies described herein provide novel insights into the evolution of host-specific strains of the enteric pathogen *Salmonella enterica*. Specifically, the robust early

fecal shedding and loss of environmental resistance phenotypes observed in *S.* Typhimurium ST313 strain D23580 are consistent with epidemiological evidence suggesting anthroponotic transmission (153). Furthermore, we have shown that D23580 has retained its ability to induce inflammatory colitis in mammalian models of infection, suggesting that the reduced incidence of diarrhea and increased incidence of invasive disease associated with these strains most likely reflect differences in host susceptibility rather than in intrinsic virulence properties of the pathogen.

Materials and Methods

Bacterial strains, genetic manipulations and growth conditions

Bacterial strains, plasmids and primers are listed in Table 4. Unless otherwise stated, all chemicals were purchased from Sigma-Aldrich (St. Louis, MO) or Fisher Scientific (Waltham, MA). Unless otherwise stated, all strains were routinely cultured in Luria-Bertani (LB) medium with shaking at 250 rpm at 37°C. Antibiotic supplementation is as follows unless otherwise stated: kanamycin (50 μg ml^{-1}), ampicillin (100 μg ml^{-1}), tetracycline (20 μg ml^{-1}) and nalidixic acid (50 μg ml^{-1}).

The λ-red recombinase system of *E. coli* was used to generate *Salmonella* mutants (147). Briefly, PCR was performed with primers containing ~40 bp of homology to the 5' or 3' end of a gene of interest and ~20 bp of homology to the kanamycin-resistance gene of pKD4 or pKD13. Confirmation of mutant construction was performed by PCR using gene-specific primers.

Construction of a multi-drug sensitive (MDS) ST313 was performed by isolating a spontaneous nalidixic acid-resistant mutant of a representative ST313 strain, D23580, by plating ~10^8 cfu of overnight culture onto LB plates containing 50 μg ml^{-1} nalidixic acid; the derivative was designated JK1124. The *gyrA* locus of JK1124 was sequenced, and a single TCC→TTC mutation was found to result in an S83F amino acid change. The *tetRA* element conferring

tetracycline resistance was PCR-amplified with primers JKP409/JKP410 using genomic DNA from strain JK18 as template. The *tetRA* element was inserted using λ red-mediated recombination (191) at bp 337269-337270 of the *Salmonella* virulence plasmid pSLT of wild-type 14028s, to create strain JK1115. A mating was performed as described (192) using donor JK1115 and recipient JK1124 at a ratio of 1:10 on a 0.45 μM filter on M9 minimal media with 0.2% glucose. The mating was incubated overnight at 37^{o}C followed by suspension of bacteria in 10 mM $MgSO_4$ and plating onto LB agar containing nalidixic acid and tetracycline. The concurrent loss of pSLT-BT and gain of pSLT-14028s::*tetRA* in D23580 was confirmed by PCR and sensitivity to multiple antibiotics.

Allelic replacement of ST19 strain 14028s KatE E177 with ST313 strain D23580 KatE G117 was performed by λ-Red homologous recombination and counter selection for tetracycline resistance (191) as follows. Genomic DNA from JK18 served as template to amplify the *tetRA* element with flanking sequences to *katE* using primers JKP539/JKP540. Subsequent λ-Red mediated recombination resulted in *tetRA* element insertion immediately following the 14028s KatE codon E117, designated JK1228. To insert the D23580 *katE* allele into 14028s primers JKP541 and JKP542 were used to amplify a 335 bp *katE* fragment from D23580. The PCR fragment was electroporated into JK1228 and by λ-Red mediated recombination and counter selection of tetracycline resistance on tetracycline sensitive plates (191) resulted in colonies with KatE G117 replacement into 14028s. Allelic replacement of KatE E117G in 14028s was confirmed by DNA sequencing and the strain designated JK1250.

The *katE* and *bcsG* mutations of D23580 were complemented by cloning the promoters and full coding sequences of the ST19 strain 14028s alleles of each gene, STM14_1600 and STM14_4364, respectively, into the *Bam*HI and *Hin*dIII sites of the low-copy expression vector pRB3 (175). The PCR product was double-digested with *Bam*HI and *Hin*dIII then ligated into the vector.

Animals

All animal experiments were approved by the University of California at Davis or the University of Washington Institutional Animal Care and Use Committee. Animal experiments were performed in accordance with guidelines regarding animal welfare.

Epithelial cell adhesion assay

Salmonella strains were grown overnight in LB broth. Stationary phase bacteria were used to infect $3x10^4$ HeLa cells/well (96-well plate) at a multiplicity of infection of ~100:1. Bacteria were centrifuged at 1000 rpm for 5 min onto HeLa monolayers to synchronize infection. Infected monolayers were incubated for 15 min at 37°C. Infected monolayers were then washed four times with sterile PBS to remove transiently associated bacteria. HeLa cells and associated bacteria were lifted from the dish by addition of 1% Triton X-100, and the adherent bacterial colony-forming units (cfu) were enumerated. Bacterial adherence is expressed as the percent of the bacterial inoculum that adhered to HeLa cells normalized to total 14028s adherence.

Epithelial cell invasion assay

Invasion assays were adapted from (193). *Salmonella* strains were grown overnight in LB broth supplemented with sodium chloride to a final concentration of 0.3 M. Overnight cultures of *Salmonella* were subcultured 1:33 in 10 ml of LB supplemented with sodium chloride and grown with shaking at 37°C for 3.5 hrs when bacteria reached late-logarithmic phase (OD_{600} ~1.0). Bacteria were used to infect $3x10^4$ HeLa cells/well (96-well plate) at a multiplicity of infection of ~100:1. Infected cells were incubated at 37°C for 10 min to promote invasion. Following invasion, epithelial cells were washed 3 times with PBS then incubated at 37°C for 20 min in antibiotic-free growth medium. After 20 min, the medium was supplemented with gentamicin at a final concentration of 50 μg ml^{-1}. Cells were incubated for 40 min at 37°C then

lysed with 1% Triton X-100 to enumerate internalized bacteria. Results are expressed as percent of the bacterial inoculum internalized.

Salmonella-induced rapid macrophage cytotoxicity assay

Salmonella strains were grown overnight in LB broth supplemented with sodium chloride to a final concentration of 0.3 M. Overnight cultures of *Salmonella* were adjusted to OD_{600} ~2.5 then subcultured 1:100 in LB supplemented with sodium chloride and grown with shaking at 37°C for 4 hrs when bacteria reached late-logarithmic phase. Bacteria were then used to infect $1.4x10^5$ RAW264.7 murine macrophage-like cells/well (96-well plate) or $3x10^5$ THP-1 human macrophage-like cells/well (24-well plate) at a multiplicity of infection of ~10:1 or 30:1, respectively. For THP-1 human macrophage-like cell infections, 72 hrs before infection THP-1 monocytes were differentiated into macrophages with 4 nM phorbol 12-myristate 13-acetate (PMA). Twenty-four hrs prior to infection, the PMA was removed, and macrophages were rested until infection. Infected monolayers were incubated at 37°C for 30 min to promote internalization. Following internalization, monolayers were washed twice with DMEM supplemented with 20 μg ml^{-1} gentamicin to kill extracellular bacteria. Infected monolayers were incubated at 37°C for 4 hrs before supernatant levels of lactate dehydrogenase were assayed using the CytoTox96 Cytotoxicity Kit (Promega, Madison, WI) per the manufacturer's protocol. Percent cytotoxicity was calculated as follows: ((Experimental release-Spontaneous release)/(Maximum release-Spontaneous release)) x 100.

Salmonella-induced delayed macrophage cytotoxicity and intramacrophage survival assay

Salmonella strains were grown overnight in LB broth. For murine macrophage infections, 1 ml of bacterial culture was centrifuged, supernatant was removed and pellets resuspended in 100 μl of 100% normal mouse serum. For human macrophage infections,

Salmonella cultures were adjusted to OD_{600} 1.0 and washed twice with sterile PBS (Cellgro). Equal parts *Salmonella* and 100% AB human serum (Cellgro) were mixed. Opsonized bacteria were incubated at 37°C for 15-20 min. Eight x 10^5 RAW246.7 murine macrophage-like cells/well or 3x10^5 THP-1 human macrophage-like cells/well were infected with opsonized *Salmonella* at a multiplicity of infection of ~10:1 or ~15:1, respectively. For THP-1 human macrophage-like cell infections, 72 hrs before infection THP-1 monocytes were differentiated into macrophages with 4 nM phorbol 12-myristate 13-acetate (PMA). Twenty-four hrs prior to infection, the PMA was removed, and macrophages were rested until infection. Infected macrophage monolayers were centrifuged at 1000 rpm for 5 min then incubated at 37°C for 15 min (RAW264.7 cells) or 1 hr (THP-1 cells) in 5% CO_2. Following internalization, macrophages were washed with RPMI 1640 1X containing 20 μg ml^{-1} gentamicin to kill extracellular bacteria, then lysed with 1% Triton X-100 to enumerate intramacrophage bacteria at 0 and 18 hrs post-infection (RAW264.7 cells) or 24 hrs post-infection (THP-1 cells). To measure *Salmonella*-induced delayed macrophage cytotoxicity, the concentration of lactate dehydrogenase in the supernatant of infected human macrophages was assayed using the CytoTox96 Cytotoxicity Kit (Promega) per the manufacturer's protocol. Percent cytotoxicity was calculated as follows: ((Experimental release-Spontaneous release)/(Maximum release-Spontaneous release)) x 100.

Mouse infections

Mouse infections were performed similarly to those previously described with modifications as noted (179). Male and female CBA/J mice were treated with 20 mg streptomycin Q1 i.g. 24 hrs prior to *Salmonella* infection. Mice were infected by gavage with 100 μl of 10^8 bacteria in LB broth. For competitive infections, a 50/50 mixture of D23580 and IR715 was used to infect mice. To determine the numbers of viable *Salmonella*, colon contents, Peyer's patches (3 per mouse), mesenteric lymph nodes, livers, and spleens were homogenized in PBS using an Ultra Turrax T25 Basic mixer (IKA). Homogenates were serially

diluted and plated on LB agar plates containing nalidixic acid (0.05 mg ml^{-1}) for IR715 or chloramphenicol (0.03 mg ml^{-1}) for D23580. After overnight growth at 37°C, cfu/gram of tissue were enumerated. Competitive indices (CI) were determined as cfu of D23580 over cfu of IR715, normalized to input inocula. Histopathological samples were scored in a blinded fashion by trained pathologist MXB.

Mouse long-term fecal shedding assay

Ten 129/Sv mice were orally infected with ~$4x10^8$ cfu of a ~1:1 mixture of *S.* Typhimurium D23580 and 14028s. The total inoculum volume was 20 µl. To harvest feces, individual mice were transferred to small cardboard buckets for 5-10 minutes. Five-to-ten fresh fecal pellets were harvested then homogenized in 1 ml sterile PBS. Homogenate was plated onto nonselective media to enumerate total cfu. The amount of D23580 in each sample was determined by patching 100 colonies onto medium containing chloramphenicol (0.03 mg ml^{-1}).

Rhesus macaque ileal loop infections

Rhesus macaque ileal loop infections were performed as described (179, 194). Briefly, 4 healthy male rhesus macaques were anesthetized prior to a laparotomy to expose the ileum. Ileal loops averaging 4 cm in length were created by ligation and infected by intra-lumenal injection of 1 ml of $1×10^9$ cfu of *Salmonella* or sterile LB broth. Five hrs following infection, loops were collected and the change in intra-lumenal fluid accumulation or RNA expression of inflammatory cytokines over mock-infected loops was measured. Monkeys were designated 37248, 36171, 38498 and 36782. Loops used in this study were loop 11 (LB media), loop 13 (IR715) and loop 14 (D23580).

Hydrogen peroxide susceptibility assays

To measure the ability of *Salmonella* strains to detoxify hydrogen peroxide (H_2O_2), 20 µl of ~8.8M H_2O_2 was added to 1 ml of an overnight culture (~16-18 hrs of growth) of *Salmonella* and incubated at room temperature for 5 minutes. The height of the oxygen bubble column correlates with the ability of a strain to detoxify H_2O_2. To measure growth in the presence of H_2O_2, overnight cultures of *Salmonella* were diluted to a final OD_{600} of 0.002 in LB broth with or without 0.5 mM H_2O_2. The OD_{600} was measured at 15 min intervals in a Bioscreen C microplate reader (Labsystems, Helsinki, Finland).

Catalase activity assay

Salmonella catalase activity was measured as described with modifications as noted (195). Briefly, 2 ml of overnight culture were washed twice and resuspended in a final volume of 400 µl wash buffer to reduce frothing during sonication. Bacteria were subjected to 4 rounds of sonication at power level 2 for 5 sec each (Mixonix, Farmingdale, NY). Lysates were centrifuged and the protein concentration of the supernatant determined using a Coomassie (Bradford) Protein Assay Kit (Pierce, Waltham, MA). Twenty µl of lysate were combined with H_2O_2 and the decay measured colorimetrically at OD_{240} over time. The specific activity of catalase was calculated using the formula: (1000 x ΔA_{240}/min (average))/(43.6 x mg of protein/ml of reaction mixture). Heat-stable KatE activity was measured by heating cell extracts to 55°C for 15 min prior to assaying catalase activity.

Detection of the RDAR colonial morphotype

Bacteria were grown overnight in LB broth then diluted to a concentration of ~100 cfu/ml. One-hundred µl were plated onto LB agar without salt and supplemented with 40 µg ml^{-1} Congo Red and 20 µg ml^{-1} Coomassie Blue. Plates were incubated at 25°C or 37°C for 7 d without inversion (162).

Water survival assay

Bacteria were grown overnight in LB broth at 37°C. Bacteria were then washed twice in sterile PBS and once in sterile water. Bacteria were inoculated into sterile water at a final concentration of ~$5x10^8$ cfu/ml and incubated at room temperature without shaking in a closed microfuge tube. At the timepoints listed, microfuge tubes were quickly vortexed to resuspend bacteria, and the cfu were enumerated on nonselective media.

Cell culture

All cell lines were obtained directly from the American Type Culture Collection (ATCC). HeLa human cervical adenocarcinoma epithelial cells were cultured in Dulbecco's Modified Eagle Medium (Mediatech, Manassas, VA) supplemented with 10% fetal bovine serum (HyClone, Logan, UT). RAW264.7 murine macrophage-like cells were cultured in RPMI 1640 1X (Mediatech, Manassas, VA) supplemented with 10% fetal bovine serum. All cell lines were propagated at 37°C in 5% CO_2.

RNA expression analysis (primates and bacteria)

RNA expression analysis of inflammatory cytokines in rhesus macaque tissues was performed as described (179). For RpoS-regulated gene expression analysis in *Salmonella* strains, RNA isolation, cDNA synthesis and quantitative PCR (qPCR) was performed as previously reported with modifications as noted (196). Briefly, bacteria were grown in LB broth to OD_{600} ~2.0. One-half ml of bacterial culture was combined with 1 ml of Qiagen RNAprotect Bacteria Reagent (Qiagen, Valencia, CA), the suspension was pelleted by centrifugation and the supernatant removed. RNA isolation was performed using a Qiagen RNeasy Mini Kit per the manufacturer's protocol. Five-hundred ng of total RNA were converted to cDNA using a QuantiTect Reverse Transcription Kit (Qiagen, Valencia, CA). Primers used for qPCR are listed in Table S1. qPCR was performed using a SYBR Green master mix and CFX96 real-time

machine (Bio-Rad, Hercules, CA). Target expression levels were normalized to the housekeeping gene *rpoD*.

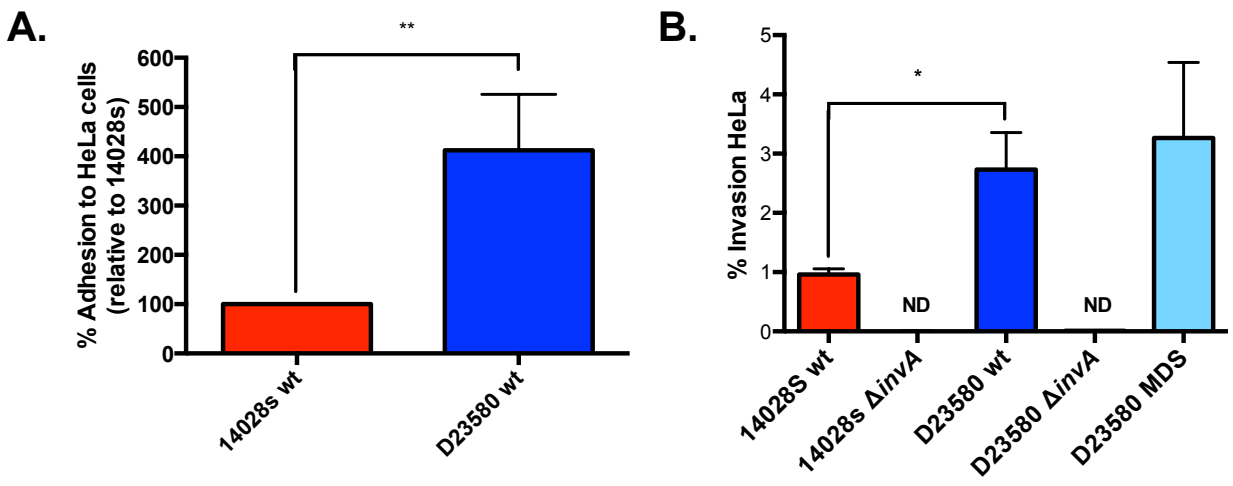

Fig. 10. D23580 is more adhesive and invasive for cultured cells than 14028s. (A) Confluent monolayers of HeLa human cervical epithelial cells were infected with stationary phase *S.* Typhimurium ST313 strain D23580 or ST19 strain 14028s at an MOI of ~100 for 15 min. Following PBS washing, intracellular cfu were enumerated by lysis and plating. Bacterial adhesion is expressed as a proportion of the starting inoculum. (B) Confluent monolayers of HeLa human cervical epithelial cells were infected with late-logarithmic phase *S.* Typhimurium ST313 strain D23580 or ST19 strain 14028s at an MOI of ~100 for 10 min. Intracellular cfu were enumerated 1 hr after internalization by lysis and plating. Bacterial invasion is expressed as a proportion of the starting inoculum. *invA* mutants were included as controls for reduced invasion. Statistical significance was determined using a paired t-test and is indicated as *, $P < 0.05$; ** $P < 0.01$.

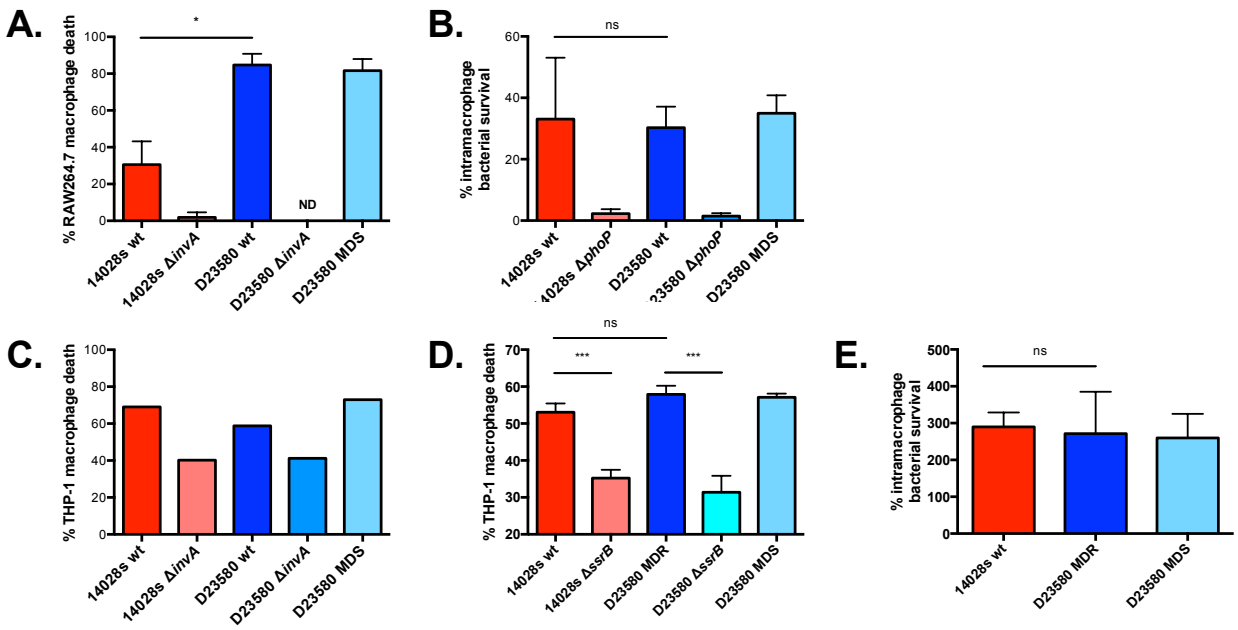

Fig. 11. D23580 is more invasive and cytotoxic for cultured cells than 14028s. (A) RAW264.7 murine macrophage-like cells were infected with late-logarithmic phase *S.* Typhimurium D23580 or 14028s at an MOI of ~10. Four hrs post-infection, culture supernatants were assayed for released lactate dehydrogenase as a measure of macrophage death. *invA* mutants were included as SPI1-deficient controls. (B) RAW264.7 murine macrophage-like cells were infected with opsonized stationary-phase *S.* Typhimurium D23580 or 14028s at an MOI of ~10. Eighteen hrs post-infection, macrophages were lysed and intracellular cfu enumerated. Bacterial survival is expressed as a proportion of internalized bacteria remaining at 18 hrs post-infection. *phoP* mutants were included as controls with reduced intramacrophage survival. (C) THP-1 human macrophage-like cells were infected with late-logarithmic phase *S.* Typhimurium D23580 or 14028s at an MOI of ~30. Four hrs post-infection, culture supernatants were assayed for released lactate dehydrogenase as a measure of macrophage death. *invA* mutants were included as SPI1-deficient controls. 1 biological replicate shown. No statistical analysis performed. (D) THP-1 human macrophage-like cells were infected with opsonized stationary-phase *S.* Typhimurium D23580 or 14028s at an MOI of ~15. Twenty-four hrs post-infection,

culture supernatants were assayed for released lactate dehydrogenase as a measure of macrophage death. *ssrB* mutants were included as SPI2-deficient controls. (E) THP-1 human macrophage-like cells were infected with opsonized stationary-phase *S.* Typhimurium D23580 or 14028s at an MOI of ~15. Twenty-four hrs post-infection, macrophages were lysed and intracellular cfu enumerated. Bacterial survival is expressed as a proportion of internalized bacteria remaining at 24 hrs post-infection. Strain D23580 MDS was included as a control to exclude effects from deletion of plasmid-borne antibiotic-resistance determinants. Bars represent the mean ± SD. ND = Not detected. Statistical significance was determined using a paired t-test and is indicated as *, $P < 0.05$; *** $P < 0.001$.

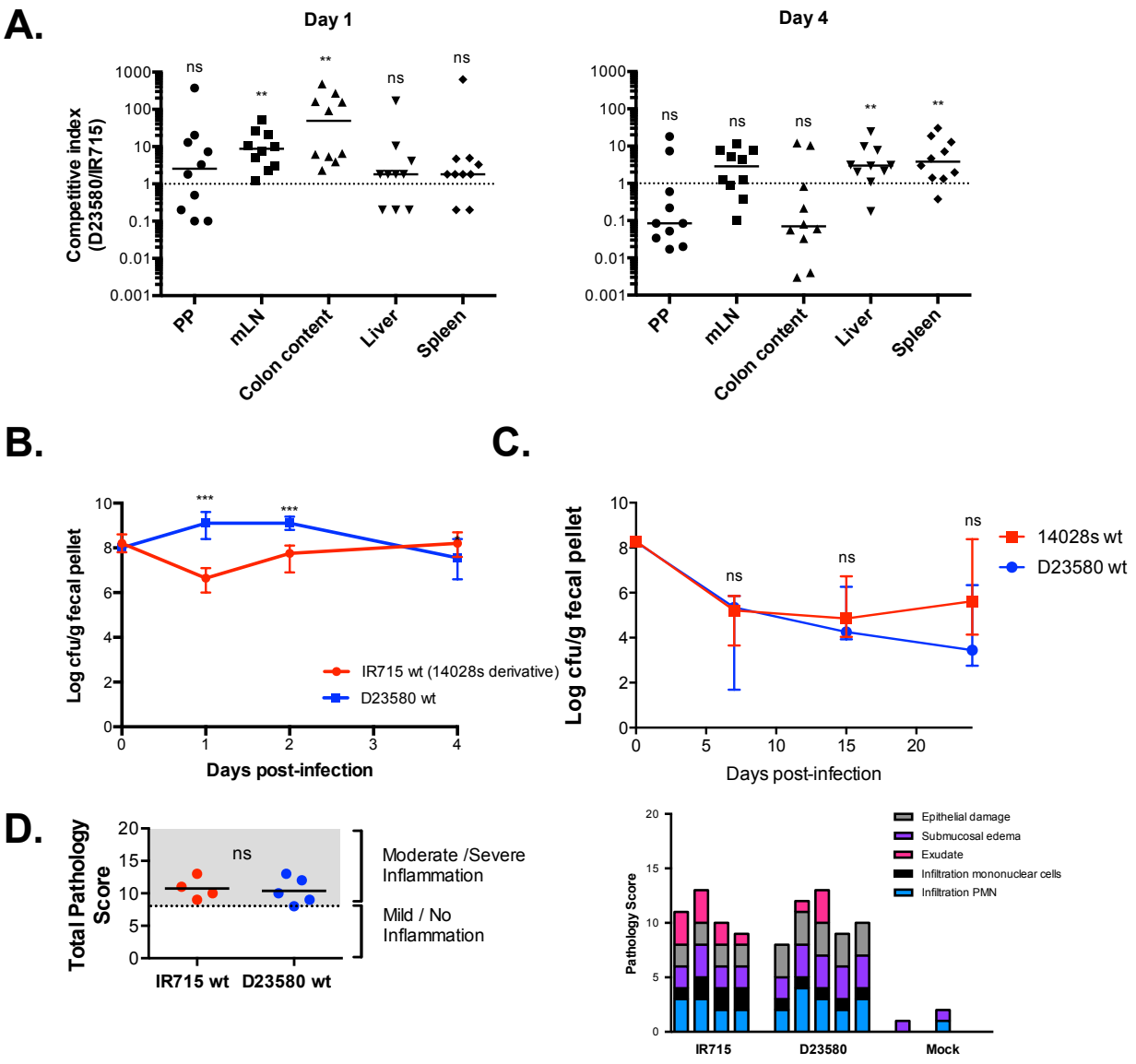

Fig. 12. D23580 efficiently colonizes the murine intestine. (A) CBA/J mice were pretreated with streptomycin for 24 hrs and i.g. infected with an ~1:1 mixture of *S.* Typhimurium ST313 strain D23580 and ST19 strain IR715. On days 1 and 4 post-infection, co-infected mice (n=10) were euthanized and cfu in Peyer's Patches (PP), mesenteric lymph nodes (mLN), colonic contents, liver and spleen were enumerated. Values greater than 1 indicate a competitive advantage of D23580 over IR715. Bars represent the median of values. Each symbol represents 1 mouse. Statistical significance was determined using an unpaired Wilcoxon signed rank test and is indicated as **, $P < 0.01$. (B) Fecal pellets from streptomycin-treated, i.g.-

infected CBA/J mice (n=10 per group) were collected and homogenized, and cfu were enumerated on days 1, 2, and 4 post-infection. Values represent the median ± range. Statistical significance was determined using a Mann-Whitney test and is indicated as *, $P < 0.05$ or ***, $P < 0.001$. (C) 129/Sv mice (n=10) were orally infected with an ~1:1 mixture of *S.* Typhimurium ST313 strain D23580 and ST19 strain 14028s. Fecal pellets of infected mice were collected and homogenized, and cfu were enumerated on days 7, 15, and 24 post-infection. Values represent the median ± range. Statistical significance was determined using a Mann-Whitney test. (D) Streptomycin-treated CBA/J mice were infected i.g. with *S.* Typhimurium D23580 or IR715. At 24 hrs post-infection, mice were euthanized followed by removal of the cecum for histopathological analysis. Blinded general and detailed cecal pathology scores for D23580- and IR715- and mock-infected mice (n=4) mice (n=4) are shown. For detailed analyses, each bar represents 1 mouse. Statistical significance was determined using a Mann-Whitney test on total histopathology scores.

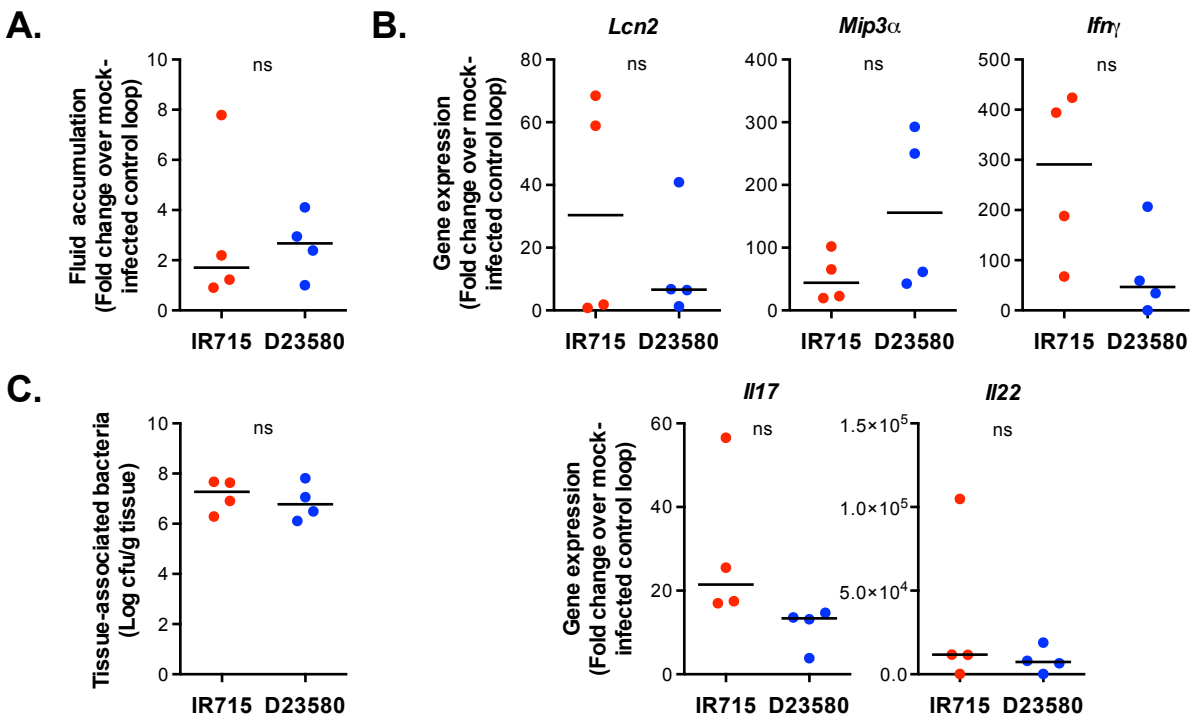

Fig. 13. D23580 elicits acute inflammation in the rhesus macaque intestine. Ligated ileal loops of anesthetized rhesus macaques (n=4) were infected with *S.* Typhimurium ST313 strain D23580, ST19 strain IR715 or an equivalent volume of sterile LB broth. (A) Fluid accumulation in the infected ileal loops was measured 5 hrs following injection. Results are expressed as the volume of fluid accumulated during infection compared to the volume of fluid accumulated following injection of sterile LB broth into a loop from the same animal. (B) Expression of inflammatory cytokines in the ileal mucosa of *S.* Typhimurium D23580- or IR715-infected ileal loops 5 hrs following injection. Results are shown as the amount of expression in infected ileal loops compared to the amount of expression in loops injected with sterile LB broth from the same animal. (C) Tissue-associated bacteria were measured 5 hrs following injection of the ileal loop. Bars represent the median of values. Each symbol represents 1 animal. Statistical significance was determined using a Wilcoxon matched-pairs signed rank test ($P > 0.05$).

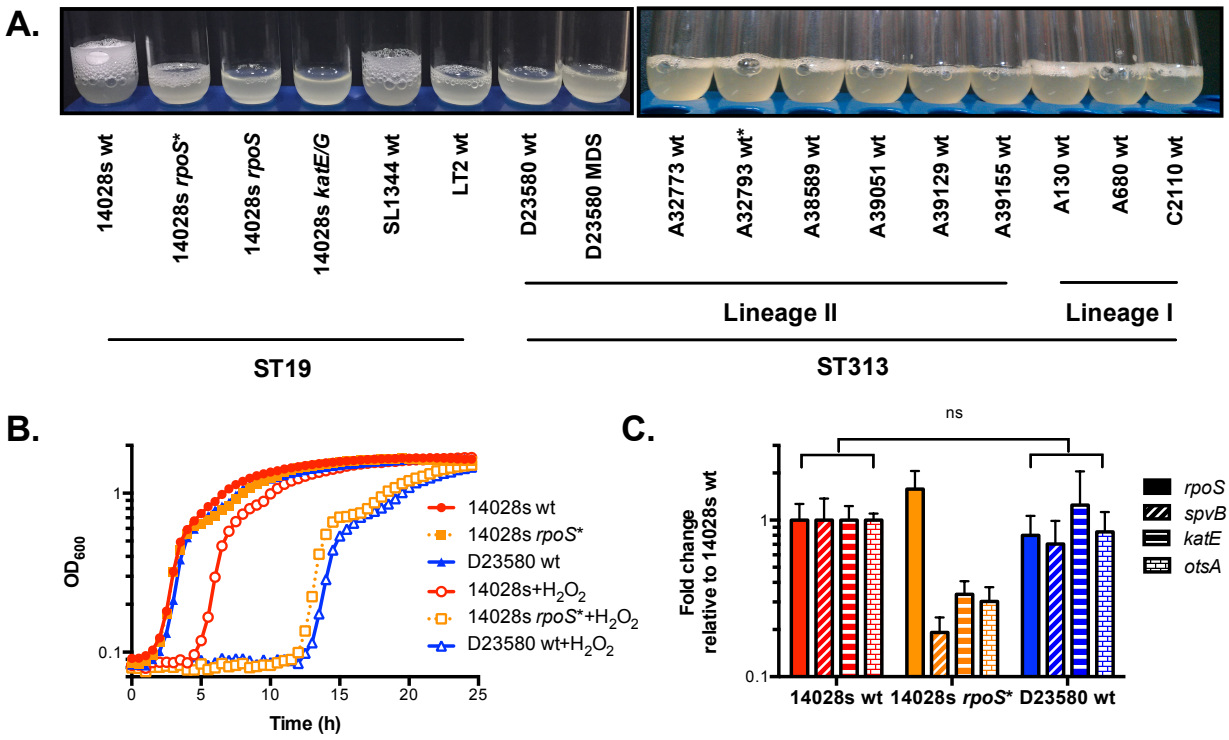

Fig. 14. D23580 exhibits deficient detoxification of hydrogen peroxide despite retaining σ^S-dependent gene expression. (A) Stationary-phase cultures of *S.* Typhimurium were grown for ~16-18 hrs before 20 µl of hydrogen peroxide (H_2O_2) were added to 1 ml of each culture. The height of the oxygen bubble column correlates with the ability of each strain to detoxify H_2O_2. (Left panel) *S.* Typhimurium strains 14028s *rpoS**, 14028s Δ*rpoS*, and LT2 are known *rpoS*-mutants and exhibit enhanced sensitivity to H_2O_2. (Right panel) Multiple independent ST313 strains exhibit deficient H_2O_2 detoxification. D23580 MDS was included as a control to exclude effects from deletion of plasmid-borne antibiotic-resistance determinants. *ST313 isolate A32793 was not sequenced and is of unknown lineage. (B) Stationary-phase cultures of *S.* Typhimurium were grown in the presence (open symbols) or absence (closed symbols) of 0.5 mM H_2O_2, and optical density was measured over time. A delay in the time to log-phase indicates an enhanced susceptibility to H_2O_2. The data shown are an average of 3 biological replicates. (C) *S.* Typhimurium strains were grown to stationary phase prior to harvesting of RNA. qPCR was performed to determine relative levels of mRNA for the σ^S (RpoS)-regulated

genes *spvB* (an ADP-ribosylating toxin), *katE* (stationary-phase catalase) and *otsA* (trehalose biosynthetic gene). Absolute qPCR values were normalized to the bacterial housekeeping gene *rpoD* and expressed as fold-change over wild-type 14028s. 14028s *rpoS** was included as a control for the effects of reduced σ^S-dependent gene expression. Statistical significance was determined using a paired t-test.

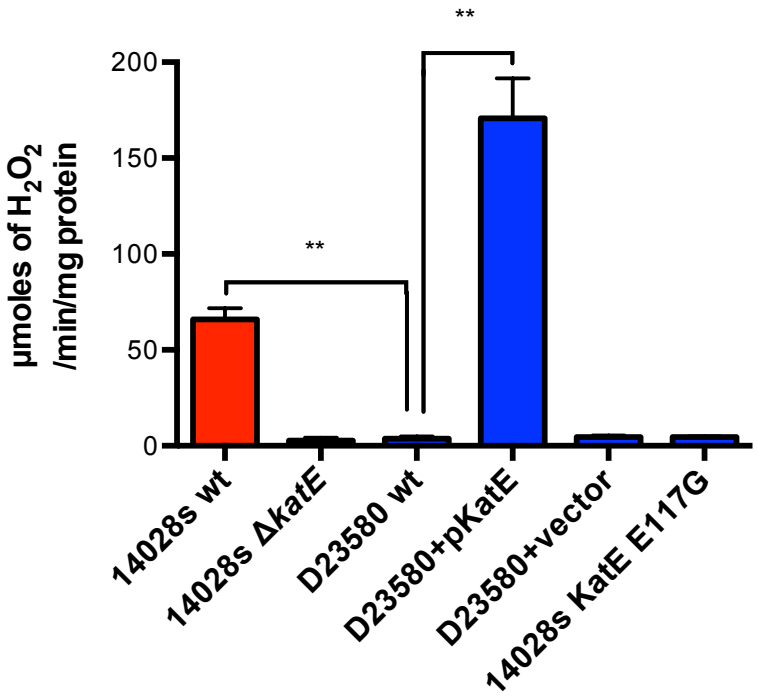

**, p < 0.01

Fig. 15. D23580 fails to detoxify hydrogen peroxide due to a mutation in the stationary-phase catalase KatE. Stationary-phase cultures of *S.* Typhimurium were sonicated over ice to release intracellular KatE before the addition of hydrogen peroxide (H_2O_2). Decay of H_2O_2 was monitored colorimetrically (A_{240}) over time. Heat-treated lysates were incubated at 55°C for 15 min to inactivate KatG, the heat-sensitive *Salmonella* catalase, before assaying for KatE activity. The strain 14028s *katE*::*tet*RA contains a targeted mutation inactivating *katE*. 14028s *katE*::*tet*RA is a KatE-null strain, a control for reduced stationary-phase catalase activity. D23580 MDS was included as a control to exclude effects of deleting plasmid-borne antibiotic-resistance determinants. Statistical significance was determined using a paired t-test and is indicated as **, P < 0.01.

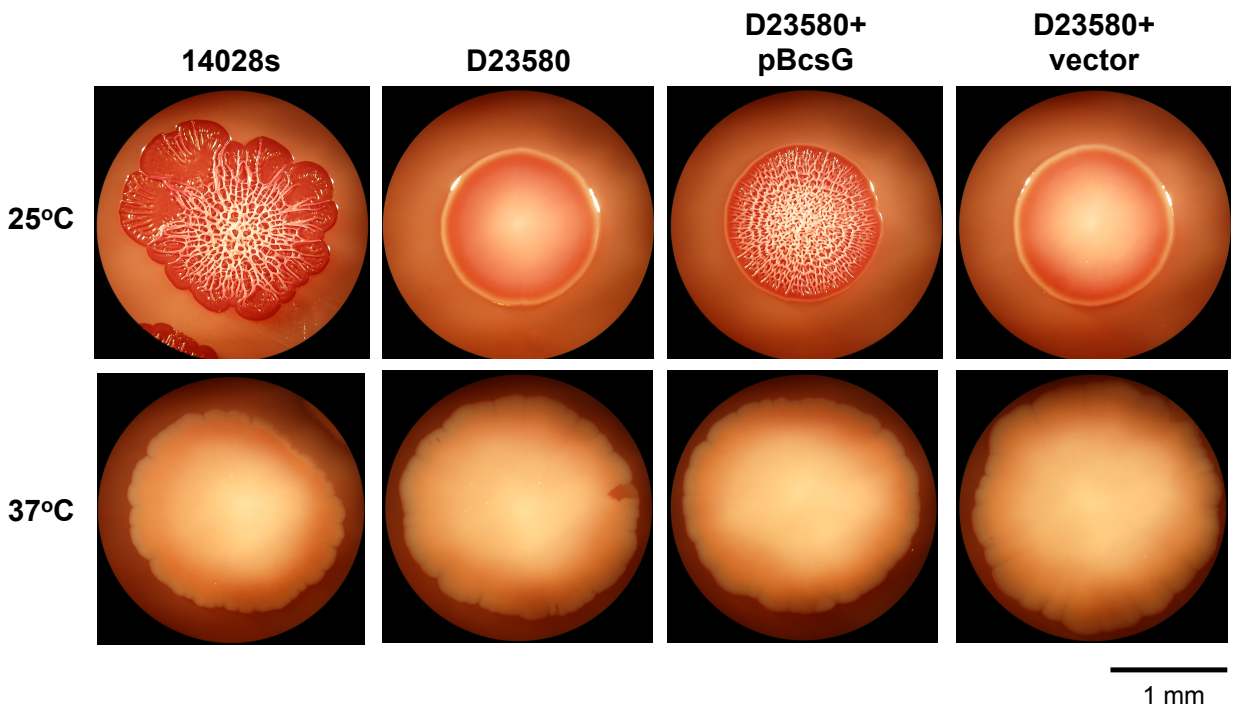

Fig. 16. D23580 is unable to form RDAR colonies due to a mutation in the cellulose synthetic enzyme BcsG. *S.* Typhimurium strains were grown overnight in LB broth and plated onto LB agar containing the dyes Congo Red and Coomassie Blue without salt. Colonies were grown for 7 d at 25°C or 37°C. RDAR (rough, dry and red) colonies are characteristically formed at 25°C and not 37°C. Pictures shown are representative examples.

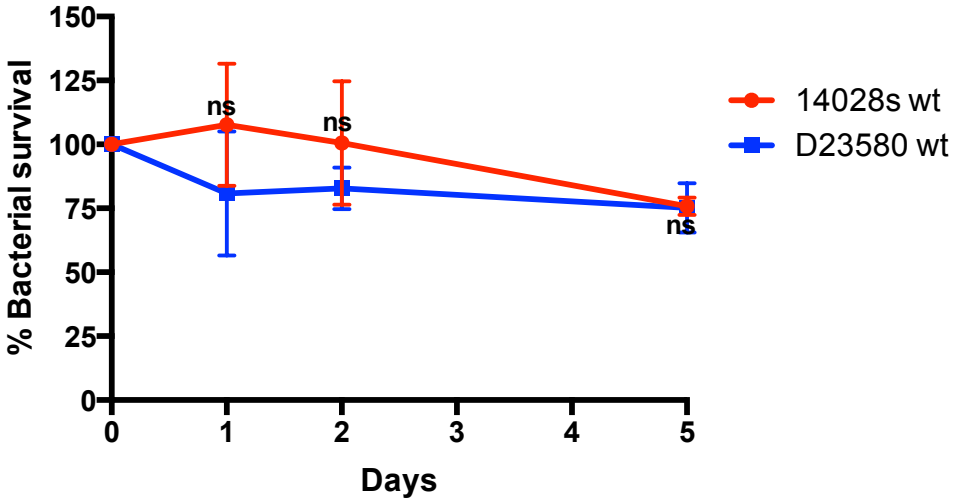

Fig. 17. Survival of D23580 and 14028s in water over 5 days. Bacteria were grown overnight in rich medium at 37°C, washed 2 times in PBS, and once in sterile water. Washed bacteria were then diluted 10-fold into sterile water, incubated without shaking at room temperature, and assayed for cfu at indicated timepoints. Data shown are the mean of three biological replicates. Statistical significance was determined using a paired t-test.

Table 4. Strains, plasmids, primers.

Strain, plasmid or primer	Genotype, relevant characteristics, or sequence[a]	Source or reference
Strains		
A130	*Salmonella* Typhimurium ST313 wild-type strain	(150)
A680	*Salmonella* Typhimurium ST313 wild-type strain	(150)
A32773	*Salmonella* Typhimurium ST313 wild-type strain	(150)
A32793	*Salmonella* Typhimurium ST313 wild-type strain	(150)
A38589	*Salmonella* Typhimurium ST313 wild-type strain	(150)
A39051	*Salmonella* Typhimurium ST313 wild-type strain	(150)
A39129	*Salmonella* Typhimurium ST313 wild-type strain	(150)
A39155	*Salmonella* Typhimurium ST313 wild-type strain	(150)
C2110	*Salmonella* Typhimurium ST313 wild-type strain	(150)
FLS267	*Salmonella* Typhimurium strain D23580 Nal^R GyrA	This study

	S83F pSLT-14028s::*tetRA* *invA*::FRT-*kan*	
FLS	*Salmonella* Typhimurium strain D23580 Nal^R GyrA S83F pSLT-14028s::*tetRA* *ssrB*::FRT-*kan*	This study
JK560	*Salmonella* Typhimurium 14028s *phoP120*::Tn*10*dCm	(197)
JK999	*Salmonella* Typhimurium 14028s *rpoS**	(21)
JK1114	*Salmonella* Typhimurium ST313 wild-type strain D23580 wild-type (Fang Lab)	(150)
JK1115	*Salmonella* Typhimurium 14028s pSLT-14028s::*tetRA*	This study
JK1124	Spontaneous Nal^R derivative (GyrA S83F) of *Salmonella* Typhimurium D23580	This study
JK1128	Multiple drug sensitive derivative of *Salmonella* Typhimurium D23580. Nal^R GyrA S83F pSLT-14028s::*tetRA*	This study
JK1168	*Salmonella* Typhimurium D23580 GyrA S83F pSLT-	This study

	14028s::*tetRA*/pKD46	
JK1217	*Salmonella* Typhimurium 14028s *invA*::FRT-*kan*	This study
JK1222	*Salmonella* Typhimurium D23580 Nal^R GyrA S83F pSLT-14028s::*tetRA* *phoP*::FRT-*kan*	This study
JK1228	*Salmonella* Typhimurium 14028s *katE*::*tetRA*	This study
JK1250	*Salmonella* Typhimurium 14028s KatE E117G	This study
JK1269	*Salmonella* Typhimurium 14028s *rpoS*::FRT-*cat*	This study
KLL6	*Salmonella* Typhimurium ST313 wild-type strain D23580 (Tsolis Lab)	(150)
KLL24	*Salmonella* Typhimurium ST19 strain IR715 (pHP45Ω) resistant to nalidixic acid, ampicillin, and streptomycin	(198) (199)
LAS18	*Salmonella* Typhimurium ST19 wild-type strain 14028s *ssrB*::FRT-*kan*	This study
LAS120	*Salmonella* Typhimurium ST19 wild-type strain 14028s	ATCC

LAS206	*Salmonella* Typhimurium ST19 wild-type strain SL1344	via C. Detweiler
LAS209	*Salmonella* Typhimurium ST19 wild-type strain LT2	ATCC
SL2759	*Salmonella* Typhimurium 14028s *katE::*Tn*10* *katG::*pRR10Δ*trfA* Pen^R	(168)
Plasmids		
pKD4	*bla* FRT *kan* FRT PS1 PS2 *ori6K*	(147)
pKD13	*bla* FRT *kan* FRT PS1 PS4 *ori6K*	(147)
pKD46	*bla araC*-P_{araB} γ β *exo* *oriR101* repA101(Ts)	(147)
pLAS1	pRB3::14028s *katE*	This study
pLAS2	pRB3::14028s *bcsG*	This study
pRB3	*par* RK2 *bla* stable low-copy-number cloning vector	(175)
Primers		
JKP409-pSLT-*tetR*	ACAACCAGCAGCGCGGAG AATTTGTGTCTGCAGAGTA AGATTAAGACCCACTTTCA CATT	This study
JKP410-pSLT-*tetA*	CACTTTACGGCTATGCCC GCGTTTCAACCAGCGATC	This study

	AGGACTAAGCACTTGTCTC CTG	
JKP428-*rpoS* F	CATCGTCAAATGGTTGTTC G	This study
JKP429-*rpoS* R	TTTCACGGCCTACATCTTC C	This study
JKP430-*katE* F	GCGGTATTCCACGCAGTT AT	This study
JKP431-*katE* R	CAGTGGAAACGGACAAAG GT	This study
JKP432-*rpoD* F	GTGGCTTGCAATTCCTTGA T	This study
JKP433-*rpoD* R	ACCAGGTTGCATAGGTGG AG	This study
JKP434-*spvB* F	GGGCGATTGTAGAGGAAT CA	This study
JKP435-*spvB* R	TCACTGGGTTCATTTGTGG A	This study
JKP444-*otsA* F	AGGCGGAACTGAAAAATG TG	This study
JKP445-*otsA* R	TAACGAATTTTTCCCCGAT G	This study
JKP507-*invA*P1	ATACCTATAGTGCTGCTTT CTCTACTTAACAGTGCTCG TTGTGTAGGCTGGAGCTG	This study

	CTTC	
JKP508-*invA*P2	TAATTAAGCCCTTATATTG TTTTTATAACATTCACTGA CTCATATGAATATCCTCCT TAG	This study
JKP511-*phoP*P1	ATGATGCGCGTACTGGTT GTAGAGGATAATGCATTAT TACGTGTAGGCTGGAGCT GCTTC	This study
JKP512-*phoP*4	GACCAGCGCCACTATGCC ATATGCCAAAGAAAGCAC CAGCATTCCGGGGATCCG TCGAC	This study
JKP539-KatE-E127-TetR	TTTTATCCTGCGCGAGAAA ATTACCCACTTTGACCATG AGTTAAGACCCACTTTCAC ATT	This study
JKP540-KatE-E127-TetA	CTGCAGATCCGCGGGCGT GAACGATCCTCTCCGGGA TGCGCTAAGCACTTGTCTC CTG	This study
LASP500-14028s *katE*-5' *Bam*HI	TCTAGAGTCGGGATCCTT CCGCTCTCCCCCAGCATA A	This study
LASP501-14028s *katE*-3’	GCATGCCTGCAAGCTTTTA	This study

*Hind*III	TGCAGGAATCGCGTTAAT	
LASP502-14028s *bcsG*-5' *Bam*HI	TCTAGAGTCGGGATCCGCCGTATCAGTGATACGACCC	This study
LASP503-14028s *bcsG*-3' *Hind*III	GCATGCCTGCAAGCTTTTACTGCGGGTAAGGCACCCA	This study
SP27-*rpoS cat* replacement F	TTGCTAGTTCCGTCAAGGGATCACGGGTAGGAGCCACCTTGTGTAGGCTGGAGCTGCTTC	This study
SP28-*rpoS cat* replacement R	AAGGCCAGTCGACAGACTGGCCTTTTTTTGACAAGGGTACATGGGAATTAGCCATGGTCC	This study
Lcn2 F	AGTTCACACTGGGCAACAT	(200)
Lcn2 R	TTCTCCTTTAGTTCCGAAG	(200)
Mip3α F	TCCTGGCTGCTTTGATGTCA	(200)
Mip3α R	GAAGGATACGGTCTGTATATCGAAGAC	(200)
Ifnγ F	CCAAGTGATGGCTGAACTGTCG	(200)
Ifnγ R	TCTGACTCCTTTTTCGCTTCCC	(200)

Il17 F	CAATCCCACGAAATCCAG GATG	(200)
Il17 R	GGTGGAGATTCCAAGGTG AGG	(200)
Il22 F	TCCGCGGAGTCAGTATGA GTGAGC	(200)
Il22 R	GAACCTATCCGATTGAGG GAGCAGC	(200)

[a]FRT, Flippase recombination target; All primer sequences are listed 5'-3'.

Chapter 4

Characterization of a novel operon contributing to *Salmonella* virulence

LAS contribution: Conceived study with F.C.F. and performed all experiments. Data in Fig. 18 were collected with assistance from Stephen J. Libby (mouse infections). Data in Fig. 19 were collected with Taylor Stepien. Unpublished preliminary data referenced in this chapter include *S*. Typhi TraDIS library construction, humanized mouse infections and bioinformatic analysis performed by Joyce Karlinsey with help from Stephen J. Libby (animal infections) and the Fred Hutchinson Cancer Research Center (FHCRC) bioinformatics group.

Abstract

Salmonella enterica serovar Typhi (*S*. Typhi), the etiologic agent of typhoid fever, causes over 20 million infections and 200,000 deaths annually. These numbers underscore the need for better strategies for typhoid prevention. *S*. Typhi is an obligate human pathogen, which makes the study of *S*. Typhi pathogenesis challenging. *Salmonella enterica* serovar Typhimurium (*S*. Typhimurium) is said to cause a 'typhoid-like' illness in mice and is employed as a model for typhoid fever. However, although *S*. Typhi and *S*. Typhimurium are genetically similar, there are substantial differences between these *Salmonella* serovars with regard to their genetic composition and interaction with host immunity. Consequently, *S.* Typhimurium infections in mice do not fully recapitulate crucial aspects of *S*. Typhi infection in humans. Human tissue culture cells and humanized mouse models of infection may provide novel insights into *S.* Typhi virulence determinants. A screen of a high-density *S*. Typhi transposon mutant library during infection of humanized mice revealed that a novel 5-gene operon was required for survival in the liver and spleen. A targeted *ppo* deletion was constructed and confirmed that this operon was also required for *S.* Typhimurium virulence in conventional mice. Based on partial sequence homology to known transport systems, the operon was tentatively

designated the "putative permease operon," henceforth referred to as *ppo*. Although some genes in the operon were related to loci involved in carbohydrate metabolism, *Salmonella ppo* mutants failed to exhibit growth defects on various single-carbon sources. Screening for the ability of a *S*. Typhi *ppo* mutant to grow a broad range of alternative nutrient sources or in the presence of chemical stressors identified a potential role for the *ppo* operon in the maintainance of membrane stability. *Salmonella ppo* mutants failed to grow as rapidly as isogenic wild-type bacteria in the presence of the metal chelator EDTA and were resistant to the toxic effects of the amino acid D-serine. EDTA-sensitivity and D-serine resistance can result from altered proton-motive force in bacteria. Using the fluorescent dye $DiOC_2(3)$, I have discovered that *Salmonella ppo* mutants exhibit hyperpolarization of the membrane potential compared to wild-type. Investigation of the contribution of this operon to *Salmonella* membrane physiology is presently under investigation.

Introduction

Salmonella enterica serovar Typhi (*S*. Typhi), the causative agent of typhoid fever, is a human-restricted pathogen. Much of what is known about human typhoid pathogenesis is gleaned from studies of *Salmonella enterica* serovar Typhimurium (*S*. Typhimurium) infection of mice. However,such studies cannot recapitulate all aspects of *S*. Typhi infection of humans as ~12% of the *S*. Typhi genome is unique and absent in generalist serovars like *S*. Typhimurium (26). Additionally, *S*. Typhimurium encodes several novel elements in its genome, not found in *S*. Typhi, that influence it's pathogenesis in both mice and humans (26, Table 2 of chapter 2). For example, *S*. Typhimurium carries the virulence plasmid pSLT that encodes an ADP-ribosylating toxin, SpvB, which is important for virulence in mice (26, 120, 121, 130) and correlates the bloodstream infections in humans (Flerer, J Infect Dis, 1992). Given the important genetic differences between *S*. Typhi and *S*. Typhimurium, there are limitations to what can be inferred about typhoid pathogenesis from animal models of *Salmonella* infection (55). Although

multiple human cell lines exist, until recently no whole animal model systems were available to allow the direct study of *S*. Typhi pathogenesis. In 2010, the our laboratory published a study characterizing the development of a humanized mouse model for acute lethal typhoid infection (124). Non-humanized mice are highly resistant to infection with *S*. Typhi, even at high infectious doses (124). However, when mice are engrafted with human hematopoietic stem cells, a human hematopoietic system is reconstituted, rendering the engrafted mice susceptible to *S*. Typhi infection (124). Following development and characterization of this humanized mouse model of typhoid infection, a high-density *S.* Typhi transposon mutant library was constructed (J. Karlinsey, unpublished data) (201, 202) and used to infect humanized mice in order to identify essential virulence factors (J. Karlinsey and S. Libby, unpublished data). This approach was validated by the demonstration that mutants harboring insertions in known *S*. Typhi virulence factors, such as the Vi capsule, were highly counterselected following intraperitoneal (ip) infection of humanized mice (J. Karlinsey, unpublished data). Mutants with insertions in a 5 gene operon (*t4474-t4478*) were also counterselected in the humanized mouse typhoid model (J. Karlinsey, unpublished data). Although this putative 5-gene operon is present in *S*. Typhimurium, it has not been previously implicated in *Salmonella* virulence.

Results

A novel operon is important for typhoid virulence in humanized mice

A transposon-mutant library of *S.* Typhi strain Ty2 was constructed using a Tn22 transposon-derivative to generate a library of over 1 million discrete Ty2 mutants (J. Karlinsey, unpublished data) (201). Typhoid-susceptible humanized mice were infected with the Ty2 mutant library to identify genes essential for systemic virulence (J. Karlinsey and S. Libby, unpublished data) (124). Upon becoming moribund, the mice were euthanized, and their livers and spleens were aseptically removed, homogenized and plated onto sterile LB agar plates (J. Karlinsey and S. Libby, unpublished data). *Salmonella* mutants counterselected during

humanized mouse infections were identified using transposon-directed insertion-site sequencing (TraDIS) (J. Karlinsey, unpublished data) (201, 203).

The *S*. Typhi Ty2 genes *t4475-4478* were counter-selected during infection (J. Karlinsey, unpublished data). These genes are not unique to *S*. Typhi and have counterparts in *S*. Typhimurium designated *STM14_5332-5335* in strain 14028s, and are also found in several non-*Salmonella* genera (139). As humanized mice are a limited and expensive resource, we elected to further investigate a possible role in virulence in a conventional mouse model of *S*. Typhimurium infection. Twenty C3H/HeN mice were infected i.p. with ~1700 cfu of a 1:1 mixture of *S*. Typhimurium 14028s wt and an isogenic, kanamycin-resistant *STM14_5332-5335* deletion mutant. Five days post-infection (pi), the mice were sacrificed and their livers and spleens aseptically removed, homogenized and plated onto sterile LB agar. Single colonies were picked and grown on kanamycin-containing LB plates to determine the proportion of *STM14_5332-5335* mutant *Salmonellae* in each organ. In liver and spleens, the 14028s *STM14_5332-5335* mutant was significantly underrepresented in comparison to wt (Fig. 18A), confirming a requirement for these genes for full virulence. We also investigated whether *STM14_5332-5335* influenced survival of non-humanized mice during *Salmonella* infection. Twelve and 13 non-humanized C3H/HeN mice were infected with 1000 cfu of 14028s wt or an isogenic *STM14_5332-5335* mutant, respectively. Mice were sacrificed once moribund or upon reaching the study end date (21 days pi), whichever came first. Mice infected with the 14028s *STM14_5332-5335* deletion mutants had a significant increase in median survival compared to wt-infected mice (Fig. 18B). These studies confirmed the results of the humanized mouse Ty2-mutant library screen indicating that this operon is important for invasive Salmonellosis in mice.

We next investigated whether *S*. Typhimurium *STM14_5332-5335* deletion mutants were defective for growth and/or *Salmonella*-induced macrophage cytotoxicity in murine RAW264.7 macrophage-like cells. RAW264.7 cells were seeded into tissue-culture wells 24h before infection. The cells were then infected with mouse-serum opsonized, stationary-phase *S*.

Typhimurium strain 14028s or an isogenic *STM14_5332-5335* mutant at a multiplicity of infection (MOI) of ~10. Bacteria were centrifuged onto macrophage monolayers to synchronize infection and internalized for 1 hr. Following internalization, monolayers were washed with medium containing the membrane-impermeant antibiotic gentamicin. Twenty-four hr pi, macrophages were lysed and intracellular cfu enumerated. Supernatants were collected and the concentration of LDH quantified as a measure of cell death. I found that 14028s *STM14_5332-5335* mutants had a more than three-fold defect in intramacrophage survival as compared to wt (Fig. 19A; performed in conjunction with T. Stepien). *S.* Typhimurium 14028s mutants lacking *ssrB*, the SPI2 T3SS, or the transcriptional regulator *phoP* were included as intramacrophage replication-deficient controls (Fig. 19A; performed in conjunction with T. Stepien). No defect in *Salmonella*-induced macrophage cytotoxicity were observed for the 14028s *STM14_5332-5335* mutant (Fig. 19B; performed in conjunction with T. Stepien). These data indicate that a defect in intramacrophage replication of 14028s *STM14_5332-5335* mutants correlates with the observed defect in mouse virulence (Fig. 18, 2).

The operon has no evident role in carbohydrate metabolism

Having identified that the *STM14_5332-5335* genes are important for *S.* Typhi and *S*. Typhimurium virulence in mice, I further investigated the possible function of the operon by employing *in silico* analytical tools such as PSI-BLAST and I-TASSER. PSI-BLAST iteratively queries protein sequence databases for similarities or matches to a target sequence (139, 204). I-TASSER (iterative threading assembly refinement) uses known protein structures from the Protein Data Bank (PDB) as templates upon which to thread or model unknown amino acid sequences of interest (205, 206). A summary of this analysis is presented in Table 5. A schematic depiction of the operon is also provided (Table 5). I included the Ty2 gene *t4474* (14028s *STM14_5331*) in my analysis, despite lack of counter-selection of this locus during the humanized mouse Ty2 mutant library screen, because of its proximity to the four highly

counterselected genes, henceforth referred to as the 5-gene operon (Table 5). Both PSI-BLAST and I-TASSER strongly predicted that *t4474*, the first gene in the putative operon, was a PTS (phosphoenolpyruvate:sugar phosphotransferase system) regulation domain (PRD)-containing protein (Table 5). PRD-containing proteins are typically associated with regulation of carbohydrate catabolism (207). I-TASSER analysis of *t4475* revealed its predicted structure had strong homology to the *Escherichia coli* (*E. coli*) ribose-5-phosphate isomerase RpiB (Table 5). Bacterial ribose-5-phosphate isomerases are part of the catabolic pentose-5-phosphate pathway and catalyze the reversible conversion of D-ribose 5-phosphate to D-ribulose 5-phosphate (208). *Salmonellae* encode one primary ribose-5-phosphate, *rpiA* (Ty2 *t2981*; 14028s *STM14_3701*), which is responsible for 99% of the ribose-5-phosphate isomerase activity in cells (209). Some bacteria such as *E. coli*, but not *S. enterica*, encode an additional ribose-5-phosphate isomerase called *rpiB* (210). The remaining genes in the operon, *t4476-4478*, were annotated as hypothetical proteins with poor and unreliable structural models generated by I-TASSER (Table 5).

As two of the 5 genes in the putative operon had potential links to carbohydrate metabolism, I examined the ability of *S*. Typhimurium lacking the 5-gene operon to grow on 13 different pentose-, hexose-, and other sole-carbon sources (Fig. 20). The Salmonella strains were grown overnight in LB broth with shaking at 37°C. Cultures were normalized to OD_{600} 2.5 and diluted 100X in M9 minimal medium lacking any carbon source. Thirty µl of this suspension was used to inoculate 270 µl of M9 minimal medium plus the carbon source of interest. Bacterial OD_{600} was monitored every 15 minutes for 24h with shaking at 37°C using a Bioscreen C microplate reader (Labsystems, Helsinki, Finland). *S*. Typhimurium 14028s *STM14_5332-5335* mutants exhibited no growth defects on any single carbon source tested (Fig. 20). All strains tested were unable to grow on D-ribulose, D-lyxose, D-xylose and D-xylulose as a sole carbon source. Although bioinformatic analysis suggested possible involvement of these genes in

carbohydrate metabolism, I was unable to demonstrate a specific growth defect of *S.* Typhimurium 14028s lacking *STM14_5332-5335* on any of the carbon sources tested.

The operon may be important for maintainance of membrane integrity in *Salmonella*

Having been unable to identify a carbohydrate utilization defect in 14028s lacking STM14_5332-5335, I performed an extensive phenotypic screen to examine growth of the mutant in the presence of other single carbon sources or in the presence of various stress conditions using a Biolog phenotypic microarray (211). *S*. Typhimurium 14028s wt, Δ*STM14_5331-5335* and Δ*spvR* (as a control for the kanamycin-resistance marker) strains were streaked onto LB agar and grown overnight, then streaked onto 0.2X TYE agar and again grown overnight. Colonies from these plates were harvested and suspended in IF-0 inoculating broth. The turbidity of each suspension was measured and equalized to 85% transmittance. Normalized suspensions were combined with a proprietary redox-sensitive dye to monitor bacterial growth and used to inoculate twenty 96-well phenotypic array microtiter plates (Biolog, Hayward, CA) (Appendices 1, 2). Growth was monitored for 48h at 37°C without shaking in an Omnilog machine (Biolog, Hayward, CA). The individual growth curves of each strain under each condition were compiled into overlapping growth curves to facilitate comparison between strains (Appendix 3). A summary of the differences in growth between 14028s wt and the *STM14_5331-5335* mutant is included in Table 6. The most dramatic differences between wt and the *STM14_5331-5335* mutant strain were during growth in the presence of the metal chelator EDTA, the amino acid D-serine, or the antibiotics phleomycin and tobramycin (Table 6).

A possible trend emerged from the significant Biolog phenotypes (Table 6). Both D-serine and the antibiotic tobramycin are toxic for bacteria (212). 14028s *STM14_5331-5335* mutants were resistant to both D-serine and tobramycin toxicity (Table 6). Uptake of tobramycin, like all aminoglycosides, is dependent upon bacterial proton-motive force (PMF) (213), and bacteria with altered PMF are resistant to tobramycin toxicity. D-serine is also toxic to some

bacteria (212) and is transported into cells via the PMF-dependent D-alanine transporter (214, 215). Therefore, resistance of 14028s *STM14_5331-5335* mutants to D-serine and tobramycin toxicity might result from perturbed PMF in these mutants. If perturbation of PMF is due to a loss of membrane integrity in the *STM14_5331-5335* mutant, then growth in the presence of the metal-ion chelator EDTA or the cell wall-damaging agent phleomycin could further destabilize bacterial cells and inhibit growth, as we observed (Table 6).

I first confirmed the most significant phenotypes observed in the phenotypic microarrays. As the phenotypic microarray conditions are largely proprietary, recapitulating the conditions under which phenotypes were observed required trial and error. *Salmonella* strains were grown overnight in LB broth with shaking at 37°C. Overnight bacterial cultures were normalized to OD_{600} 2.5 then diluted 100X in LB medium lacking EDTA. Thirty µl of this suspension was used to inoculate 270 µl of M9 minimal medium plus varying concentrations of EDTA. Bacterial OD_{600} was measured every 15 min for 48h with shaking at 37°C using a Bioscreen C microplate reader (Labsystems, Helsinki, Finland). Both *S*. Typhi Ty2 and *S*. Typhimurium 14028s and their isogenic 5-gene deletion mutants were tested for EDTA sensitivity. Although I had some difficulty precisely replicating the EDTA-sensitivity phenotype in 14028s, I was able to demonstrate that the Ty2 *t4474-4478* mutant was more sensitive to EDTA compared to wt (Fig. 21). An increased lag phase during growth in the presence of EDTA is indicative of an organism's increased sensitivity to that compound. Additional conditions are presently being employed to assess the *S*. Typhimurium *STM14_5332-5335* deletion mutant.

As for EDTA-sensitivity, confirming the D-serine resistance phenotype in the 5-gene deletion mutants of *S*. Typhi Ty2 and *S*. Typhimurium 14028s proved difficult. Various concentrations of D-serine were employed but failed to inhibit *Salmonella* growth (Fig. 22). It is possible that additional modifications of the culture medium will be required to observe this phenotype.

I next investigated whether PMF was altered in mutant bacteria lacking the 5-gene operon. PMF is generated from electrical and chemical gradients according to the following equation: PMF = Δψ-60ΔpH where Δψ is the membrane potential and ΔpH is the proton gradient. A ratiometric assay was employed to measure bacterial membrane potential (216). Salmonella strains were grown overnight in LB broth. Bacteria were diluted 1000X into fresh LB and grown to ~OD_{600} 1.5 at 37°C with shaking. Two µl of OD_{600} 1.5 bacterial culture were added to 1 ml of permeabilization buffer containing the membrane polarization-sensitive dye $DiOC_2(3)$ (216). The suspension was vortexed and incubated for 15 min in the dark before assaying a LSRII flow cytometer (Becton Dickinson). Both *S*. Typhi Ty2 and *S*. Typhimurium 14028s 5-gene mutant strains exhibited membrane hyperpolarization in comparison to their respective wt parental strains (Fig. 23). Membrane hyperpolarization may be a compensatory response to changes in the proton gradient resulting from reduced membrane integrity. Further experimentation will be required to test this hypothesis.

Discussion

Although many studies to identify *S*. Typhimurium genes required for virulence in mice have been performed, some important virulence loci may have been overlooked. Our laboratory recently performed a screen of *S*. Typhi Ty2 transposon mutants during infection of a unique humanized mice model. The novel candidate virulence genes identified included a 5-gene operon designated *t4474-4478* (screen performed by J. Karlinsey and S. Libby, unpublished data). This operon is also found in *S*. Typhimurium 14028s (*STM14_5331-5335*) and in several other enteric bacteria, but has not been previously implicated in virulence. As humanized mice are a scarce resource, we further evaluated the possible contribution of these genes to *Salmonella* virulence using a conventional mouse model and *S*. Typhimurium strain 14028s.

A *S*. Typhimurium 14028s *STM14_5332-5335* mutant was found to be deficient in competitive infections with wt *S*. Typhimurium in C3H/HeN mice (Fig. 18A). In addition,

STM14_5332-5335 mutants were found to cause reduced mortality than isogenic wt *S.* Typhimurium (Fig. 18B). I further found that *STM14_5331-5335* mutants were defective in their ability to replicate in cultured macrophages but not in their ability to induce macrophage cell death (Fig. 19, performed in conjunction with T. Stepien). The observed defect in intramacrophage replication may help to account for the virulence defect (Fig. 18), as the ability to survive inside macrophages is required for systemic infection of mice (64).

A bioinformatic analysis of *t4474-4478* using NCBI's PSI-BLAST and I-TASSER (205, 206, 217, 218) suggested that *t4474* and *t4475* might be involved in bacterial carbohydrate metabolism (Table 5). Ty2 *t4474* was predicted to encode a protein contaning a phosphoenolpyruvate:sugar phosphotransferase system (PTS) regulation domain (Table 5). PTS regulation domain (PRD)-containing proteins are almost exclusively found in proteins associated with carbohydrate uptake and metabolism (207) and are activated in response to specific carbon source availability (219), acting as transcriptional antiterminators or activators (207, 219). *S.* Typhi *t4475* was predicted to encode a ribose-5-phosphate isomerase (Table 5). Bacterial ribose-5-phosphate isomerases catalyze the reversible conversion of ribose-5-phosphate to ribulose-5-phosphate in the pentose phosphate pathway (208). *S. enterica* encodes a constitutively expressed ribose-5-phosphate isomerase called RpiA that is responsible for 99% of the ribose-5-phosphate isomerase activity in cells (209). Some bacteria including *E. coli*, but not *S. enterica*, encode an additional ribose-5-phosphate isomerase called RpiB (210). The specific *in vivo* conditions under which RpiB isomerase activity is important have not been studied. However, RpiB has been implicated in the utilization of the rare sugar D-allose, a C-3 epimer of glucose (220). However, if Ty2 T4475 is a functional homolog of *E. coli* RpiB as predicted (Table 5), it would be unlikely to be involved in *Salmonella* D-allose catabolism, as the D-allose degradative pathway is absent in both *S*. Typhi and *S*. Typhimurium (139). Perhaps T4475 is expressed when RpiA is inactive (221, 222).

Despite *in silico* evidence for the involvement of these genes in carbohydrate metabolism, *S.* Typhimurium 14028s *STM14_5332-5335* deletion mutants had no observable defects in growth on various single-carbon sources (Fig. 20). Growth on D-allose was only measured in the Biolog phenotypic microarray screen at a single unknown concentration, and no growth defect was observed (Appendix 3). However, both *S*. Typhi Ty2 and *S*. Typhimurium 14028s have intact *rpiA* genes, so that a defect in carbon source utilization might not be apparent unless the primary ribose-5-phosphate isomerase encoded by *rpiA* is abrogated. Reexamining single carbon source utilization in an *rpiAB* null background might yield insights into the function of the *STM14_5331-5335* and *t4474-4478* operons.

Finding no role for the operon during carbohydrate metabolism, I took a broader approach to identifying a possible role of these genes in *Salmonella* metabolism, employing Biolog phenotypic microarrays to examine the growth of wt 14028s and its isogenic *STM14_5331-5335* mutant derivative during 1,920 different growth conditions (211). A summary of the significant advantageous and disadvantageous mutant phenotypes is listed in Table 6. Multiple mutant phenotypes hinted at a role for these genes in maintaining membrane integrity, the most significant of which were sensitivity to the metal-ion chelator EDTA and resistance to the toxic host metabolite D-serine and antibiotic tobramycin (Table 6; Fig. 21B; Appendix 3) (212, 223). The metal chelator EDTA destabilizes bacterial cell membranes by binding to calcium and magnesium (224). D-serine is transported into cells via the PMF-dependent D-alanine transporter (214, 215). While some bacteria, including *Salmonella*, encode a D-serine tolerance locus *dsdA*, this locus can be ineffective at high D-serine concentrations (225, 226). Like D-serine, the antibiotic tobramycin is imported in a PMF-dependent manner (213). Bacteria with impaired PMF are resistant to tobramycin (227). PMF is generated from electrical and chemical gradients according to the following equation: $PMF = \Delta\psi - 60\Delta pH$, in which $\Delta\psi$ is the membrane potential and ΔpH is the proton gradient. I measured the membrane potential of *S*. Typhi Ty2 and *S*. Typhimurium 14028s mutants and found that for mutant strains lacking the 5-

gene operon exhibited a *higher* membrane potential than wt (Fig. 23) (216). I hypothesize that this might represent a compensatory response to the loss of the physiologic trans-membrane pH gradient. Additional studies to measure the intracellular pH will test this hypothesis.

A possible role of this novel operon is to indirectly maintain bacterial membrane integrity by translocating carbohydrate intermediates, such as pentose phosphate pathway (PPP)-generated products. A variety of metabolic precursors are generated by the PPP, such as erythrose 4-phosphate, generated during the non-oxidative phase of the PPP and used for the biosynthesis of aromatic amino acids (228). Ribose-5-phosphate, also generated during the non-oxidative phase of the PPP, is a precursor for nucleotide synthesis (228). Frucose-6-phosphate, one of the final products of the PPP, serves as a precursor for the synthesis of N-acetylglucosamine (NAG) and N-acetylmuramic acid (MurNAc) (228). NAG and MurNAc are the backbone of peptidoglycan, an essential component of the bacterial cell wall (229). It is important to note that *Salmonella aro* mutants, defective in their synthesis of aromatic amino acids, have cell wall defects (230). Moreover, *E. coli* cell wall mutants are hypersusceptible to EDTA-stress as well as resistant to the toxic effects of D-methionine in an energy-dependent manner (231, 232). If *STM14_5331-5335* mutants have altered levels of PPP intermediates like erythrose 4-phosphate, this may result in reductions in membrane integrity and the trans-membrane proton gradient, leading to EDTA hypersusceptibility and D-serine/tobramycin resistance (Table 6). In future studies, it may be worth investigating whether these mutants are hypersensitive to osmotic shock or lysis by agents such as lysozyme (233).

In conclusion, my observations indicate that *STM14_5331-5335* and *t4474-4478* play an important role in *Salmonella* physiology and virulence, and may link carbohydrate metabolism to the maintenance of PMF. Additional studies to identify the substrate or substrates transported by the proteins encoded by this operon may reveal their specific function. One possible approach would be to embed the proteins were in lipid vesicles and analyze the contents by mass spectrometry (234).

Materials and Methods

Bacterial strains, genetic manipulations and growth conditions

Bacterial strains and primers are listed in Table 7. Unless otherwise stated, all chemicals were purchased from Sigma-Aldrich (St. Louis, MO) or Fisher Scientific (Waltham, MA). The λ-red recombinase system of *E. coli* was used to generate *Salmonella* mutants (147). Briefly, PCR was performed with primers containing ~40 bp of homology to the 5' or 3' end of a gene of interest and ~20 bp of homology to the kanamycin-resistance gene of pKD4 or pKD13. Confirmation of mutant construction was performed by PCR. Strains were cultured in Luria-Bertani (LB) medium for 18 hrs with shaking at 250 rpm at 37°C. Kanamycin was supplemented at 50 μg ml^{-1} unless otherwise stated.

Animals

All animal experiments were approved by the University of Washington Institutional Animal Care and Use Committee and performed in accordance with guidelines regarding animal welfare.

Cell culture

All cell lines were obtained directly from the American Type Culture Collection (ATCC). RAW264.7 murine macrophage-like cells were cultured in RPMI 1640 1X (Mediatech, Manassas, VA) supplemented with 10% heat-inactivated fetal bovine serum (Cellgro). All cell lines were propagated according to ATCC recommendations at 37°C in 5% CO_2.

Non-humanized mouse infections

For competitive infections, 20 non-humanized C3H/HeN mice were infected i.p. with ~2000 cfu of a 1:1 mixture of wt *S*. Typhimurium 14028s and 14028s Δ*STM14_5332*-

5335::FRT-*kan*. Five dpi, mice were sacrificed; livers and spleens were aseptically removed and homogenized using a Power Gen 125 (Fisher Scientific) and plated onto sterile LB agar. Single colonies were picked and then grown on kanamycin-containing LB agar to determine the proportion of mutant *Salmonella* in each organ. Competitive indices were determined as the cfu of wt 14028s divided by the cfu of 14028s Δ*STM14_5332-5335*::FRT-*kan*, normalized to input inocula. For mouse survival experiments, 12 and 13 non-humanized C3H/HeN mice were infected with ~1000 cfu of wt or Δ*STM14_5332-5335*::FRT-*kan S*. Typhimurium, respectively. Mice were sacrificed upon becoming moribund or on the study end date (21 dpi), whichever came first. These data represent two biological replicates.

***Salmonella* intramacrophage survival assay**

For murine macrophage infections, $7.5x10^4$ RAW264.7 murine macrophage-like cells were seeded into 96-well tissue-culture plates 24 hrs before infection. *Salmonella* strains were grown in LB broth for 18 hrs with shaking at 37°C. *Salmonella* cultures were adjusted to OD_{600} 1.0 and washed twice with sterile PBS (Cellgro). Equal parts *Salmonella* and ice-thawed 100% mouse serum (Cellgro) were mixed and incubated at 37°C in 5% CO_2 for 20 min to opsonize bacteria. Opsonized bacteria were added to 1X RPMI 1640 (ATCC) and used to infect RAW264.7 murine macrophages an MOI of ~10. Infected monolayers were centrifuged for 5 min at 1000 rpm to synchronize infection then incubated at 37°C for 1 hr to promote internalization. Following internalization, monolayers were washed with RPMI supplemented with 20 μg ml^{-1} gentamicin to kill extracellular bacteria. Twenty-four hpi, medium was removed from wells and macrophages lysed with 1% Triton X-100 to enumerate intramacrophage bacteria. Survival is expressed as the percent intracellular *Salmonella* surviving as compared to T_0.

***Salmonella*-induced human macrophage cytotoxicity assay**

RAW264.7 murine macrophage-like cells were infected as for the *Salmonella* intramacrophage survival assays. Twenty-four hpi, supernatants from *Salmonella*-infected macrophages were collected and the concentration of lactate dehydrogenase quantified using the CytoTox96 Cytotoxicity Kit (Promega) per the manufacturer's protocol. Percent cytotoxicity was calculated as follows: ((Experimental release-Spontaneous release)/(Maximum release-Spontaneous release)) x 100.

Bioinformatic analysis of genes of unknown function (PSI-BLAST and I-TASSER)

The amino acid sequences of *S*. Typhi Ty2 *t4474, t4475, t4476, t4477* and *t4478* were obtained from the National Center for Biotechnology Information's (NCBI) GenBank (AE014613.1) (235, 236). Amino acid sequences were submitted to the NCBI's standard protein basic local alignment tool (BLAST) using the position-specific iterated BLAST (PSI-BLAST) algorithm (217). Each amino acid sequence was also submitted to the University of Michigan's iterative threading assembly refinement (I-TASSER) server for protein structure and function prediction (205, 206, 218).

Analysis of *Salmonella* growth on sole carbon sources

To measure growth of Salmonella strains on single carbon sources, overnight cultures of *Salmonella* were diluted to a final OD_{600} of 0.0025 in M9 minimal broth supplemented with the carbon sources indicated at a final concentration of 0.04% w/v. The OD_{600} was measured at 15 min intervals for 24h with vigorous shaking at 37°C in a Bioscreen C microplate reader (Labsystems, Helsinki, Finland).

EDTA and D-serine susceptibility assays

To measure the ability of *Salmonella* strains to grow in the presence of the toxic compounds EDTA or D-serine, overnight cultures of *Salmonella* were diluted to a final OD_{600} of

0.0025 in dilute LB broth (1:5 in sterile water) with or without EDTA or D-serine at the concentrations listed. The OD_{600} was measured at 15 min intervals for 48h with shaking at 37°C in a Bioscreen C microplate reader (Labsystems, Helsinki, Finland).

Phenotypic microarray growth analysis

Bacteria were prepared for phenotypic microarray growth analysis as described (237). Briefly, *S*. Typhimurium 14028s wt, Δ*STM14_5331-5335*::kan-FRT and Δ*spvR*::kan-FRT (a control for the kanamycin-resistance marker) strains were streaked onto LB agar and grown overnight. LB-agar grown *Salmonella* were then streaked onto 0.2X TYE agar and grown overnight. Colonies from these plates were harvested and suspended in IF-0 inoculating broth. The turbidity of each suspension was measured and equalized to 85% transmittance. Normalized suspensions were diluted then used to inoculate 20 phenotypic microarray plates according to the manufacturer's recommended protocol. Biolog Phenotypic MicroArrays were used to evaluate the growth of *Salmonella* strains under 1,920 different conditions. The following phenotyping plates were used: PM1, PM2A, PM3B, PM4A, PM5, PM6, PM7, PM8, PM9, PM10, PM11C, PM12B, PM13B, PM14A, PM15B, PM16A, PM17A, PM18C, PM19, PM20B. *Salmonella* growth was monitored for 48h without shaking at 37°C on an Omnilog machine (Biolog, Hayward, CA).

Membrane potential assay

The membrane potential of *S*. Typhi Ty2 wt, Ty2 Δ*t4474-4478*::kan-FRT, *S*. Typhimurium 14028s wt and 14028s Δ*STM14_5331-5335*::kan-FRT strains was assayed by a ratiometric method using the fluorescent dye 3,3'-Diethyloxacarbocyanine iodide ($DiOC_2(3)$) (216). Salmonella strains were grown overnight in LB broth with shaking at 37°C. Overnight cultures were diluted 100X into fresh LB medium and grown to late-logarithmic phase with shaking at 37°C. Cultures were diluted into permeabilization buffer (1 mM EDTA in 10 mM Tric-

HCl) containing the 30 μM of the dye $DiOC_2(3)$. Cultures were incubated for 15 min in the dark before immediate analysis on a LSRII flow cytometer (Becton Dickinson).

Acknowledgments

We thank Colin Manoil and Samuel Lee (Manoil lab) for their help in performing the Biolog phenotypic microarrays.

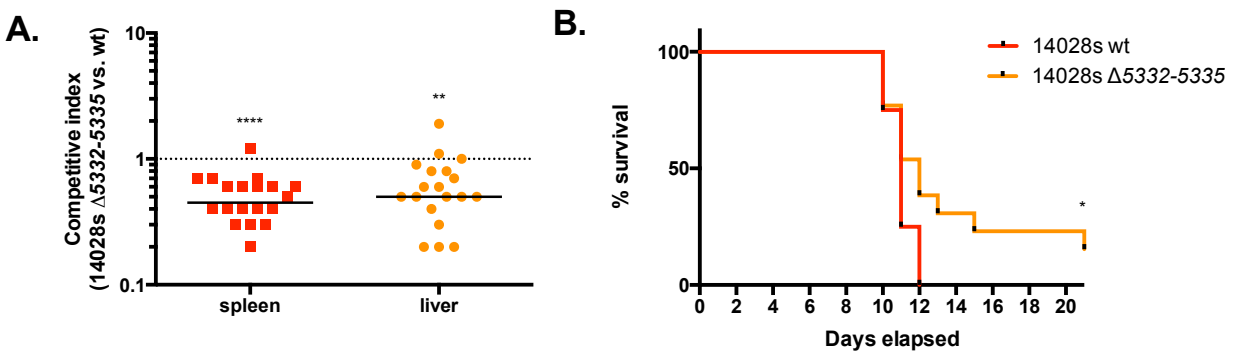

Figure 18. *S.* Typhimurium *STM14_5332-5335* mutants are attenuated for virulence in conventional mice. (A) Twenty C3H/HeN mice were infected ip with ~2000 cfu of a ~1:1 mixture of *S.* Typhimurium 14028s wt and an isogenic *STM14_5332-5335* mutant strain. Five days post-infection, mice were sacrificed and the organism burden (cfu) of each strain in the liver and spleen enumerated. Values less than one indicate a competitive disadvantage of the *STM14_5332-5335* mutant. Bars represent the median of values. Each symbol represents one mouse. Statistical significance was determined using an unpaired Wilcoxon signed rank test and is indicated as ** P < 0.01; **** P <0.0001. (B) Twelve and 13 C3H/HeN mice were infected ip with ~1000 cfu of *S.* Typhimurium 14028s wt or the *STM14_5332-5335* mutant, respectively. Mice were sacrificed upon becoming moribund or on the study end date 21d post-infection. Statistical significance was determined using a log-rank test and is indicated as * P = 0.05.

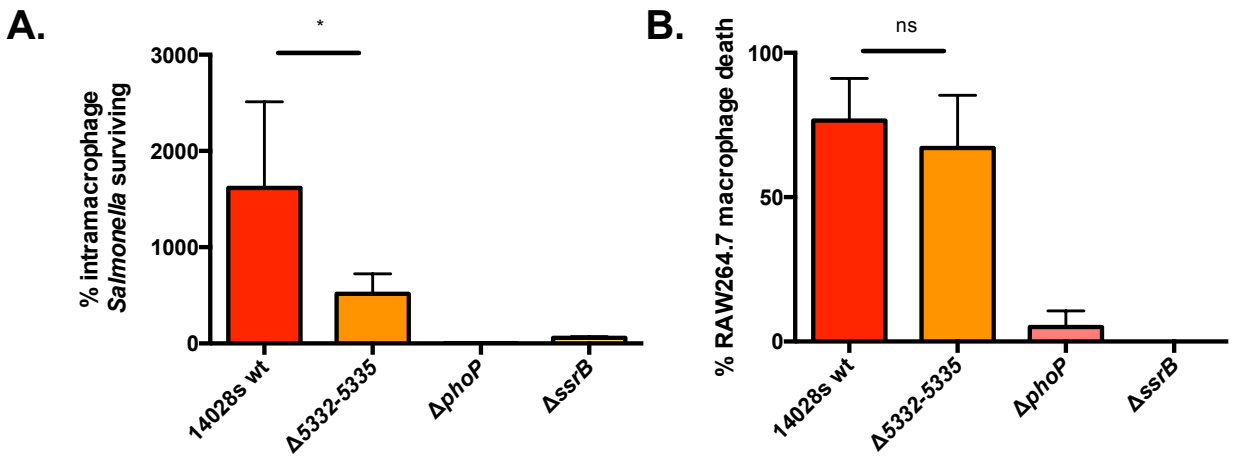

Figure 19. Survival of *Salmonella* in a murine macrophage cell line. Murine RAW264.7 macrophage-like cells were infected with opsonized stationary-phase *S.* Typhimurium 14028s wt or an *STM14_5332-5335* mutant at a MOI of ~10. At 24h post-infection, macrophages were lysed and intracellular bacteria enumerated. Bacterial survival is expressed as the proportion of internalized bacteria compared to T_0. (B) Supernatants were collected 24h post-infection and LDH quantified as a measure of macrophage cell death. Statistical significance was determined using a ordinary one-way ANOVA and is indicated as *, P = 0.05.

Ty2 #	NCBI annotation	Protein structure/function prediction	Source
T4474	Hypothetical protein	Glycine dehydrogenase; PRD-containing protein EF_0829 superfamily (PRD domain protein) PRD-containing transcriptional regulator (*strong predicted structure*)	PSI-BLAST I-TASSER
T4475	Hypothetical protein	Hypothetical protein; transcriptional regulator Gly-rich-SFCGS and EF_0830 superfamily Ribose-5-phosphate isomerase B RpiB (*good predicted structure*)	PSI-BLAST I-TASSER
T4476	Hypothetical protein	Hypothetical protein; cytoplasmic protein DUF4312 superfamily and EF_0831 Poor model generated	PSI-BLAST I-TASSER
T4477	Putative membrane protein	Membrane protein; hypothetical protein; permease DUF4311 superfamily and EF_0832 Poor model generated	PSI-BLAST I-TASSER
T4478	Putative membrane protein	Membrane protein; hypothetical protein; phosphotransferase DUF4310 Poor model generated	PSI-BLAST I-TASSER

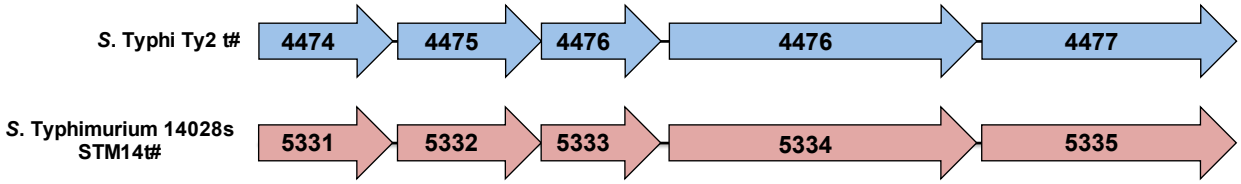

Table 5. Protein structure/function prediction analysis reveals a potential role of T4474-4478 in carbohydrate metabolism. The amino acid sequences of *S*. Typhi Ty2 T4474-4478 were submitted to PSI-BLAST and I-TASSER for structure/function prediction analysis. A summary of the results is presented. A schematic depiction of the operons in *S*. Typhi Ty2 and *S*. Typhimurium 14028s is shown.

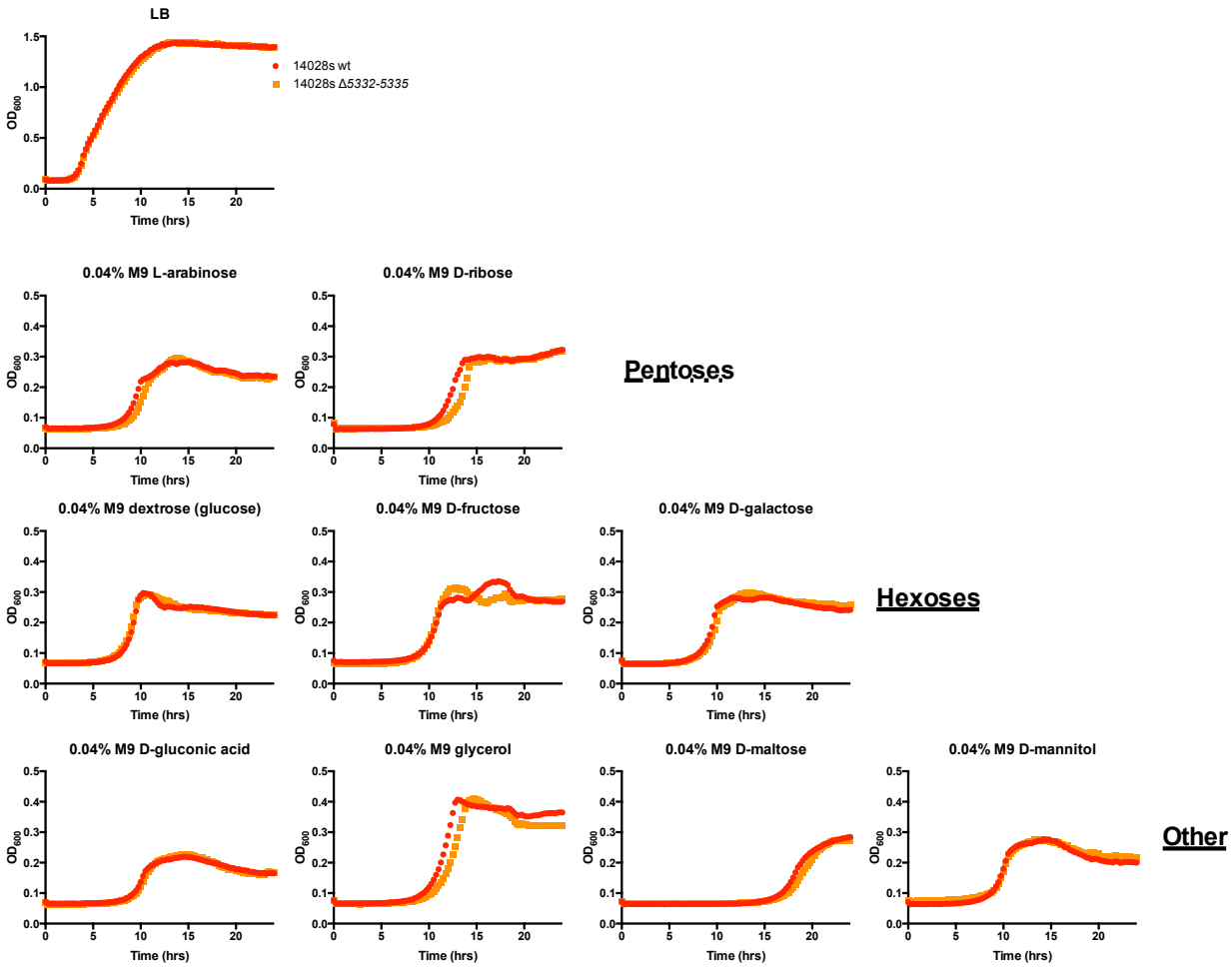

Figure 20. Growth of *Salmonella* strains on single carbon sources. *S.* Typhimurium 14028s wt or the isogenic mutant Δ*STM14_5332-5335* were grown in the presence of the single carbon sources indicated. A delay in the time to log-phase indicates a defect in the ability of the organism to utilize the specified carbon source. The data shown are representative growth curves.

Advantageous mutant phenotypes	
Compound	***Function***
Menadione	Superoxide generator
α-keto-butyric acid	Metabolism intermediate, precursor of citric acid cycle substrates
NaCl	Osmolyte
Urea	Chaotropic agent; osmolyte
Tobramycin	Aminoglycoside antibiotic; interferes with ribosome function
5,7-Dichloro-8-hydroxyquinoline (chloroxine)	Antibiotic; causes DNA damage
Chlorpromazine	May inhibit proton motive force-dependent pumps in gram positive bacteria [Marquez, 2005]
D-serine	Toxic to some bacteria like E. coli
Oxytetracycline	Tetracycline antibiotic; interferes with ribosome function

Disadvantageous mutant phenotypes	
Compound	***Function***
EDTA	Metal ion chelator
Phleomycin	Intercalates within DNA
Sodium azide	Bacteriostatic agent
Antimony trichloride	Genotoxic agent; can influence the pH of media
Iodonitrotetrazolium violet	Redox sensitive dye
8-hydroxy-quinoline	Metal ion chelator

Table 6. Biolog phenotypic microarray results summary. Growth of *S.* Typhimurium 14028s wt and its isogenic *STM14_5331-5335* mutant was monitored under 1,920 different conditions. The most significant advantageous and disadvantageous mutant growth phenotypes are summarized above.

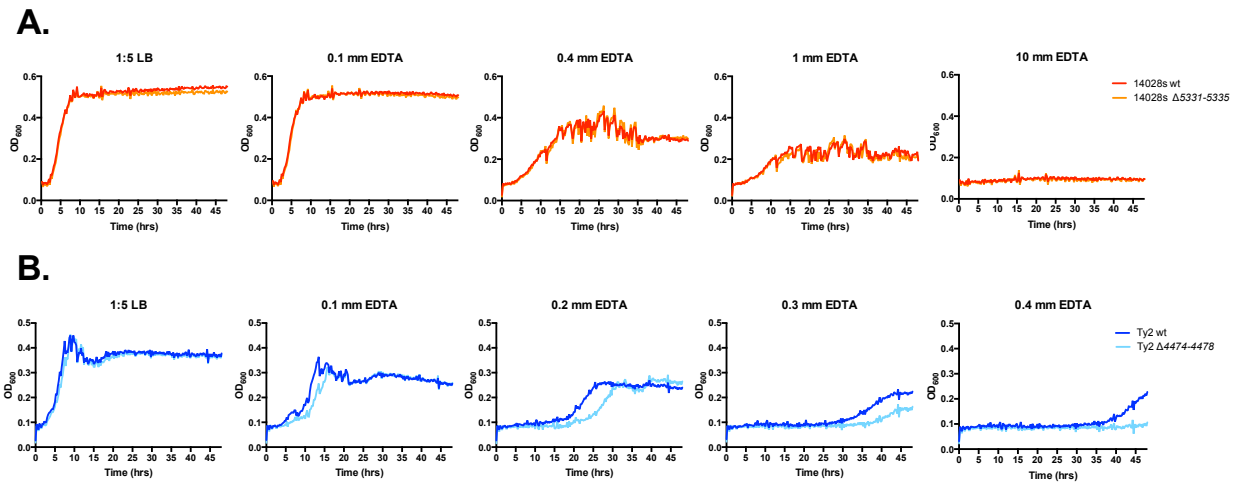

Figure 21. Ty2 *t4474-4478* mutants are hyper-susceptible to EDTA stress. (A) *S.* Typhimurium 14028s wt and 14028s Δ*STM14_5331-5335* or (B) *S.* Typhi Ty2 wt and Ty2 Δ*t4474-4478* strains were grown in dilute LB broth with or without the addition of EDTA at the listed concentrations. A delay in the time to log-phase indicates increased susceptibility to EDTA stress. The data shown are representative growth curves.

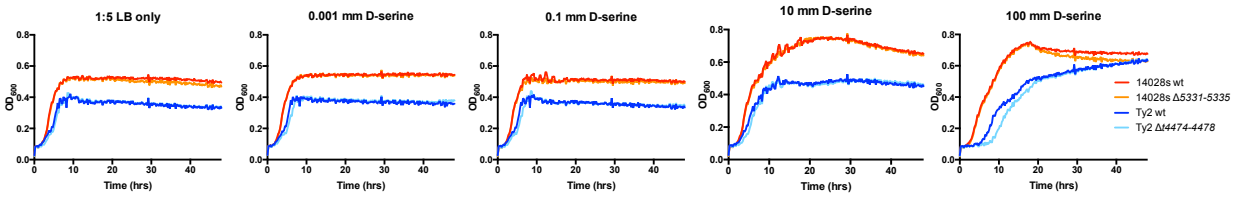

Figure 22. Growth of *Salmonella* in the presence of the toxic host-metabolite D-serine. *S.* Typhimurium 14028s wt, 14028s Δ*STM14_5331-5335, S.* Typhi Ty2 wt and Ty2 Δ*t4474-4478* strains were grown in dilute LB broth with or without the addition of D-serine at the concentrations indicated. A delay in the time to log-phase indicates increased susceptibility to D-serine toxicity.

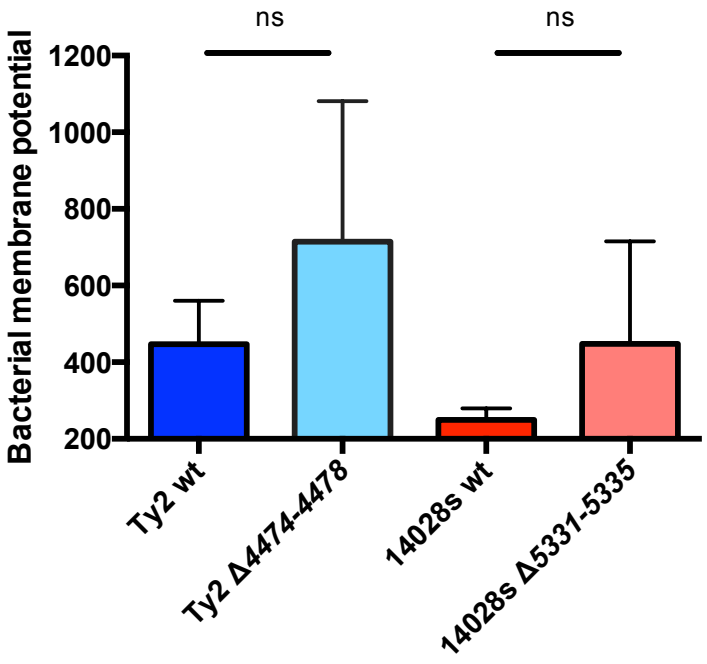

Figure 23. *Salmonella* STM14_5331-5335 and *t4474-4478* operon mutants exhibit membrane hyper-polarization. *S*. Typhimurium 14028s wt, 14028s Δ*STM14_5331-5335*, *S*. Typhi Ty2 wt and Ty2 Δ*t4474-4478* strains were grown to late-logarithmic phase, stained with the membrane potential sensitive dye $DiOC_2$ and analyzed by flow cytometry. Statistical significance was determined using a ratio paired t-test.

Table 7. Strains and primers.

Strain, plasmid or primer	Genotype, relevant characteristics, or sequence	Source or reference
Strains		
LAS5	*Salmonella* Typhimurium wild-type strain 14028s	ATCC
LAS93	*Salmonella* Typhimurium 14028s *STM14_5332-5335*::FRT-*kan*	This study
LAS155	*Salmonella* Typhimurium 14028s *STM14_5331-5335*::FRT-*kan*	This study
TY3	*Salmonella* Typhi wild-type strain Ty2	JSG624 from J. Gunn
LAS275	*Salmonella* Typhi Ty2 *t4474-4478*::FRT-*kan*	This study
SL2678	*Salmonella* Typhimurium 14028s *spvR*::Tn5-*kan*	(238)
Primers		
14028s S*TM14_5332-5335 kan* replacement F	ATGGAACAGATTACCGTC GTGATTGGCGATCGCCTG GGTATGTGTAGGCTGGAG CTGCT	This study
14028s S*TM14_5332-5335*	TTAGCTAATCGCAACCGG	This study

kan replacement R	GAAGATGGAACCGAGGAT CATCCATATGAATATCCTC CTTA	
Ty2 *t4475-4478 kan* replacement F	ATGGAACAGATTACCGTC GTAATTGGCGATCGCCTG GGTATGTGTAGGCTGGAG CTGCT	This study
Ty2 *t4475-4478 kan* replacement R	TTAGCTAATCGAAACCGG GAAGATGGAACCGAGGAT CATCCATATGAATATCCTC CTTA	This study
Ty2 *t4474-4478*/14028s S*TM14_5331-5335 kan* replacement F	TGGATAACGGAGCAGTAA AACACGATGCCGGTGAGC GAATGTGTAGGCTGGAGC TGCTTC	This study
Ty2 *t4474-4478* /14028s S*TM14_5331-5335 kan* replacement R	ACCAGAGAGCCCAGACCA ATAGGAATCGATGCCGTC ATGGCATATGAATATCCTC CTTAG	This study

Appendix 1. Growth analysis for *S*. Typhimurium 14028s wt, Δ*STM14_5331-5335,* and Δ*spvR* on plates PM1-20. Black lines = 14028s wt; yellow lines = Δ*STM14_5331-5335*, red lines = Δ*spvR* (control strain for kanamycin-resistance marker).

Chapter 5:

Future directions

Typhoid fever presents a significant burden to developing countries, yet current typhoid vaccines are suboptimal. Typhoid vaccine development is limited by the current models of *Salmonella* pathogenesis, which have relied upon the use of non-typhoidal *Salmonella* serovars in mice. The work presented here employs novel models for studying *Salmonella* pathogenesis and has implications for typhoid vaccine research and design.

Preventing *S*. Typhi infection in humans will become more important as the number of multi-drug resistant strains of *S*. Typhi increase and novel antibiotic discovery stagnates (29–33, 239). Current typhoid vaccines are suboptimal and have ~50-80% efficacy rates (51); Vivotif, the only live-attenuated typhoid vaccine available, has a combined three-dose efficacy of ~51%. While the Vivotif mechanism of protection is largely attributed to humoral responses, it has been shown that cell-mediated responses are key to resolving *Salmonella* infection possibly explaining the reduced efficacy of the Vivotif vaccine (114, 117, 240, 241).

Vaccine efficacy could be improved through better understanding of how *S*. Typhi interacts with and manipulates the human immune response to infection. Due to the use of *S*. Typhimurium infection of mice as a model for *S*. Typhi infection of humans, we may have a fundamental misunderstanding of *S*. Typhi's interaction with the human immune system. I have shown that *S*. Typhi decreases expression of SPI2 inside human macrophages and that this may account for its ability to avoid a M1/T_h1 response in human cells (Figures 4,8). This suggests that higher intramacrophage SPI2 expression *promotes* macrophage activation during infection, as is observed during *S*. Typhimurium infection of human macrophages. In contrast, several studies of *S*. Typhimurium infection of conventional mice have emphasized the importance of SPI2 in *avoiding* phagocyte activation. *Cheminay et al.* demonstrated that increased resistance to *Salmonella* reinfection occurred after vaccinating mice with a SPI2

mutant of *S*. Typhimurium compared to a SPI2-proficient strain (242). *Halici et al.* demonstrated that several SPI2 effectors are responsible for interfering with antigen presentation by dendritic cells during *Salmonella* infection (243). Given that Ty21a, the Vivotif vaccine strain, was indiscriminately chemically mutagenized during development it likely retains the ability to interfere with M1/T_h1 responses to infection, through reduced intramacrophage SPI2 expression, thereby possibly explaining one reason for its poor efficacy and lack of cell-mediated responses (241). Further studies to specifically understand how down-regulation of SPI2 expression by *S*. Typhi influences the M1/T_h1 response to infection may prove useful in development of a better live attenuated typhoid vaccine. Additionally, future typhoid vaccine research should focus on creating vaccines that target human immune responses specifically provoked by *S*. Typhi, not murine responses to *S*. Typhimurium.

The need to study *S*. Typhi infection of human-based systems highlights an additional need for development in this area. Currently, only two humanized mouse models of typhoid infection exist. One model, previously developed by the Fang lab in collaboration with scientists at the University of Massachusetts and Jackson Laboratories, is described in chapter two of this dissertation. Briefly, non-obese diabetic-scid *IL2rγ*^{null} (NOD-*scid IL2rγ*^{null}) mouse pups are irradiated then engrafted with T cell depleted, CD34$^+$ human umbilical cord blood partially reconstituting a human immune system in these mice (heretofore referred to as humanized mice) (124–126). Not only does *S*. Typhi replicate in these mice, but infected mice display several pathological and immunological hallmarks of typhoid fever (124). The second humanized mouse model of typhoid infection engrafts human fetal liver CD34$^+$ hematopoietic stem cells onto Rag2$^{-/-}$γc$^{-/-}$ mice in order to reconstitute a partial human immune system (244). *S*. Typhi replicates proficiently in these mice and they develop innate and adaptive immune responses to infection; however, these mice display no clinical symptoms of infection, in contrast to the former model (124, 244). Despite the advantages of the *Libby et al.* humanized mouse model, these mice are costly, laborious and variable in their engraftment levels.

Additionally, these mice do not contain Peyer's patches, a site of early immune responses to *Salmonella* infection and the gateway to the mesenteric lymph nodes. Without Peyer's patches, oral infection studies cannot be performed, hindering our understanding of early immune responses to *S*. Typhi infection.

The 5-gene operon identified during the TraDIS mutant screen in humanized mice is important to *Salmonella* virulence and could present a novel therapeutic target independent of and/or complementary to antibiotics. It has been demonstrated that this novel 5-gene operon is important to survival of *Salmonella* in both humanized and non-humanized mice (Figure 18; J. Karlinsey unpublished data). Structural prediction has implicated the involvement of these genes in carbohydrate metabolism (Table 5). I demonstrated that the absence of this operon influences membrane stability and polarization in *S*. Typhi, which are essential to maintaining the structural and physiological integrity of the bacterial cell. (Figures 21, 23). This operon could be targeted in combination with drugs that weaken the bacterial cell wall to synergistically treat infection. One such drug is ceftriaxone, an inhibitor of bacterial cell wall synthesis, which is commonly prescribed to typhoid fever patients.

In contrast to *S*. Typhi, invasive nontyphoidal Salmonellosis (iNTS) appears to cause systemic infection by exploiting the impaired immune system of its hosts (165). Due to the immunocompromised nature of iNTS patients, vaccination against iNTS-causing *S.* Typhimurium and other enteriditis strains is unlikely to be effective (240). Instead, a better understanding of the mode of transmission of these pathogens may prove useful. I, and others, have provided evidence that *S*. Typhimurium ST313 strains have adapted to an anthroponotic mode of transmission (Figure 14, 15, 16) (152, 153). In-depth epidemiological studies would be required to determine if this hypothesis is true. Future directions will investigate the role of SPI1 in the differences in transmission between ST313 and ST19 strains. Both fecal shedding and epithelial cell invasion by *Salmonella* are influenced by the SPI1 T3SS (181). Anthroponotic transmission of ST313 bacteria may be enhanced due to increased fecal shedding of bacteria in

infected individuals (Figure 12B). Additionally, ST313 is more invasive for human epithelial cells as compared to ST19 (Figure 10B). Previous studies have reported differential expression of the SPI1 effector *sopE2* between ST19 and ST313 strains (157). Future studies aimed at better understanding the differences in SPI1 regulation between ST313 and ST19 may help explain enhanced fecal shedding of ST313 strains.

The best remedy for invasive and noninvasive Salmonellosis is improvements in public infrastructure that promote clean water and food sources. However, changes like these are costly and difficult to implement. In the meantime, a better understanding of how these pathogens cause disease will continue to inform preventative and therapeutic research and design in the hopes of reducing the burden of these diseases globally.

References

1. **Papagrigorakis, MJ, Synodinos, PN, Yapijakis, C**. 2007. Ancient typhoid epidemic reveals possible ancestral strain of *Salmonella enterica* serovar Typhi. Infect Genet Evol **7**:126–127.
2. **Crump, JA, Luby, SP, Mintz, ED**. 2004. The global burden of typhoid fever. Bull World Health Organ **82**:346–353.
3. **Wain, J, Hendriksen, RS, Mikoleit, ML, Keddy, KH, Ochiai, RL**. 2015. Typhoid fever. Lancet **385**:1136–1145.
4. **Mabey, DC, Brown, A, Greenwood, BM**. 1987. *Plasmodium falciparum* malaria and *Salmonella* infections in Gambian children. J Infect Dis **155**:1319–1321.
5. **Gordon, MA, Graham, SM, Walsh, AL, Wilson, L, Phiri, A, Molyneux, E, Zijlstra, EE, Heyderman, RS, Hart, CA, Molyneux, ME**. 2008. Epidemics of invasive *Salmonella enterica* serovar enteritidis and *S. enterica* Serovar typhimurium infection associated with multidrug resistance among adults and children in Malawi. Clin Infect Dis **46**:963–969.
6. **Reddy, EA, Shaw, AV, Crump, JA**. 2010. Community-acquired bloodstream infections in Africa: a systematic review and meta-analysis. Lancet Infect Dis **10**:417–432.
7. **Ao, TT, Feasey, NA, Gordon, MA, Keddy, KH, Angulo, FJ, Crump, JA**. 2015. Global burden of invasive nontyphoidal *Salmonella* disease, 2010(1). Emerg Infect Dis **21**
8. **Duggan, MB, Beyer, L**. 1975. Enteric fever in young Yoruba children. Arch Dis Child **50**:67–71.
9. **Jonas, C, Van de Perre, P, Reding, P, Burette, A, Deprez, C, Clumeck, N, Deltenre, M**. 1984. [Severe digestive complications of AIDS in a group of patients from Zaire]. Acta Gastroenterol Belg **47**:396–402.
10. **Piot, P, Quinn, TC, Taelman, H, Feinsod, FM, Minlangu, KB, Wobin, O, Mbendi, N, Mazebo, P, Ndangi, K, Stevens, W**. 1984. Acquired immunodeficiency syndrome in a heterosexual population in Zaire. Lancet **2**:65–69.
11. **Gilks, CF, Brindle, RJ, Otieno, LS, Simani, PM, Newnham, RS, Bhatt, SM, Lule, GN, Okelo, GB, Watkins, WM, Waiyaki, PG**. 1990. Life-threatening bacteraemia in HIV-1 seropositive adults admitted to hospital in Nairobi, Kenya. Lancet **336**:545–549.
12. **Bäumler, AJ**. 1997. The record of horizontal gene transfer in *Salmonella*. Trends Microbiol **5**:318–322.
13. **Bäumler, AJ, Tsolis, RM, Ficht, TA, Adams, LG**. 1998. Evolution of host adaptation in *Salmonella enterica*. Infect Immun **66**:4579–4587.
14. **Li, J, Ochman, H, Groisman, EA, Boyd, EF, Solomon, F, Nelson, K, Selander, RK**. 1995. Relationship between evolutionary rate and cellular location among the Inv/Spa invasion proteins of *Salmonella enterica*. Proc Natl Acad Sci U S A **92**:7252–7256.
15. **Mills, DM, Bajaj, V, Lee, CA**. 1995. A 40 kb chromosomal fragment encoding *Salmonella* typhimurium invasion genes is absent from the corresponding region of the *Escherichia coli* K-12 chromosome. Mol Microbiol **15**:749–759.
16. **Ochman, H, Groisman, EA**. 1995. The evolution of invasion by enteric bacteria. Can J Microbiol **41**:555–561.
17. **Que, F, Wu, S, Huang, R**. 2013. *Salmonella* pathogenicity island 1(SPI-1) at work. Curr Microbiol **66**:582–587.
18. **Ochman, H, Groisman, EA**. 1996. Distribution of pathogenicity islands in *Salmonella* spp. Infect Immun **64**:5410–5412.
19. **Hensel, M**. 2000. *Salmonella* pathogenicity island 2. Mol Microbiol **36**:1015–1023.
20. **Sorek, R, Zhu, Y, Creevey, CJ, Francino, MP, Bork, P, Rubin, EM**. 2007. Genome-wide experimental determination of barriers to horizontal gene transfer. Science **318**:1449–1452.

21. **Navarre, WW, Porwollik, S, Wang, Y, McClelland, M, Rosen, H, Libby, SJ, Fang, FC**. 2006. Selective silencing of foreign DNA with low GC content by the H-NS protein in *Salmonella*. Science **313**:236–238.
22. **Will, WR, Bale, DH, Reid, PJ, Libby, SJ, Fang, FC**. 2014. Evolutionary expansion of a regulatory network by counter-silencing. Nat Commun **5**:5270.
23. **Will, WR, Navarre, WW, Fang, FC**. 2015. Integrated circuits: how transcriptional silencing and counter-silencing facilitate bacterial evolution. Curr Opin Microbiol **23**:8–13.
24. **Liu, B, Knirel, YA, Feng, L, Perepelov, AV, Senchenkova, SN, Reeves, PR, Wang, L**. 2014. Structural diversity in *Salmonella* O antigens and its genetic basis. FEMS Microbiol Rev **38**:56–89.
25. **Bäumler, A, Fang, FC**. 2013. Host specificity of bacterial pathogens. Cold Spring Harb Perspect Med **3**:a010041.
26. **Sabbagh, SC, Forest, CG, Lepage, C, Leclerc, JM, Daigle, F**. 2010. So similar, yet so different: uncovering distinctive features in the genomes of *Salmonella enterica* serovars Typhimurium and Typhi. FEMS Microbiol Lett **305**:1–13.
27. **Parry, CM, Hien, TT, Dougan, G, White, NJ, Farrar, JJ**. 2002. Typhoid fever. N Engl J Med **347**:1770–1782.
28. **Levine, MM, Black, RE, Lanata, C**. 1982. Precise estimation of the numbers of chronic carriers of *Salmonella* typhi in Santiago, Chile, an endemic area. J Infect Dis **146**:724–726.
29. **Chau, TT, Campbell, JI, Galindo, CM, Van Minh Hoang, N, Diep, TS, Nga, TT, Van Vinh Chau, N, Tuan, PQ, Page, AL, Ochiai, RL, Schultsz, C, Wain, J, Bhutta, ZA, Parry, CM, Bhattacharya, SK, Dutta, S, Agtini, M, Dong, B, Honghui, Y, Anh, DD, Canh, DG, Naheed, A, Albert, MJ, Phetsouvanh, R, Newton, PN, Basnyat, B, Arjyal, A, La, TT, Rang, NN, Phuong, LT, Van Be Bay, P, von Seidlein, L, Dougan, G, Clemens, JD, Vinh, H, Hien, TT, Chinh, NT, Acosta, CJ, Farrar, J, Dolecek, C**. 2007. Antimicrobial drug resistance of *Salmonella enterica* serovar typhi in asia and molecular mechanism of reduced susceptibility to the fluoroquinolones. Antimicrob Agents Chemother **51**:4315–4323.
30. **Azmatullah, A, Qamar, FN, Thaver, D, Zaidi, AK, Bhutta, ZA**. 2015. Systematic review of the global epidemiology, clinical and laboratory profile of enteric fever. J Glob Health **5**:020407.
31. **Rahman, BA, Wasfy, MO, Maksoud, MA, Hanna, N, Dueger, E, House, B**. 2014. Multi-drug resistance and reduced susceptibility to ciprofloxacin among *Salmonella enterica* serovar Typhi isolates from the Middle East and Central Asia. New Microbes New Infect **2**:88–92.
32. **Wong, VK, Baker, S, Pickard, DJ, Parkhill, J, Page, AJ, Feasey, NA, Kingsley, RA, Thomson, NR, Keane, JA, Weill, FX, Edwards, DJ, Hawkey, J, Harris, SR, Mather, AE, Cain, AK, Hadfield, J, Hart, PJ, Thieu, NT, Klemm, EJ, Glinos, DA, Breiman, RF, Watson, CH, Kariuki, S, Gordon, MA, Heyderman, RS, Okoro, C, Jacobs, J, Lunguya, O, Edmunds, WJ, Msefula, C, Chabalgoity, JA, Kama, M, Jenkins, K, Dutta, S, Marks, F, Campos, J, Thompson, C, Obaro, S, MacLennan, CA, Dolecek, C, Keddy, KH, Smith, AM, Parry, CM, Karkey, A, Mulholland, EK, Campbell, JI, Dongol, S, Basnyat, B, Dufour, M, Bandaranayake, D, Naseri, TT, Singh, SP, Hatta, M, Newton, P, Onsare, RS, Isaia, L, Dance, D, Davong, V, Thwaites, G, Wijedoru, L, Crump, JA, De Pinna, E, Nair, S, Nilles, EJ, Thanh, DP, Turner, P, Soeng, S, Valcanis, M, Powling, J, Dimovski, K, Hogg, G, Farrar, J, Holt, KE, Dougan, G**. 2015. Phylogeographical analysis of the dominant multidrug-resistant H58 clade of *Salmonella* Typhi identifies inter- and intracontinental transmission events. Nat Genet **47**:632–639.
33. **Holt, KE, Phan, MD, Baker, S, Duy, PT, Nga, TV, Nair, S, Turner, AK, Walsh, C, Fanning, S, Farrell-Ward, S, Dutta, S, Kariuki, S, Weill, FX, Parkhill, J, Dougan, G, Wain, J**. 2011. Emergence of a globally dominant IncHI1 plasmid type associated with multiple drug resistant typhoid. PLoS Negl Trop Dis **5**:e1245.

34. **Marineli, F, Tsoucalas, G, Karamanou, M, Androutsos, G**. 2013. Mary Mallon (1869-1938) and the history of typhoid fever. Ann Gastroenterol **26**:132–134.
35. **Lai, CW, Chan, RC, Cheng, AF, Sung, JY, Leung, JW**. 1992. Common bile duct stones: a cause of chronic salmonellosis. Am J Gastroenterol **87**:1198–1199.
36. **Prouty, AM, Schwesinger, WH, Gunn, JS**. 2002. Biofilm formation and interaction with the surfaces of gallstones by *Salmonella* spp. Infect Immun **70**:2640–2649.
37. **McGovern, VJ, Slavutin, LJ**. 1979. Pathology of *salmonella* colitis. Am J Surg Pathol **3**:483–490.
38. **McCormick, BA, Colgan, SP, Delp-Archer, C, Miller, SI, Madara, JL**. 1993. *Salmonella* typhimurium attachment to human intestinal epithelial monolayers: transcellular signalling to subepithelial neutrophils. J Cell Biol **123**:895–907.
39. **Lee, CA, Silva, M, Siber, AM, Kelly, AJ, Galyov, E, McCormick, BA**. 2000. A secreted *Salmonella* protein induces a proinflammatory response in epithelial cells, which promotes neutrophil migration. Proc Natl Acad Sci U S A **97**:12283–12288.
40. **Day, DW, Mandal, BK, Morson, BC**. 1978. The rectal biopsy appearances in *Salmonella* colitis. Histopathology **2**:117–131.
41. **Tükel, C, Raffatellu, M, Chessa, D, Wilson, RP, Akçelik, M, Bäumler, AJ**. 2006. Neutrophil influx during non-typhoidal salmonellosis: who is in the driver's seat. FEMS Immunol Med Microbiol **46**:320–329.
42. **SAPHRA, I, WINTER, JW**. 1957. Clinical manifestations of salmonellosis in man; an evaluation of 7779 human infections identified at the New York *Salmonella* Center. N Engl J Med **256**:1128–1134.
43. **Buchwald, DS, Blaser, MJ**. 1984. A review of human salmonellosis: II. Duration of excretion following infection with nontyphi *Salmonella*. Rev Infect Dis **6**:345–356.
44. **Gordon, MA, Banda, HT, Gondwe, M, Gordon, SB, Boeree, MJ, Walsh, AL, Corkill, JE, Hart, CA, Gilks, CF, Molyneux, ME**. 2002. Non-typhoidal *salmonella* bacteraemia among HIV-infected Malawian adults: high mortality and frequent recrudescence. AIDS **16**:1633–1641.
45. **Feasey, NA, Dougan, G, Kingsley, RA, Heyderman, RS, Gordon, MA**. 2012. Invasive non-typhoidal *salmonella* disease: an emerging and neglected tropical disease in Africa. Lancet **379**:2489–2499.
46. **Whitaker, JA, Franco-Paredes, C, del Rio, C, Edupuganti, S**. 2009. Rethinking typhoid fever vaccines: implications for travelers and people living in highly endemic areas. J Travel Med **16**:46–52.
47. **Wilson, RP, Winter, SE, Spees, AM, Winter, MG, Nishimori, JH, Sanchez, JF, Nuccio, SP, Crawford, RW, Tükel, Ç, Bäumler, AJ**. 2011. The Vi capsular polysaccharide prevents complement receptor 3-mediated clearance of *Salmonella enterica* serotype Typhi. Infect Immun **79**:830–837.
48. **Looney, RJ, Steigbigel, RT**. 1986. Role of the Vi antigen of *Salmonella* typhi in resistance to host defense in vitro. J Lab Clin Med **108**:506–516.
49. **Raffatellu, M, Santos, RL, Chessa, D, Wilson, RP, Winter, SE, Rossetti, CA, Lawhon, SD, Chu, H, Lau, T, Bevins, CL, Adams, LG, Bäumler, AJ**. 2007. The capsule encoding the *viaB* locus reduces interleukin-17 expression and mucosal innate responses in the bovine intestinal mucosa during infection with *Salmonella enterica* serotype Typhi. Infect Immun **75**:4342–4350.
50. **Raffatellu, M, Chessa, D, Wilson, RP, Dusold, R, Rubino, S, Bäumler, AJ**. 2005. The Vi capsular antigen of *Salmonella enterica* serotype Typhi reduces Toll-like receptor-dependent interleukin-8 expression in the intestinal mucosa. Infect Immun **73**:3367–3374.
51. **Martin, LB**. 2012. Vaccines for typhoid fever and other salmonelloses. Curr Opin Infect Dis **25**:489–499.
52. **Crump, JA, Mintz, ED**. 2010. Global trends in typhoid and paratyphoid Fever. Clin Infect Dis **50**:241–246.

53. **Pakkanen, SH, Kantele, JM, Kantele, A**. 2012. Cross-reactive gut-directed immune response against *Salmonella enterica* serovar Paratyphi A and B in typhoid fever and after oral Ty21a typhoid vaccination. Vaccine **30**:6047–6053.
54. **Bodhidatta, L, Taylor, DN, Thisyakorn, U, Echeverria, P**. 1987. Control of typhoid fever in Bangkok, Thailand, by annual immunization of schoolchildren with parenteral typhoid vaccine. Rev Infect Dis **9**:841–845.
55. **Tsolis, RM, Xavier, MN, Santos, RL, Bäumler, AJ**. 2011. How to become a top model: impact of animal experimentation on human *Salmonella* disease research. Infect Immun **79**:1806–1814.
56. **Watson, KG, Holden, DW**. 2010. Dynamics of growth and dissemination of *Salmonella* in vivo. Cell Microbiol **12**:1389–1397.
57. **Galán, JE, Curtiss, R**. 1989. Cloning and molecular characterization of genes whose products allow *Salmonella* typhimurium to penetrate tissue culture cells. Proc Natl Acad Sci U S A **86**:6383–6387.
58. **Clark, MA, Jepson, MA, Simmons, NL, Hirst, BH**. 1994. Preferential interaction of *Salmonella* typhimurium with mouse Peyer's patch M cells. Res Microbiol **145**:543–552.
59. **Clark, MA, Hirst, BH, Jepson, MA**. 1998. Inoculum composition and *Salmonella* pathogenicity island 1 regulate M-cell invasion and epithelial destruction by *Salmonella* typhimurium. Infect Immun **66**:724–731.
60. **Eichelberg, K, Galán, JE**. 1999. Differential regulation of *Salmonella* typhimurium type III secreted proteins by pathogenicity island 1 (SPI-1)-encoded transcriptional activators InvF and hilA. Infect Immun **67**:4099–4105.
61. **Jones, BD, Ghori, N, Falkow, S**. 1994. *Salmonella* typhimurium initiates murine infection by penetrating and destroying the specialized epithelial M cells of the Peyer's patches. J Exp Med **180**:15–23.
62. **Richter-Dahlfors, A, Buchan, AM, Finlay, BB**. 1997. Murine salmonellosis studied by confocal microscopy: *Salmonella* typhimurium resides intracellularly inside macrophages and exerts a cytotoxic effect on phagocytes in vivo. J Exp Med **186**:569–580.
63. **Vazquez-Torres, A, Jones-Carson, J, Bäumler, AJ, Falkow, S, Valdivia, R, Brown, W, Le, M, Berggren, R, Parks, WT, Fang, FC**. 1999. Extraintestinal dissemination of *Salmonella* by CD18-expressing phagocytes. Nature **401**:804–808.
64. **Fields, PI, Swanson, RV, Haidaris, CG, Heffron, F**. 1986. Mutants of *Salmonella* typhimurium that cannot survive within the macrophage are avirulent. Proc Natl Acad Sci U S A **83**:5189–5193.
65. **Figueira, R, Holden, DW**. 2012. Functions of the *Salmonella* pathogenicity island 2 (SPI-2) type III secretion system effectors. Microbiology **158**:1147–1161.
66. **Cirillo, DM, Valdivia, RH, Monack, DM, Falkow, S**. 1998. Macrophage-dependent induction of the *Salmonella* pathogenicity island 2 type III secretion system and its role in intracellular survival. Mol Microbiol **30**:175–188.
67. **Forest, CG, Ferraro, E, Sabbagh, SC, Daigle, F**. 2010. Intracellular survival of *Salmonella enterica* serovar Typhi in human macrophages is independent of *Salmonella* pathogenicity island (SPI)-2. Microbiology **156**:3689–3698.
68. **Daigle, F, Graham, JE, Curtiss, R**. 2001. Identification of *Salmonella* typhi genes expressed within macrophages by selective capture of transcribed sequences (SCOTS). Mol Microbiol **41**:1211–1222.
69. **Desjardins, M, Celis, JE, van Meer, G, Dieplinger, H, Jahraus, A, Griffiths, G, Huber, LA**. 1994. Molecular characterization of phagosomes. J Biol Chem **269**:32194–32200.
70. **Harrison, RE, Bucci, C, Vieira, OV, Schroer, TA, Grinstein, S**. 2003. Phagosomes fuse with late endosomes and/or lysosomes by extension of membrane protrusions along microtubules: role of Rab7 and RILP. Mol Cell Biol **23**:6494–6506.

71. **Rathman, M, Sjaastad, MD, Falkow, S**. 1996. Acidification of phagosomes containing *Salmonella* typhimurium in murine macrophages. Infect Immun **64**:2765–2773.
72. **Quinn, MT, Gauss, KA**. 2004. Structure and regulation of the neutrophil respiratory burst oxidase: comparison with nonphagocyte oxidases. J Leukoc Biol **76**:760–781.
73. **Fang, FC**. 2004. Antimicrobial reactive oxygen and nitrogen species: concepts and controversies. Nat Rev Microbiol **2**:820–832.
74. **Xie, Q, Nathan, C**. 1994. The high-output nitric oxide pathway: role and regulation. J Leukoc Biol **56**:576–582.
75. **Kamijo, R, Harada, H, Matsuyama, T, Bosland, M, Gerecitano, J, Shapiro, D, Le, J, Koh, SI, Kimura, T, Green, SJ**. 1994. Requirement for transcription factor IRF-1 in NO synthase induction in macrophages. Science **263**:1612–1615.
76. **Tam, MA, Rydström, A, Sundquist, M, Wick, MJ**. 2008. Early cellular responses to *Salmonella* infection: dendritic cells, monocytes, and more. Immunol Rev **225**:140–162.
77. **Vidal, S, Tremblay, ML, Govoni, G, Gauthier, S, Sebastiani, G, Malo, D, Skamene, E, Olivier, M, Jothy, S, Gros, P**. 1995. The *Ity/Lsh/Bcg* locus: natural resistance to infection with intracellular parasites is abrogated by disruption of the *Nramp1* gene. J Exp Med **182**:655–666.
78. **Fink, SL, Cookson, BT**. 2007. Pyroptosis and host cell death responses during *Salmonella* infection. Cell Microbiol **9**:2562–2570.
79. **Chen, LM, Kaniga, K, Galán, JE**. 1996. *Salmonella* spp. are cytotoxic for cultured macrophages. Mol Microbiol **21**:1101–1115.
80. **Monack, DM, Raupach, B, Hromockyj, AE, Falkow, S**. 1996. *Salmonella* typhimurium invasion induces apoptosis in infected macrophages. Proc Natl Acad Sci U S A **93**:9833–9838.
81. **Miao, EA, Leaf, IA, Treuting, PM, Mao, DP, Dors, M, Sarkar, A, Warren, SE, Wewers, MD, Aderem, A**. 2010. Caspase-1-induced pyroptosis is an innate immune effector mechanism against intracellular bacteria. Nat Immunol **11**:1136–1142.
82. **Fantuzzi, G, Dinarello, CA**. 1999. Interleukin-18 and interleukin-1 beta: two cytokine substrates for ICE (caspase-1). J Clin Immunol **19**:1–11.
83. **Hersh, D, Monack, DM, Smith, MR, Ghori, N, Falkow, S, Zychlinsky, A**. 1999. The *Salmonella* invasin SipB induces macrophage apoptosis by binding to caspase-1. Proc Natl Acad Sci U S A **96**:2396–2401.
84. **Brennan, MA, Cookson, BT**. 2000. *Salmonella* induces macrophage death by caspase-1-dependent necrosis. Mol Microbiol **38**:31–40.
85. **Fink, SL, Cookson, BT**. 2006. Caspase-1-dependent pore formation during pyroptosis leads to osmotic lysis of infected host macrophages. Cell Microbiol **8**:1812–1825.
86. **Mariathasan, S, Newton, K, Monack, DM, Vucic, D, French, DM, Lee, WP, Roose-Girma, M, Erickson, S, Dixit, VM**. 2004. Differential activation of the inflammasome by caspase-1 adaptors ASC and Ipaf. Nature **430**:213–218.
87. **Lundberg, U, Vinatzer, U, Berdnik, D, von Gabain, A, Baccarini, M**. 1999. Growth phase-regulated induction of *Salmonella*-induced macrophage apoptosis correlates with transient expression of SPI-1 genes. J Bacteriol **181**:3433–3437.
88. **Kofoed, EM, Vance, RE**. 2011. Innate immune recognition of bacterial ligands by NAIPs determines inflammasome specificity. Nature **477**:592–595.
89. **Zhao, Y, Yang, J, Shi, J, Gong, YN, Lu, Q, Xu, H, Liu, L, Shao, F**. 2011. The NLRC4 inflammasome receptors for bacterial flagellin and type III secretion apparatus. Nature **477**:596–600.
90. **Zhao, Y, Shao, F**. 2016. Diverse mechanisms for inflammasome sensing of cytosolic bacteria and bacterial virulence. Curr Opin Microbiol **29**:37–42.
91. **Yang, J, Zhao, Y, Shi, J, Shao, F**. 2013. Human NAIP and mouse NAIP1 recognize bacterial type III secretion needle protein for inflammasome activation. Proc Natl Acad Sci U S A **110**:14408–14413.

92. **Qu, Y, Misaghi, S, Newton, K, Maltzman, A, Izrael-Tomasevic, A, Arnott, D, Dixit, VM**. 2016. NLRP3 recruitment by NLRC4 during *Salmonella* infection. J Exp Med **213**:877–885.
93. **van der Velden, AW, Lindgren, SW, Worley, MJ, Heffron, F**. 2000. *Salmonella* pathogenicity island 1-independent induction of apoptosis in infected macrophages by *Salmonella enterica* serotype typhimurium. Infect Immun **68**:5702–5709.
94. **Monack, DM, Detweiler, CS, Falkow, S**. 2001. *Salmonella* pathogenicity island 2-dependent macrophage death is mediated in part by the host cysteine protease caspase-1. Cell Microbiol **3**:825–837.
95. **Miao, EA, Mao, DP, Yudkovsky, N, Bonneau, R, Lorang, CG, Warren, SE, Leaf, IA, Aderem, A**. 2010. Innate immune detection of the type III secretion apparatus through the NLRC4 inflammasome. Proc Natl Acad Sci U S A **107**:3076–3080.
96. **Faucher, SP, Porwollik, S, Dozois, CM, McClelland, M, Daigle, F**. 2006. Transcriptome of *Salmonella enterica* serovar Typhi within macrophages revealed through the selective capture of transcribed sequences. Proc Natl Acad Sci U S A **103**:1906–1911.
97. **Lyons, S, Wang, L, Casanova, JE, Sitaraman, SV, Merlin, D, Gewirtz, AT**. 2004. *Salmonella* typhimurium transcytoses flagellin via an SPI2-mediated vesicular transport pathway. J Cell Sci **117**:5771–5780.
98. **Uchiya, K, Nikai, T**. 2008. *Salmonella* virulence factor SpiC is involved in expression of flagellin protein and mediates activation of the signal transduction pathways in macrophages. Microbiology **154**:3491–3502.
99. **Guilloteau, LA, Wallis, TS, Gautier, AV, MacIntyre, S, Platt, DJ, Lax, AJ**. 1996. The *Salmonella* virulence plasmid enhances *Salmonella*-induced lysis of macrophages and influences inflammatory responses. Infect Immun **64**:3385–3393.
100. **Libby, SJ, Lesnick, M, Hasegawa, P, Weidenhammer, E, Guiney, DG**. 2000. The *Salmonella* virulence plasmid *spv* genes are required for cytopathology in human monocyte-derived macrophages. Cell Microbiol **2**:49–58.
101. **Browne, SH, Lesnick, ML, Guiney, DG**. 2002. Genetic requirements for *salmonella*-induced cytopathology in human monocyte-derived macrophages. Infect Immun **70**:7126–7135.
102. **Schwan, WR, Huang, XZ, Hu, L, Kopecko, DJ**. 2000. Differential bacterial survival, replication, and apoptosis-inducing ability of *Salmonella* serovars within human and murine macrophages. Infect Immun **68**:1005–1013.
103. **Conlan, JW**. 1997. Critical roles of neutrophils in host defense against experimental systemic infections of mice by *Listeria monocytogenes, Salmonella* typhimurium, and *Yersinia enterocolitica*. Infect Immun **65**:630–635.
104. **Spees, AM, Kingsbury, DD, Wangdi, T, Xavier, MN, Tsolis, RM, Bäumler, AJ**. 2014. Neutrophils are a source of gamma interferon during acute *Salmonella enterica* serovar Typhimurium colitis. Infect Immun **82**:1692–1697.
105. **Cheminay, C, Chakravortty, D, Hensel, M**. 2004. Role of neutrophils in murine salmonellosis. Infect Immun **72**:468–477.
106. **Kupz, A, Scott, TA, Belz, GT, Andrews, DM, Greyer, M, Lew, AM, Brooks, AG, Smyth, MJ, Curtiss, R, Bedoui, S, Strugnell, RA**. 2013. Contribution of Thy1+ NK cells to protective IFN-γ production during *Salmonella* typhimurium infections. Proc Natl Acad Sci U S A **110**:2252–2257.
107. **Rydström, A, Wick, MJ**. 2007. Monocyte recruitment, activation, and function in the gut-associated lymphoid tissue during oral *Salmonella* infection. J Immunol **178**:5789–5801.
108. **Sierro, F, Dubois, B, Coste, A, Kaiserlian, D, Kraehenbuhl, JP, Sirard, JC**. 2001. Flagellin stimulation of intestinal epithelial cells triggers CCL20-mediated migration of dendritic cells. Proc Natl Acad Sci U S A **98**:13722–13727.
109. **Bumann, D**. 2003. T cell receptor-transgenic mouse models for studying cellular immune responses to *Salmonella* in vivo. FEMS Immunol Med Microbiol **37**:105–109.

110. **McSorley, SJ, Asch, S, Costalonga, M, Reinhardt, RL, Jenkins, MK**. 2002. Tracking *salmonella*-specific CD4 T cells in vivo reveals a local mucosal response to a disseminated infection. Immunity **16**:365–377.
111. **Mittrücker, HW, Kaufmann, SH**. 2000. Immune response to infection with *Salmonella* typhimurium in mice. J Leukoc Biol **67**:457–463.
112. **Michetti, P, Mahan, MJ, Slauch, JM, Mekalanos, JJ, Neutra, MR**. 1992. Monoclonal secretory immunoglobulin A protects mice against oral challenge with the invasive pathogen *Salmonella* typhimurium. Infect Immun **60**:1786–1792.
113. **Martinoli, C, Chiavelli, A, Rescigno, M**. 2007. Entry route of *Salmonella* typhimurium directs the type of induced immune response. Immunity **27**:975–984.
114. **Pham, OH, McSorley, SJ**. 2015. Protective host immune responses to *Salmonella* infection. Future Microbiol **10**:101–110.
115. **Andrews, T, Sullivan, KE**. 2003. Infections in patients with inherited defects in phagocytic function. Clin Microbiol Rev **16**:597–621.
116. **MacLennan, C, Fieschi, C, Lammas, DA, Picard, C, Dorman, SE, Sanal, O, MacLennan, JM, Holland, SM, Ottenhoff, TH, Casanova, JL, Kumararatne, DS**. 2004. Interleukin (IL)-12 and IL-23 are key cytokines for immunity against *Salmonella* in humans. J Infect Dis **190**:1755–1757.
117. **Jantsch, J, Chikkaballi, D, Hensel, M**. 2011. Cellular aspects of immunity to intracellular *Salmonella enterica*. Immunol Rev **240**:185–195.
118. **Zaki, SA, Karande, S**. 2011. Multidrug-resistant typhoid fever: a review. J Infect Dev Ctries **5**:324–337.
119. **Akhtar, S, Sarker, MR, Jabeen, K, Sattar, A, Qamar, A, Fasih, N**. 2015. Antimicrobial resistance in *Salmonella enterica* serovar typhi and paratyphi in South Asia-current status, issues and prospects. Crit Rev Microbiol **41**:536–545.
120. **Fierer, J**. 2001. Extra-intestinal *Salmonella* infections: the significance of spv genes. Clin Infect Dis **32**:519–520.
121. **Heffernan, EJ, Fierer, J, Chikami, G, Guiney, D**. 1987. Natural history of oral *Salmonella* dublin infection in BALB/c mice: effect of an 80-kilobase-pair plasmid on virulence. J Infect Dis **155**:1254–1259.
122. **Shalini, S, Dorstyn, L, Dawar, S, Kumar, S**. 2015. Old, new and emerging functions of caspases. Cell Death Differ **22**:526–539.
123. **Griffin, AJ, McSorley, SJ**. 2011. Development of protective immunity to *Salmonella*, a mucosal pathogen with a systemic agenda. Mucosal Immunol **4**:371–382.
124. **Libby, SJ, Brehm, MA, Greiner, DL, Shultz, LD, McClelland, M, Smith, KD, Cookson, BT, Karlinsey, JE, Kinkel, TL, Porwollik, S, Canals, R, Cummings, LA, Fang, FC**. 2010. Humanized nonobese diabetic-scid IL2rgammanull mice are susceptible to lethal *Salmonella* Typhi infection. Proc Natl Acad Sci U S A **107**:15589–15594.
125. **Pearson, T, Greiner, DL, Shultz, LD**. 2008. Humanized SCID mouse models for biomedical research. Curr Top Microbiol Immunol **324**:25–51.
126. **Brehm, MA, Shultz, LD, Greiner, DL**. 2010. Humanized mouse models to study human diseases. Curr Opin Endocrinol Diabetes Obes **17**:120–125.
127. **Trinchieri, G**. 2003. Interleukin-12 and the regulation of innate resistance and adaptive immunity. Nat Rev Immunol **3**:133–146.
128. **Deiwick, J, Nikolaus, T, Erdogan, S, Hensel, M**. 1999. Environmental regulation of *Salmonella* pathogenicity island 2 gene expression. Mol Microbiol **31**:1759–1773.
129. **Lee, AK, Detweiler, CS, Falkow, S**. 2000. OmpR regulates the two-component system SsrA-ssrB in *Salmonella* pathogenicity island 2. J Bacteriol **182**:771–781.
130. **Guiney, DG, Fierer, J**. 2011. The Role of the *spv* Genes in *Salmonella* Pathogenesis. Front Microbiol **2**:129.

131. **Rauch, I, Müller, M, Decker, T**. 2013. The regulation of inflammation by interferons and their STATs. JAKSTAT **2**:e23820.
132. **Pallmer, K, Oxenius, A**. 2016. Recognition and Regulation of T Cells by NK Cells. Front Immunol **7**:251.
133. **Toshchakov, V, Jones, BW, Perera, PY, Thomas, K, Cody, MJ, Zhang, S, Williams, BR, Major, J, Hamilton, TA, Fenton, MJ, Vogel, SN**. 2002. TLR4, but not TLR2, mediates IFN-beta-induced STAT1alpha/beta-dependent gene expression in macrophages. Nat Immunol **3**:392–398.
134. **Sheikh, F, Dickensheets, H, Gamero, AM, Vogel, SN, Donnelly, RP**. 2014. An essential role for IFN-β in the induction of IFN-stimulated gene expression by LPS in macrophages. J Leukoc Biol **96**:591–600.
135. **Wilson, RP, Raffatellu, M, Chessa, D, Winter, SE, Tükel, C, Bäumler, AJ**. 2008. The Vi-capsule prevents Toll-like receptor 4 recognition of *Salmonella*. Cell Microbiol **10**:876–890.
136. **Ibarra, JA, Knodler, LA, Sturdevant, DE, Virtaneva, K, Carmody, AB, Fischer, ER, Porcella, SF, Steele-Mortimer, O**. 2010. Induction of *Salmonella* pathogenicity island 1 under different growth conditions can affect *Salmonella*-host cell interactions in vitro. Microbiology **156**:1120–1133.
137. **Ahmad, KA, Khan, LH, Roshan, B, Bhutta, ZA**. 2011. Factors associated with typhoid relapse in the era of multiple drug resistant strains. J Infect Dev Ctries **5**:727–731.
138. **Griffin, AJ, Li, LX, Voedisch, S, Pabst, O, McSorley, SJ**. 2011. Dissemination of persistent intestinal bacteria via the mesenteric lymph nodes causes typhoid relapse. Infect Immun **79**:1479–1488.
139. **Altschul, SF, Gish, W, Miller, W, Myers, EW, Lipman, DJ**. 1990. Basic local alignment search tool. J Mol Biol **215**:403–410.
140. **Coombes, BK, Wickham, ME, Lowden, MJ, Brown, NF, Finlay, BB**. 2005. Negative regulation of *Salmonella* pathogenicity island 2 is required for contextual control of virulence during typhoid. Proc Natl Acad Sci U S A **102**:17460–17465.
141. **Rytkönen, A, Poh, J, Garmendia, J, Boyle, C, Thompson, A, Liu, M, Freemont, P, Hinton, JC, Holden, DW**. 2007. SseL, a *Salmonella* deubiquitinase required for macrophage killing and virulence. Proc Natl Acad Sci U S A **104**:3502–3507.
142. **Le Negrate, G, Faustin, B, Welsh, K, Loeffler, M, Krajewska, M, Hasegawa, P, Mukherjee, S, Orth, K, Krajewski, S, Godzik, A, Guiney, DG, Reed, JC**. 2008. *Salmonella* secreted factor L deubiquitinase of *Salmonella* typhimurium inhibits NF-kappaB, suppresses IkappaBalpha ubiquitination and modulates innate immune responses. J Immunol **180**:5045–5056.
143. **Gal-Mor, O, Elhadad, D, Deng, W, Rahav, G, Finlay, BB**. 2011. The *Salmonella* enterica PhoP directly activates the horizontally acquired SPI-2 gene *sseL* and is functionally different from a *S. bongori* ortholog. PLoS One **6**:e20024.
144. **Wood, MW, Jones, MA, Watson, PR, Hedges, S, Wallis, TS, Galyov, EE**. 1998. Identification of a pathogenicity island required for *Salmonella* enteropathogenicity. Mol Microbiol **29**:883–891.
145. **Arricau, N, Hermant, D, Waxin, H, Popoff, MY**. 1997. Molecular characterization of the *Salmonella* typhi StpA protein that is related to both *Yersinia* YopE cytotoxin and YopH tyrosine phosphatase. Res Microbiol **148**:21–26.
146. **Tobar, JA, González, PA, Kalergis, AM**. 2004. *Salmonella* escape from antigen presentation can be overcome by targeting bacteria to Fc gamma receptors on dendritic cells. J Immunol **173**:4058–4065.
147. **Datsenko, KA, Wanner, BL**. 2000. One-step inactivation of chromosomal genes in *Escherichia coli* K-12 using PCR products. Proc Natl Acad Sci U S A **97**:6640–6645.
148. **Singletary, LA, Karlinsey, JE, Libby, SJ, Mooney, JP, Lokken, KL, Tsolis, RM, Byndloss, MX, Hirao, LA, Gaulke, CA, Crawford, RW, Dandekar, S, Kingsley, RA, Msefula,**

CL, Heyderman, RS, Fang, FC. 2016. Loss of Multicellular Behavior in Epidemic African Nontyphoidal *Salmonella enterica* Serovar Typhimurium ST313 Strain D23580. MBio **7**:e02265.
149. **Kariuki, S, Revathi, G, Kariuki, N, Kiiru, J, Mwituria, J, Hart, CA**. 2006. Characterisation of community acquired non-typhoidal *Salmonella* from bacteraemia and diarrhoeal infections in children admitted to hospital in Nairobi, Kenya. BMC Microbiol **6**:101.
150. **Kingsley, RA, Msefula, CL, Thomson, NR, Kariuki, S, Holt, KE, Gordon, MA, Harris, D, Clarke, L, Whitehead, S, Sangal, V, Marsh, K, Achtman, M, Molyneux, ME, Cormican, M, Parkhill, J, MacLennan, CA, Heyderman, RS, Dougan, G**. 2009. Epidemic multiple drug resistant *Salmonella* Typhimurium causing invasive disease in sub-Saharan Africa have a distinct genotype. Genome Res **19**:2279–2287.
151. **Okoro, CK, Kingsley, RA, Connor, TR, Harris, SR, Parry, CM, Al-Mashhadani, MN, Kariuki, S, Msefula, CL, Gordon, MA, de Pinna, E, Wain, J, Heyderman, RS, Obaro, S, Alonso, PL, Mandomando, I, MacLennan, CA, Tapia, MD, Levine, MM, Tennant, SM, Parkhill, J, Dougan, G**. 2012. Intracontinental spread of human invasive *Salmonella* Typhimurium pathovariants in sub-Saharan Africa. Nat Genet **44**:1215–1221.
152. **Kariuki, S, Revathi, G, Gakuya, F, Yamo, V, Muyodi, J, Hart, CA**. 2002. Lack of clonal relationship between non-typhi *Salmonella* strain types from humans and those isolated from animals living in close contact. FEMS Immunol Med Microbiol **33**:165–171.
153. **Kariuki, S, Revathi, G, Kariuki, N, Kiiru, J, Mwituria, J, Muyodi, J, Githinji, JW, Kagendo, D, Munyalo, A, Hart, CA**. 2006. Invasive multidrug-resistant non-typhoidal *Salmonella* infections in Africa: zoonotic or anthroponotic transmission. J Med Microbiol **55**:585–591.
154. **Parsons, BN, Humphrey, S, Salisbury, AM, Mikoleit, J, Hinton, JC, Gordon, MA, Wigley, P**. 2013. Invasive non-typhoidal *Salmonella* typhimurium ST313 are not host-restricted and have an invasive phenotype in experimentally infected chickens. PLoS Negl Trop Dis **7**:e2487.
155. **Herrero-Fresno, A, Wallrodt, I, Leekitcharoenphon, P, Olsen, JE, Aarestrup, FM, Hendriksen, RS**. 2014. The role of the *st313-td* gene in virulence of *Salmonella* Typhimurium ST313. PLoS One **9**:e84566.
156. **Yang, J, Barrila, J, Roland, KL, Kilbourne, J, Ott, CM, Forsyth, RJ, Nickerson, CA**. 2015. Characterization of the Invasive, Multidrug Resistant Non-typhoidal *Salmonella* Strain D23580 in a Murine Model of Infection. PLoS Negl Trop Dis **9**:e0003839.
157. **Carden, S, Okoro, C, Dougan, G, Monack, D**. 2015. Non-typhoidal *Salmonella* Typhimurium ST313 isolates that cause bacteremia in humans stimulate less inflammasome activation than ST19 isolates associated with gastroenteritis. Pathog Dis **73**
158. **Ramachandran, G, Perkins, DJ, Schmidlein, PJ, Tulapurkar, ME, Tennant, SM**. 2015. Invasive *Salmonella* Typhimurium ST313 with naturally attenuated flagellin elicits reduced inflammation and replicates within macrophages. PLoS Negl Trop Dis **9**:e3394.
159. **Okoro, CK, Barquist, L, Connor, TR, Harris, SR, Clare, S, Stevens, MP, Arends, MJ, Hale, C, Kane, L, Pickard, DJ, Hill, J, Harcourt, K, Parkhill, J, Dougan, G, Kingsley, RA**. 2015. Signatures of adaptation in human invasive *Salmonella* Typhimurium ST313 populations from sub-Saharan Africa. PLoS Negl Trop Dis **9**:e0003611.
160. **Kingsley, RA, Humphries, AD, Weening, EH, De Zoete, MR, Winter, S, Papaconstantinopoulou, A, Dougan, G, Bäumler, AJ**. 2003. Molecular and phenotypic analysis of the CS54 island of *Salmonella enterica* serotype typhimurium: identification of intestinal colonization and persistence determinants. Infect Immun **71**:629–640.
161. **Ma, M, Eaton, JW**. 1992. Multicellular oxidant defense in unicellular organisms. Proc Natl Acad Sci U S A **89**:7924–7928.
162. **Römling, U, Sierralta, WD, Eriksson, K, Normark, S**. 1998. Multicellular and aggregative behaviour of *Salmonella* typhimurium strains is controlled by mutations in the *agfD* promoter. Mol Microbiol **28**:249–264.

163. **White, AP, Gibson, DL, Kim, W, Kay, WW, Surette, MG**. 2006. Thin aggregative fimbriae and cellulose enhance long-term survival and persistence of *Salmonella*. J Bacteriol **188**:3219–3227.
164. **MacKenzie, KD, Wang, Y, Shivak, DJ, Wong, CS, Hoffman, LJ, Lam, S, Kröger, C, Cameron, AD, Townsend, HG, Köster, W, White, AP**. 2015. Bistable expression of CsgD in *Salmonella enterica* serovar Typhimurium connects virulence to persistence. Infect Immun **83**:2312–2326.
165. **Lokken, KL, Mooney, JP, Butler, BP, Xavier, MN, Chau, JY, Schaltenberg, N, Begum, RH, Müller, W, Luckhart, S, Tsolis, RM**. 2014. Malaria parasite infection compromises control of concurrent systemic non-typhoidal *Salmonella* infection via IL-10-mediated alteration of myeloid cell function. PLoS Pathog **10**:e1004049.
166. **Vazquez-Torres, A, Fang, FC**. 2000. Cellular routes of invasion by enteropathogens. Curr Opin Microbiol **3**:54–59.
167. **Clark, L, Perrett, CA, Malt, L, Harward, C, Humphrey, S, Jepson, KA, Martinez-Argudo, I, Carney, LJ, La Ragione, RM, Humphrey, TJ, Jepson, MA**. 2011. Differences in *Salmonella enterica* serovar Typhimurium strain invasiveness are associated with heterogeneity in SPI-1 gene expression. Microbiology **157**:2072–2083.
168. **Buchmeier, NA, Libby, SJ, Xu, Y, Loewen, PC, Switala, J, Guiney, DG, Fang, FC**. 1995. DNA repair is more important than catalase for *Salmonella* virulence in mice. J Clin Invest **95**:1047–1053.
169. **Wilmes-Riesenberg, MR, Foster, JW, Curtiss, R**. 1997. An altered *rpoS* allele contributes to the avirulence of *Salmonella* typhimurium LT2. Infect Immun **65**:203–210.
170. **Sutton, A, Buencamino, R, Eisenstark, A**. 2000. *rpoS* mutants in archival cultures of *Salmonella enterica* serovar typhimurium. J Bacteriol **182**:4375–4379.
171. **Zogaj, X, Nimtz, M, Rohde, M, Bokranz, W, Römling, U**. 2001. The multicellular morphotypes of *Salmonella* typhimurium and *Escherichia coli* produce cellulose as the second component of the extracellular matrix. Mol Microbiol **39**:1452–1463.
172. **Römling, U**. 2005. Characterization of the rdar morphotype, a multicellular behaviour in *Enterobacteriaceae*. Cell Mol Life Sci **62**:1234–1246.
173. **Simm, R, Ahmad, I, Rhen, M, Le Guyon, S, Römling, U**. 2014. Regulation of biofilm formation in *Salmonella enterica* serovar Typhimurium. Future Microbiol **9**:1261–1282.
174. **Solano, C, García, B, Valle, J, Berasain, C, Ghigo, JM, Gamazo, C, Lasa, I**. 2002. Genetic analysis of *Salmonella enteritidis* biofilm formation: critical role of cellulose. Mol Microbiol **43**:793–808.
175. **Berggren, RE, Wunderlich, A, Ziegler, E, Schleicher, M, Duke, RC, Looney, D, Fang, FC**. 1995. HIV gp120-specific cell-mediated immune responses in mice after oral immunization with recombinant *Salmonella*. J Acquir Immune Defic Syndr Hum Retrovirol **10**:489–495.
176. **Kader, A, Simm, R, Gerstel, U, Morr, M, Römling, U**. 2006. Hierarchical involvement of various GGDEF domain proteins in rdar morphotype development of *Salmonella enterica* serovar Typhimurium. Mol Microbiol **60**:602–616.
177. **Graham, SM, Walsh, AL, Molyneux, EM, Phiri, AJ, Molyneux, ME**. 2000. Clinical presentation of non-typhoidal *Salmonella* bacteraemia in Malawian children. Trans R Soc Trop Med Hyg **94**:310–314.
178. **Haneda, T, Winter, SE, Butler, BP, Wilson, RP, Tükel, C, Winter, MG, Godinez, I, Tsolis, RM, Bäumler, AJ**. 2009. The capsule-encoding *viaB* locus reduces intestinal inflammation by a *Salmonella* pathogenicity island 1-independent mechanism. Infect Immun **77**:2932–2942.
179. **Mooney, JP, Butler, BP, Lokken, KL, Xavier, MN, Chau, JY, Schaltenberg, N, Dandekar, S, George, MD, Santos, RL, Luckhart, S, Tsolis, RM**. 2014. The mucosal

inflammatory response to non-typhoidal *Salmonella* in the intestine is blunted by IL-10 during concurrent malaria parasite infection. Mucosal Immunol **7**:1302–1311.
180. **Maclennan, CA**. 2014. Out of Africa: links between invasive nontyphoidal *Salmonella* disease, typhoid fever, and malaria. Clin Infect Dis **58**:648–650.
181. **Kingsley, RA, van Amsterdam, K, Kramer, N, Bäumler, AJ**. 2000. The *shdA* gene is restricted to serotypes of *Salmonella enterica* subspecies I and contributes to efficient and prolonged fecal shedding. Infect Immun **68**:2720–2727.
182. **Fang, FC, Libby, SJ, Buchmeier, NA, Loewen, PC, Switala, J, Harwood, J, Guiney, DG**. 1992. The alternative sigma factor katF (rpoS) regulates *Salmonella* virulence. Proc Natl Acad Sci U S A **89**:11978–11982.
183. **Robbe-Saule, V, Norel, F**. 1999. The *rpoS* mutant allele of *Salmonella* typhi Ty2 is identical to that of the live typhoid vaccine Ty21a. FEMS Microbiol Lett **170**:141–143.
184. **Robbe-Saule, V, Algorta, G, Rouilhac, I, Norel, F**. 2003. Characterization of the RpoS status of clinical isolates of *Salmonella enterica*. Appl Environ Microbiol **69**:4352–4358.
185. **Santander, J, Wanda, SY, Nickerson, CA, Curtiss, R**. 2007. Role of RpoS in fine-tuning the synthesis of Vi capsular polysaccharide in *Salmonella enterica* serotype Typhi. Infect Immun **75**:1382–1392.
186. **Gerstel, U, Römling, U**. 2001. Oxygen tension and nutrient starvation are major signals that regulate *agfD* promoter activity and expression of the multicellular morphotype in *Salmonella* typhimurium. Environ Microbiol **3**:638–648.
187. **White, AP, Gibson, DL, Grassl, GA, Kay, WW, Finlay, BB, Vallance, BA, Surette, MG**. 2008. Aggregation via the red, dry, and rough morphotype is not a virulence adaptation in *Salmonella enterica* serovar Typhimurium. Infect Immun **76**:1048–1058.
188. **Römling, U, Bokranz, W, Rabsch, W, Zogaj, X, Nimtz, M, Tschäpe, H**. 2003. Occurrence and regulation of the multicellular morphotype in *Salmonella* serovars important in human disease. Int J Med Microbiol **293**:273–285.
189. **Eguale, T, Marshall, J, Molla, B, Bhatiya, A, Gebreyes, WA, Engidawork, E, Asrat, D, Gunn, JS**. 2014. Association of multicellular behaviour and drug resistance in *Salmonella enterica* serovars isolated from animals and humans in Ethiopia. J Appl Microbiol **117**:961–971.
190. **Zaragoza, WJ, Noel, JT, Teplitski, M**. 2012. Spontaneous non-rdar mutations increase fitness of *Salmonella* in plants. Environ Microbiol Rep **4**:453–458.
191. **Karlinsey, JE**. 2007. lambda-Red genetic engineering in *Salmonella enterica* serovar Typhimurium. Methods Enzymol **421**:199–209.
192. **Ahmer, BM, Tran, M, Heffron, F**. 1999. The virulence plasmid of *Salmonella* typhimurium is self-transmissible. J Bacteriol **181**:1364–1368.
193. **Steele-Mortimer, O**. 2008. Infection of epithelial cells with *Salmonella enterica*. Methods Mol Biol **431**:201–211.
194. **Hirao, LA, Grishina, I, Bourry, O, Hu, WK, Somrit, M, Sankaran-Walters, S, Gaulke, CA, Fenton, AN, Li, JA, Crawford, RW, Chuang, F, Tarara, R, Marco, ML, Bäumler, AJ, Cheng, H, Dandekar, S**. 2014. Early mucosal sensing of SIV infection by paneth cells induces IL-1β production and initiates gut epithelial disruption. PLoS Pathog **10**:e1004311.
195. **Visick, JE, Clarke, S**. 1997. RpoS- and OxyR-independent induction of HPI catalase at stationary phase in *Escherichia coli* and identification of *rpoS* mutations in common laboratory strains. J Bacteriol **179**:4158–4163.
196. **Velayudhan, J, Karlinsey, JE, Frawley, ER, Becker, LA, Nartea, M, Fang, FC**. 2014. Distinct roles of the *Salmonella enterica* serovar Typhimurium CyaY and YggX proteins in the biosynthesis and repair of iron-sulfur clusters. Infect Immun **82**:1390–1401.
197. **Guo, L, Lim, KB, Gunn, JS, Bainbridge, B, Darveau, RP, Hackett, M, Miller, SI**. 1997. Regulation of lipid A modifications by *Salmonella* typhimurium virulence genes *phoP-phoQ*. Science **276**:250–253.

198. **Stojiljkovic, I, Bäumler, AJ, Heffron, F**. 1995. Ethanolamine utilization in *Salmonella* typhimurium: nucleotide sequence, protein expression, and mutational analysis of the *cchA cchB eutE eutJ eutG eutH* gene cluster. J Bacteriol **177**:1357–1366.
199. **Prentki, P, Krisch, HM**. 1984. In vitro insertional mutagenesis with a selectable DNA fragment. Gene **29**:303–313.
200. **Raffatellu, M, Santos, RL, Verhoeven, DE, George, MD, Wilson, RP, Winter, SE, Godinez, I, Sankaran, S, Paixao, TA, Gordon, MA, Kolls, JK, Dandekar, S, Bäumler, AJ**. 2008. Simian immunodeficiency virus-induced mucosal interleukin-17 deficiency promotes *Salmonella* dissemination from the gut. Nat Med **14**:421–428.
201. **Langridge, GC, Phan, MD, Turner, DJ, Perkins, TT, Parts, L, Haase, J, Charles, I, Maskell, DJ, Peters, SE, Dougan, G, Wain, J, Parkhill, J, Turner, AK**. 2009. Simultaneous assay of every *Salmonella* Typhi gene using one million transposon mutants. Genome Res **19**:2308–2316.
202. **Barquist, L, Mayho, M, Cummins, C, Cain, AK, Boinett, CJ, Page, AJ, Langridge, GC, Quail, MA, Keane, JA, Parkhill, J**. 2016. The TraDIS toolkit: sequencing and analysis for dense transposon mutant libraries. Bioinformatics **32**:1109–1111.
203. **Zomer, A, Burghout, P, Bootsma, HJ, Hermans, PW, van Hijum, SA**. 2012. ESSENTIALS: software for rapid analysis of high throughput transposon insertion sequencing data. PLoS One **7**:e43012.
204. **Schäffer, AA, Aravind, L, Madden, TL, Shavirin, S, Spouge, JL, Wolf, YI, Koonin, EV, Altschul, SF**. 2001. Improving the accuracy of PSI-BLAST protein database searches with composition-based statistics and other refinements. Nucleic Acids Res **29**:2994–3005.
205. **Zhang, Y**. 2008. I-TASSER server for protein 3D structure prediction. BMC Bioinformatics **9**:40.
206. **Yang, J, Zhang, Y**. 2015. Protein Structure and Function Prediction Using I-TASSER. Curr Protoc Bioinformatics **52**:5.8.1–15.
207. **Deutscher, J, Aké, FM, Derkaoui, M, Zébré, AC, Cao, TN, Bouraoui, H, Kentache, T, Mokhtari, A, Milohanic, E, Joyet, P**. 2014. The bacterial phosphoenolpyruvate:carbohydrate phosphotransferase system: regulation by protein phosphorylation and phosphorylation-dependent protein-protein interactions. Microbiol Mol Biol Rev **78**:231–256.
208. **Sprenger, GA**. 1995. Genetics of pentose-phosphate pathway enzymes of *Escherichia coli* K-12. Arch Microbiol **164**:324–330.
209. **Rangarajan, ES, Sivaraman, J, Matte, A, Cygler, M**. 2002. Crystal structure of D-ribose-5-phosphate isomerase (RpiA) from *Escherichia coli*. Proteins **48**:737–740.
210. **Essenberg, MK, Cooper, RA**. 1975. Two ribose-5-phosphate isomerases from *Escherichia coli* K12: partial characterisation of the enzymes and consideration of their possible physiological roles. Eur J Biochem **55**:323–332.
211. **Shea, A, Wolcott, M, Daefler, S, Rozak, DA**. 2012. Biolog phenotype microarrays. Methods Mol Biol **881**:331–373.
212. **Cosloy, SD**. 1973. D-serine transport system in *Escherichia coli* K-12. J Bacteriol **114**:679–684.
213. **Taber, HW, Mueller, JP, Miller, PF, Arrow, AS**. 1987. Bacterial uptake of aminoglycoside antibiotics. Microbiol Rev **51**:439–457.
214. **Robbins, JC, Oxender, DL**. 1973. Transport systems for alanine, serine, and glycine in *Escherichia coli* K-12. J Bacteriol **116**:12–18.
215. **Clark, VL, Young, FE**. 1974. Active transport of D-alanine and related amino acids by whole cells of *Bacillus subtilis*. J Bacteriol **120**:1085–1092.
216. **Novo, D, Perlmutter, NG, Hunt, RH, Shapiro, HM**. 1999. Accurate flow cytometric membrane potential measurement in bacteria using diethyloxacarbocyanine and a ratiometric technique. Cytometry **35**:55–63.

217. **Altschul, SF, Madden, TL, Schäffer, AA, Zhang, J, Zhang, Z, Miller, W, Lipman, DJ**. 1997. Gapped BLAST and PSI-BLAST: a new generation of protein database search programs. Nucleic Acids Res **25**:3389–3402.
218. **Roy, A, Kucukural, A, Zhang, Y**. 2010. I-TASSER: a unified platform for automated protein structure and function prediction. Nat Protoc **5**:725–738.
219. **Stülke, J, Arnaud, M, Rapoport, G, Martin-Verstraete, I**. 1998. PRD--a protein domain involved in PTS-dependent induction and carbon catabolite repression of catabolic operons in bacteria. Mol Microbiol **28**:865–874.
220. **Poulsen, TS, Chang, YY, Hove-Jensen, B**. 1999. D-Allose catabolism of *Escherichia coli*: involvement of *alsI* and regulation of *als* regulon expression by allose and ribose. J Bacteriol **181**:7126–7130.
221. **Skinner, AJ, Cooper, RA**. 1974. Genetic studies on ribose 5-phosphate isomerase mutants of *Escherichia coli* K-12. J Bacteriol **118**:1183–1185.
222. **Sørensen, KI, Hove-Jensen, B**. 1996. Ribose catabolism of *Escherichia coli*: characterization of the *rpiB* gene encoding ribose phosphate isomerase B and of the *rpiR* gene, which is involved in regulation of *rpiB* expression. J Bacteriol **178**:1003–1011.
223. **Flora, SJ, Pachauri, V**. 2010. Chelation in metal intoxication. Int J Environ Res Public Health **7**:2745–2788.
224. **Vaara, M**. 1992. Agents that increase the permeability of the outer membrane. Microbiol Rev **56**:395–411.
225. **Nørregaard-Madsen, M, McFall, E, Valentin-Hansen, P**. 1995. Organization and transcriptional regulation of the *Escherichia coli* K-12 D-serine tolerance locus. J Bacteriol **177**:6456–6461.
226. **Anfora, AT, Welch, RA**. 2006. DsdX is the second D-serine transporter in uropathogenic Escherichia coli clinical isolate CFT073. J Bacteriol **188**:6622–6628.
227. **Fraimow, HS, Greenman, JB, Leviton, IM, Dougherty, TJ, Miller, MH**. 1991. Tobramycin uptake in *Escherichia coli* is driven by either electrical potential or ATP. J Bacteriol **173**:2800–2808.
228. 1996. **Medical Microbiology**, S, B (ed), University of Texas Medical Branch, Galveston.
229. **Heath, EC**. 1971. Complex polysaccharides. Annu Rev Biochem **40**:29–56.
230. **Sebkova, A, Karasova, D, Crhanova, M, Budinska, E, Rychlik, I**. 2008. *aro* mutations in *Salmonella enterica* cause defects in cell wall and outer membrane integrity. J Bacteriol **190**:3155–3160.
231. **Gál, J, Szvetnik, A, Schnell, R, Kálmán, M**. 2002. The *metD* D-methionine transporter locus of *Escherichia coli* is an ABC transporter gene cluster. J Bacteriol **184**:4930–4932.
232. **Kadner, RJ, Winkler, HH**. 1975. Energy coupling for methionine transport in *Escherichia coli*. J Bacteriol **123**:985–991.
233. **Russell, AB, Hood, RD, Bui, NK, LeRoux, M, Vollmer, W, Mougous, JD**. 2011. Type VI secretion delivers bacteriolytic effectors to target cells. Nature **475**:343–347.
234. **Krumpochova, P, Sapthu, S, Brouwers, JF, de Haas, M, de Vos, R, Borst, P, van de Wetering, K**. 2012. Transportomics: screening for substrates of ABC transporters in body fluids using vesicular transport assays. FASEB J **26**:738–747.
235. **Clark, K, Karsch-Mizrachi, I, Lipman, DJ, Ostell, J, Sayers, EW**. 2016. GenBank. Nucleic Acids Res **44**:D67–72.
236. **Deng, W, Liou, SR, Plunkett, G, Mayhew, GF, Rose, DJ, Burland, V, Kodoyianni, V, Schwartz, DC, Blattner, FR**. 2003. Comparative genomics of *Salmonella enterica* serovar Typhi strains Ty2 and CT18. J Bacteriol **185**:2330–2337.
237. **Starkey, M, Hickman, JH, Ma, L, Zhang, N, De Long, S, Hinz, A, Palacios, S, Manoil, C, Kirisits, MJ, Starner, TD, Wozniak, DJ, Harwood, CS, Parsek, MR**. 2009. *Pseudomonas aeruginosa* rugose small-colony variants have adaptations that likely promote persistence in the cystic fibrosis lung. J Bacteriol **191**:3492–3503.

238. **Krause, M, Fang, FC, Guiney, DG**. 1992. Regulation of plasmid virulence gene expression in *Salmonella* dublin involves an unusual operon structure. J Bacteriol **174**:4482–4489.
239. **Davies, J**. 2006. Where have All the Antibiotics Gone. Can J Infect Dis Med Microbiol **17**:287–290.
240. **Doffinger, R, Patel, S, Kumararatne, DS**. 2005. Human immunodeficiencies that predispose to intracellular bacterial infections. Curr Opin Rheumatol **17**:440–446.
241. **MacLennan, CA, Martin, LB, Micoli, F**. 2014. Vaccines against invasive *Salmonella* disease: current status and future directions. Hum Vaccin Immunother **10**:1478–1493.
242. **Cheminay, C, Möhlenbrink, A, Hensel, M**. 2005. Intracellular *Salmonella* inhibit antigen presentation by dendritic cells. J Immunol **174**:2892–2899.
243. **Halici, S, Zenk, SF, Jantsch, J, Hensel, M**. 2008. Functional analysis of the *Salmonella* pathogenicity island 2-mediated inhibition of antigen presentation in dendritic cells. Infect Immun **76**:4924–4933.
244. **Song, J, Willinger, T, Rongvaux, A, Eynon, EE, Stevens, S, Manz, MG, Flavell, RA, Galán, JE**. 2010. A mouse model for the human pathogen *Salmonella* typhi. Cell Host Microbe **8**:369–376.